Elucidating mechanisms of protection against dengue severity through immunity to dengue virus nonstructural protein 1

by

Marcus Poon Wong

A dissertation submitted in partial fulfillment of the

requirements for the degree of

Doctor of Philosophy

in

Infectious Diseases and Immunity

in the

Graduate Division

of the

University of California, Berkeley

Committee in charge:

Professor Eva Harris, Chair
Professor Sarah Stanley
Professor Russell Vance
Professor Laurent Coscoy

Fall 2023

Abstract

Elucidating mechanisms of protection against dengue severity through immunity to dengue virus nonstructural protein 1

by

Marcus Poon Wong

Doctor of Philosophy in Infectious Diseases and Immunity

University of California, Berkeley

Professor Eva Harris, Chair

Almost half of the world's population is at risk of infection by dengue virus (DENV), a mosquito-borne flavivirus consisting of serotypes DENV1-4 that is the causative agent of dengue disease. Of the estimated 50-100 million dengue cases annually, 5% develop severe complications known as dengue hemorrhagic fever/dengue shock syndrome (DHF/DSS), which are characterized by severe vascular leak of fluid from the blood into tissues. The triggers of pathogenic DENV-associated vascular leak are still under investigation, but recent work has identified secreted DENV non-structural protein 1 (NS1) as a direct mediator of endothelial cell hyperpermeability and vascular leak. Antibodies against NS1 have been shown to prevent morbidity and mortality in mouse models of DENV infection and can inhibit DENV NS1-induced endothelial dysfunction *in vitro*, highlighting their potential as a therapeutic against DENV and a target for vaccine design. The mechanistic basis by which anti-NS1 antibodies prevent endothelial dysfunction is largely unknown. DENV NS1 is a multifunctional viral protein that plays many roles in the viral life cycle. In addition to inducing endothelial dysfunction, it has been shown to participate in the formation of the viral replication complex, antagonize the complement cascade, and activate innate immune cells. The mechanisms underlying NS1-induced innate immune activation, in particular, are not well understood, and the contribution of this activation during DENV infection is unclear. This dissertation details the exploration of how both innate immunity and antibodies targeting NS1 inhibit DENV pathogenesis.

First, we identify inflammasomes, a class of cytosolic innate immune sensors in the nucleotide-binding oligomerization domain-like receptor (NLR) family, as sensors of DENV NS1. Inflammasomes can sense pathogenic stimuli through NLRs like NLRP3, which leads to activation of caspase-1 and release of IL-1 family cytokines such as IL-1β. We show that DENV NS1 activates inflammasomes in mouse and human macrophages in a caspase-1/11-dependent manner. In mice, we find that DENV NS1-induced inflammasome activation is independent of the NLRP3 inflammasome and does not result in detectable inflammatory cell death. Using caspase-1/11- and NLRP3-deficient mice, we find that caspase-1/11 deficiency makes mice more susceptible to DENV compared to caspase-1/11-functional mice, whereas NLRP3 deficiency has no effect on morbidity and mortality during DENV infection, mirroring the pattern of NS1-induced inflammasome activation. Taken together, we demonstrate that NS1 can trigger inflammasome

activation and identify a beneficial role for the inflammasome pathway in DENV infection, broadening our understanding of innate immune-mediated protective responses to DENV.

Next, we characterized the mechanisms behind the protective ability of an NS1-specific monoclonal antibody (mAb), 2B7. mAb 2B7 inhibits NS1 binding to endothelial cells and NS1-induced hyperpermeability *in vitro* and prevents vascular leak and mortality *in vivo*. We mutated amino acids within the 2B7 epitope guided by a recent crystal structure of the 2B7 antigen-binding fragment (F'ab) in complex with NS1 in order to define the basis of antibody-mediated inhibition of NS1-induced endothelial dysfunction. We found that several amino acids within the core of the 2B7 epitope are conserved across flaviviruses, imbuing 2B7 with pan-flavivirus NS1 cross-reactivity. We also identified several mutants that could still bind to endothelial cells but were unable to induce hyperpermeability, suggesting that amino acids within the 2B7 epitope are molecular determinants of NS1 pathogenesis. The structures and mutagenesis results suggest that 2B7 prevents NS1-induced endothelial dysfunction though two mechanisms: 1) indirect steric hinderance of the cell-binding domain of NS1, abrogating interaction with endothelial cells and 2) direct blockade of amino acids responsible for an additional step in NS1 pathogenesis downstream of binding. Lastly, we find that humans infected with DENV can generate 2B7-like antibody responses against DENV NS1, opening the possibility for rational vaccine design targeting this important epitope.

Taken together, these findings highlight the importance of immune responses to DENV NS1 in preventing disease and elucidate new aspects of DENV NS1's protective and pathogenic roles during DENV infection.

Dedication

To the countless lives that make life possible
Who grow the food we eat, make the clothes we wear, build the homes we live in

To those unafraid to speak truth to power,
despite the personal cost, because it was the right thing to do

To those who want to better the world
even when the world pushes you to the margins

thank you

Table of Contents

Acknowledgements

15 years ago, I was assigned to a group project in my high school biology class to make our own lesson teaching the class about a specific organ system. We chose to do the project on the immune system, a choice that subsequently changed the story of my life. Up to this point, I had never really been the most engaged student, but something about how this complex system of cells in our body worked tirelessly to fight off infection really captured my attention. I set out to turn this spark of inspiration into something I could spend the rest of my life studying. At the time I had little conception of what graduate school was, had never even heard of a PhD, nor knew what research was. All I knew was that the immune system was pretty freaking cool and I wanted to learn even more. This was my call to action, the start of my coming-of-age story. Completing this PhD, thus feels like the last chapter of my own personal bildungsroman. Like every good story, there was plenty of struggle, complete with plagues (COVID-19!), natural disasters (wildfires and PG&E shutdowns), and profound social change (Black Lives Matter and grad student strikes). One might even criticize the writer for being too on the nose; after all, how often does someone get a PhD in infectious disease when a new global pandemic happens to emerge? Seems like a convenient plot device to me. Despite it all, I have come out the other side, changed indelibly by the experience. However, the hero's journey can't be completed without the help of others. In fact, this journey was never really about the final destination, but about the community forged and lessons learned. The best part of this whole chapter in my life has definitely been the things I have learned and the people I have met along the way. So, I'd like to take a moment to highlight all the support I have received throughout my PhD.

I'd first like to thank my thesis committee (Sarah Stanley, Russell Vance, and Laurent Coscoy) for all of their support throughout this process. They have been so generous with their time, reagents, and mentorship and I could not be where I am today without their guidance. Of course, I have to give special thanks to Eva Harris, my thesis advisor, for giving me the opportunity to grow as a scientist and person in her lab. I have learned so much about what it takes to run a lab, what it means to be a mentor, and how to be a champion for global health. Thank you so much for the guidance throughout the years and for giving me the opportunity to pursue a project with as much independence as possible.

The Harris lab is a special, kind of crazy (in a good way!) place. I don't think I have ever met a lab full of such intelligent people coming from a diverse range of backgrounds and perspectives. Thank you to all of the members of the Harris lab, including Paulina Andrade, Dustin Glasner, Scott Biering, Diego Espinosa, P. Robert Beatty, Francielle Tramontini Gomes De Sousa, Josefina Coloma, Chunling Wang, Magelda Montoya, Claudia Sanchez San Martin, Tulika Singh, Jeffery Li, Jasmine Larrick, Samantha Hernandez, Luis Lopez, Michelle Meas, Jaime Cardona-Ospina, Vanessa Jimenez-Posada, Pedro Carneiro, Maria Jose Andrade, Nharae Lee, Reinaldo Mercado-Hernandez, Michael Verdolin, Agam Baljot, Eduarda Lopes, and Elin Lee. You are all amazing people and scientists and I have learned so much from each and every one of you. I will carry our many shared memories with me for years to come.

I'd like to especially give special shout-outs to Sophie Blanc, Laurentia Tjang, Susan Roodsari, Xinyi Feng, Amir Balakhmet, Julia Huffaker, Bryan Castillo-Rojas, Sandra Bos, Aaron Graber, Elias Duarte, Hannah Nilson, Isabel Lamb-Echegaray, and Felix Pahmeier, all of whom have had

to deal with my many shenanigans/crazy ideas/ rants during lunch time and in lab. I am so grateful for our friendships throughout the years and all of the help you have provided both personally and professionally. Thank you for helping weather the storm and being so supportive when things weren't going well. If I am the main character, then you are all the supporting cast that really steal the show.

Thank you to Evan Juan, Phoebe Wang, Sai Chelluri for tolerating me as your research supervisor. It has been such an honor to be your mentor and see you grow in innumerable ways. I truly could not have completed this PhD without your help and I am forever in your debt because of it. I am sure you all will become amazing individuals in the future, and I can't wait to see the good you will do in the future.

I'd also like to thank all of the past and present members of the IDI PhD program, including Eric Lee, Alexandra Tsitsiklis, Derek Jordan Bangs, Gina Borgo, Kristi Geiger, Perri Callaway, Eric Jedel, Kishen Patel, Claire Mastrangelo, Abigail Kane, Carolina Agudelo, Scott Espich, Marize Rizkalla, and Zahra Zubair-Nizami. I truly think IDI was the perfect PhD program for me, in large part because of you all. Thank you for taking me under your wing when I was just a naïve first year and teaching me how to navigate graduate school, for the countless post-seminar coffee chats, for the much-needed socializing when grad school was getting to me. Special shout out to my cohort mates Jo Vinden and Cuong Joseph Tran; we have faced so many challenges together and I am grateful for our trauma bond. I truly hope we all keep in touch, and I wish you all the future success you deserve.

My research journey first got its start as an undergraduate researcher in the Raffatellu lab, and I am absolutely the scientist today because of my time there. Thank you to Suzi Klaus and Manuela Raffatellu for taking a chance on me when I was just a clueless undergrad armed with nothing but an enthusiasm for science. Many people would not have accommodated my absolutely insane class and work schedule, but I am so grateful that you saw my potential even when I didn't.

Thank you to my friends for all of their unwavering support throughout the years. Thank you for sticking with me, even when grad school took up 150% of my time and left nothing for me to give to you. I could fill another 130 pages with how much you all mean to me. I will be forever grateful for our continued friendship and look forward to our adventures together now that I'm done with this part of my life.

I'd also like to take some time to remember the 5th floor view of LKS (In memoriam, 2010-Febuary 1st, 2023). The view definitely helped me get through the tough days and long nights. While I may never be able to see the sun set over the Golden Gate Bridge ever again from the bench at the end of the hallway, it will live forever in my memory (and my Google photo account).

There is so much more I wish I could say but I am running out of room. I do have some brief words for the lifelong friends I have made in the Bay.
To Nicholas Lo, disturbance. To Joel Reyes, bop.

Lastly, I am deeply indebted to the immeasurable sacrifices my family has made to get me to this point. Coming from an immigrant family and being the first person in my family to obtain graduate degree and as a child of immigrants, this PhD represents so much more than my own personal accomplishment. It is the hopes and realization of my parents and grandparents, who uprooted their lives to move to a completely foreign place with absolutely nothing. Having the freedom to study what is interesting to me instead of focusing on pure survival is such a privilege and it makes me truly appreciate this path I chose. I am especially grateful for the resilience and determination they instilled in me. In the face of the adversity they faced, the grad school struggle seems so insignificant. Truly, this degree is for them.

Curriculum Vitae

Education

University of California, Berkeley
Berkeley, CA
Ph.D in Infectious Diseases and Immunity
2018-2023

University of California, Irvine
Irvine, CA
B.S: Biological Sciences
B.A: Comparative Literature
Minor: Asian-American Studies
2011-2015

Research Experience

Graduate Student Researcher
Advisor**: Eva Harris**
University of California, Berkeley
2019-2023
Thesis Project: Elucidating mechanisms of protection to severe dengue disease through immunity to dengue virus non-structural protein 1

Staff Research Associate
Advisor**: Donald Forthal**
University of California, Irvine
2015-2018
Antibody effector functions during HIV infections and vaccinations.

Undergraduate Researcher
Advisor**: Manuela Raffatellu**
University of California, Irvine
2013-2015
Neutrophil responses to *Salmonella typhimurium* in the inflamed gut

Teaching Experience & Service

Graduate Student Instructor
University of California, Berkeley

- MCB 150L: Immunology Lab (Jan-May 2020)
- MCB 150: Molecular Immunology (Aug-Dec 2021)
- MCB 150: Molecular Immunology (Jan-May 2023)

President - (2022-2023)
Infectious Diseases and Immunity Doctoral Student Group, *University of California, Berkeley*

Admissions Committee Member - (2021-2022)
Infectious Diseases and Immunity PhD Program, University of California, Berkeley

Publications

1. **Wong MP**, Juan EYW, Chelluri SS, Wang P, Castillo-Rojas B, Pahmeier F, Blanc SB, Biering SB, Vance RE, Harris E.
   The Inflammasome is Activated by Dengue Virus Non-structural Protein 1 and is Protective during Dengue Virus Infection
   bioRxiv. 2023 Sep 21;. doi: 10.1101/2023.09.21.558875.

2. Biering SB, Gomes de Sousa FT, Tjang LV, Pahmeier F, Zhu C, Ruan R, Blanc SF, Patel TS, Worthington CM, Glasner DR, Castillo-Rojas B, Servellita V, Lo NTN, **Wong MP**, Sandoval DR, Clausen TM, Santos YA, Fox DM, Ortega V, Näär AM, Baric RS, Stanley SA, Aguilar HC, Esko JD, Chiu CY, Pak JE, Beatty PR, Harris E.
   SARS-CoV-2 Spike triggers barrier dysfunction and vascular leak via integrins and TGF-β signaling.
   Nature Communications. 2022 Dec 9;13(1):7630.

3. Lo NTN, Roodsari SZ, Tin NL, **Wong MP**, Biering SB, Harris E.
   Molecular Determinants of Tissue Specificity of Flavivirus Nonstructural Protein 1 Interaction with Endothelial Cells.
   Journal of Virology. 2022 Oct 12;96(19):e0066122. doi: 10.1128/jvi.00661-22. Epub 2022 Sep 15.

4. Solomon O, Adams C, Horton M, **Wong MP**, Meas M, Shao X, Fedrigo I, Hernandez S, Quach HL, Quach DL, Barcellos AL, Coloma J, Busch MP, Harris E, Barcellos LF
   COVID-19 vaccine antibody response is associated with side-effects, chronic health conditions, and vaccine type in a large Northern California cohort
   medRxiv. 2022.09.30.22280166

5. Adams C, Horton M, Solomon O, **Wong MP**, Wu SL, Fuller S, Shao X, Fedrigo I, Quach HL, Quach DL, Meas MA, Lopez L, Broughton A, Barcellos AL, Shim J, Seymens Y, Hernandez SM, Montoya M, Johnson DM, Beckman KB, Busch MP, Coloma J, Lewnard JA, Harris E, Barcellos LF.
   Health inequities in SARS-CoV-2 infection, seroprevalence, and COVID-19 vaccination: Results from the East Bay COVID-19 study
   PLOS Global Public Health. 2022 Aug 15. 2(8): e0000647.

6. **Wong MP**, Meas MA, Adams C, Hernandez S, Green V, Montoya M, Hirsch BM, Horton M, Quach HL, Quach DL, Shao X, Fedrigo I, Zermeno A, Huffaker J, Montes R, Madden A, Cyrus S, McDowell D, Williamson P, Contestable P, Stone M, Coloma J, Busch MP, Barcellos LF, Harris E.
Development and Implementation of Dried Blood Spot-Based COVID-19 Serological Assays for Epidemiologic Studies.
Microbiology Spectrum 2022 May 25:e0247121.

7. Mora AM, Lewnard JA, Kogut K, Rauch SA, Hernandez S, **Wong MP,** Huen K, Chang C, Jewell NP, Holland N, Harris E, Cuevas M, Eskenazi B.
Risk Factors Associated With SARS-CoV-2 Infection Among Farmworkers in Monterey County, California.
JAMA Network Open. 2021 Sep 1;4(9):e2124116. doi: 10.1001/jamanetworkopen.2021.24116.

8. Lewnard JA, Mora AM, Nkwocha O, Kogut K, Rauch SA, Morga N, Hernandez S, **Wong MP**, Huen K, Andrejko K, Jewell NP, Parra KL, Holland N, Harris E, Cuevas M, Eskenazi B.
Prevalence and Clinical Profile of Severe Acute Respiratory Syndrome Coronavirus 2 Infection among Farmworkers, California, June-November 2020
Emerging Infectious Diseases. 2021 Mar 3;27(5).

9. Biering SB & Akey DL, **Wong MP**, Brown WC, Lo NTN, Puerta-Guardo H, Wang C, Konwerski JR, Tramontini F, Espinosa DA, Glasner DR, Li J, Blanc SF, Elledge SJ, Mina MJ, Beatty PR, Smith JL, Harris E
Structural basis for antibody-mediated inhibition of flavivirus NS1-triggered endothelial dysfunction
Science. 2021 Jan 8;371(6525):194-200.

10. Young E, Carnahan RH, Andrade DV, Kose N, Nargi RS, Fritch EJ, Munt JE, Doyle MP, White L, Baric TJ, Stoops M, DeSilva AM, Tse LV, Martinez DR, Zhu D, Metz S, **Wong MP**, Espinosa DA, Montoya M, Biering SB, Sukulpolvi-Petty S, Kuan G, Balmaseda A, Diamond MS, Harris E, Crowe, Jr. JE, Baric RH
Identification of Dengue Virus Serotype 3 Specific Antigenic Sites Targeted by Neutralizing Human Antibodies
Cell Host & Microbe 2020 May 13;27(5):710-724.e7.

11. Vaccari M, Fourati S, Gordon SN, Brown DR, Bissa M, Schifanella L, Silva de Castro I, Doster MN, Galli V, Omsland M, Fujikawa D, Gorini G, Liyanage NP, Trinh HV, McKinnon KM, Foulds K, Keele BF, Roederer M, Koup R, Shen X, Tomaras GD, **Wong MP**, Munoz KJ, Gach JS, Forthal DN, Montefiori DC, Venzon DJ, Felber BK, Rosati M, Pavlakis GN, Rao M, Sekaly RP and Franchini G
HIV vaccine candidate activation of hypoxia and inflammasome in CD14^{+} monocytes is associated with a decreased risk of SIV$_{mac251}$ acquisition.
Nature Medicine 2018 Jun; 24(6):847-856

12. Gach JS, Bouzin M, **Wong MP**, Chromikova V, Gorlani A, Yu KT, Sharma B, Gratton E, and Forthal DN.
Human Immunodeficiency Virus Type-1 (HIV-1) Evades Antibody-Dependent Phagocytosis.
PLOS Pathogens 2017 Dec 27; 13(12): e1006793.

Presentations

The inflammasome is activated by dengue non-structural protein 1 and plays a protective role during viral infection.
Oral Presentation- American Society for Virology annual meeting, Athens, GA. June 2023.

The inflammasome is activated by dengue non-structural protein 1 and plays a protective role during viral infection.
Poster Presentation- Bay Area Virology Symposium, San Francisco, CA. Dec 2022.

The inflammasome is activated by dengue non-structural protein 1 and plays a protective role during viral infection.
Poster Presentation- American Society for Tropical Medicine and Hygiene annual meeting, Seattle, WA. Nov 2022.

Investigating the role of inflammasome activation by dengue virus non-structural protein 1 during infection
Oral Presentation- American Society for Virology annual meeting, Madison, WI. July 2022.

Investigating the role of inflammasome activation by dengue virus non-structural protein 1 during infection
Oral and Poster Presentation- American Association of Immunologists annual meeting, Portland, OR, May 2022.

Investigating the role of inflammasome activation by dengue virus non-structural protein 1 during infection
Poster Presentation- Bay Area Microbial Pathogenesis Symposium, San Francisco, CA, March 2022.

Investigation of a pandemic, during a pandemic: Results from the UC Berkeley East Bay COVID-19 Study.
Oral Presentation- School of Public Health Brown Bag Talks, UC Berkeley, March 9th 2021.
Co-presented with Cameron Adams and Mary Horton (Barcellos Lab, UC Berkeley)

Characterization of a protective antibody against dengue virus non-structural protein 1 (NS1) reveals critical domains required for NS1-triggered pathogenesis.
Oral Presentation- Infectious Diseases & Immunity Seminar Series, UC Berkeley, October 5th 2020.

Characterization of a protective antibody against dengue virus non-structural protein 1 (NS1) reveals critical domains required for NS1-triggered pathogenesis.
Poster Presentation- American Association of Immunologists annual meeting, Honolulu HI, May 2020.
Conference cancelled due to COVID-19

Awards and Fellowships

Sydney Mac Donald Russell Fellow
Center for Emerging and Neglected Diseases, UC Berkeley
Awarded: 2022

Dean's Honor List
University of California, Irvine
Awarded: 2012-2015

Excellence in Research in Biological Sciences
School of Biological Sciences, University of California, Irvine
Awarded: 2015

Chapter 1

Introduction

Dengue as a threat to global public health

Dengue virus (DENV) is a mosquito-borne arbovirus in the *Flavivirus* genus and is the most prevalent mosquito-borne viral disease in humans globally. DENV represents a major burden on global public health, infecting an estimated 100 million people worldwide and causing annual losses of up to US $8.9 billion and 2,922,630 disability-adjusted life years (1–3). Over 3.8 billion people are at risk of infection with DENV, mostly those residing in low- and middle-income countries within the tropical and sub-tropical regions where the *Aedes* mosquito vector is endemic (4). Dengue incidence rates have increased rapidly, with cases increasing 10-fold over the past 20 years alone, likely due to globalization, urbanization, and climate change expanding the range of the mosquito vector. As climate change increases and urban populations grow, an estimated 6.1 billion people will be at risk for DENV infection by 2080 (5). Indeed, the National Institute of Allergy and Infectious Diseases has recently listed flaviviruses such as DENV and the closely related Zika virus (ZIKV), as priority pathogens due to "their ability to cause severe disease in humans, established pandemic potential, and general lack of countermeasures", underscoring the need to study and develop countermeasures against DENV (6).

Dengue: Clinical manifestations and management

A majority of the estimated 105 million people infected by DENV annually are asymptomatic; however, ~51 million develop classical dengue fever (DF) (1). DF presents as an acute febrile illness characterized by high fever, muscle, joint and bone pain, and rash (7). However, some patients progress to severe disease characterized by thrombocytopenia, hemorrhagic manifestations, and vascular leakage, potentially resulting in shock and organ failure (7). Severe dengue was initially described as dengue hemorrhagic fever (DHF)/ dengue shock syndrome (DSS), but a new classification scheme of disease severity was introduced by the World Health Organization in 2009 to facilitate clinical management, which classifies dengue as Dengue without Warning Signs, Dengue with Warning Signs, and Severe Dengue (8). Approximately 5% of DF cases progress to DHF/DSS; however, it is difficult to predict which patients will progress to severe disease (9). Clinical warning signs for severe dengue can arise less than one day before the onset of severe disease and late during the infection when patients are beginning to recover, challenging clinical management (10). No biomarkers or treatment options specific to severe dengue currently exist, due in part to an incomplete understanding of dengue pathogenesis (11). Ultimately, while severe dengue can be managed successfully in hospital settings with supportive care, more effective treatments and biomarkers for severe disease are sorely needed to direct care to patients with the most need and reduce patient burden in hospitals.

Dengue: Virion and genome structure

DENV exists as a serocomplex of 4 genetically similar but antigenically distinct serotypes, DENV1-4 (12). All DENV serotypes are positive-sense single-stranded RNA viruses whose ~10.7-kb genome encodes for three structural proteins (capsid, C; pre-membrane/membrane, prM/M; envelope, E) and seven non-structural proteins (NS1, NS2A, NS2B, NS3, NS4A, NS4B, NS5) (13,14). The virion is composed of 180 copies of the E and pr/M proteins arranged in icosahedral-like symmetry surrounding a nucleocapsid composed of the viral genome complexed to multiple copies of C (15–17). The non-structural proteins play critical roles in viral replication, viral pathogenesis, and innate immune evasion. The role of specific NS proteins during viral replication is described briefly below:

- NS1 is involved in both viral replication and viral pathogenesis and will be further discussed in detail (18).
- NS2A orchestrates nucleocapsid formation by recruiting viral RNA, structural proteins, and proteases to sites of virion assembly (19).
- NS2B is a cofactor essential for the function of NS3 as a viral protease; the NS2B-NS3 complex is responsible for the proteolytic processing of the translated flavivirus polyprotein (20,21).
- NS3 has additional functions as a helicase that unwinds dsRNA during viral RNA synthesis and as an 5' RNA triphosphatase, which is the first step required for RNA capping by NS5 (22–24)
- NS4A/4B support viral replication by remodeling host membranes to form the viral replication complex through interactions with NS1 and NS3 (25–29).
- NS5 is a RNA-dependent RNA polymerase and a methyltransferase essential for viral RNA replication and RNA capping (30–32).

DENV replication and the viral life cycle

DENV primarily infects myeloid cells including monocytes, macrophages, and dendritic cells (DCs) in humans and mice (33–37). While a DENV-specific entry receptor has yet to be identified, DENV can use interactions with cell surface-bound glycosaminoglycans (GAGs), C-type lectins (e.g., dendritic-cell-specific intracellular adhesion molecule-3-grabbing non-integrin [DC-SIGN]) and proteins of the T-cell immunoglobulin domain and mucin domain (TIM) and Tyro3, Axl and Mertk (TAM) family of phosphatidylserine receptors as attachment factors to enhance infection (38–41). After attachment, DENV is internalized into endosomes via clathrin-mediated endocytosis (42). Endosomal acidification induces conformational changes in the E protein, allowing membrane fusion and release of the viral nucleocapsid into the cytoplasm (15,16,43,44). The viral genome is then translated directly in the endoplasmic reticulum (ER) as a single polyprotein, which is then cleaved into individual proteins by both the NS2B-NS3 viral protease and host proteases (21,45,46). Cleaved viral proteins then induce dramatic remodeling of the ER to form viral replication organelles though recruitment of host proteins such as atlastins and reticulons, as well as through the actions of NS1 and NS4A/B (25,29,47–49). Within these replication organelles, replication of the viral genome by NS3 and NS5 and assembly of the immature viral particle occurs (47). The nascent viral particles are then transported through the Golgi apparatus, where pH changes and furin-mediated cleavage of prM leads to maturation of the virion (50,51). It should be noted that furin cleavage is inefficient, resulting in the release of partially mature virions that display different epitopes than that of mature virions, impacting neutralizing antibody responses to DENV (52). After processing in the Golgi apparatus, infectious virions are released from the cell to continue the infectious cycle. Targeting the interactions between NS proteins during the viral life cycle is a promising therapeutic strategy, as most recently demonstrated by the development of JNJ-A07, potent pan-serotype DENV anti-viral that blocks the interaction between NS3 and NS4B (53) .

Innate immune responses to DENV

Innate immune sensing and effector function

In mammals, the host innate immune response is crucial for the initial sensing and subsequent antiviral response to DENV. Infection of myeloid cells by DENV triggers the activation of several pathogen recognition receptors (PRRs) that recognize conserved pathogen or damage-associated molecular patterns (PAMPs/DAMPs) (54). Toll-like receptors (TLR), such as TLR3 and TLR7 recognize DENV viral dsRNA and ssRNA, respectively, within the endosomal compartment (55–58). Ligand binding triggers the dimerization of TLRs and results in the recruitment of adaptor molecules such as myeloid differentiation primary response gene 88 (MyD88) in the case of TLR7 and TIR domain-containing adaptor inducing IFN-β (TRIF) in the case of TLR3 (59). Subsequent signaling events result in the nuclear translocation of interferon (IFN) regulatory transcription factors 3 and 7 (IRF3 and IRF7) and NF-κB, which induce expression of type I IFNs (IFN-α and IFN-β) and pro-inflammatory cytokines including tumor necrosis factor-α (TNF-α) and interleukin-6 (IL-6) (59). Retinoic acid-inducible gene I (RIG-I) and melanoma-differentiation-associated gene 5 (MDA5) recognize DENV RNA in the cytoplasm; it has been recently suggested that RIG-I binds to the 5' regions of nascently generated uncapped DENV RNA (57,60–62). Sensing of viral RNA results in translocation of RIG-I/MDA5 to the mitochondrial membrane and activation of the mitochondrial antiviral signaling protein (MAVS), resulting in the activation of IRF3/7 and subsequent expression of type I IFNs (63). The cyclic GMP-AMP synthase (cGAS) sensor binds to mitochondrial DNA released into the cytosol as a result of DENV infection and produces cyclic diguanylate monophosphate (c-di-GMP) as a second messenger that binds to the stimulator of IFN genes (STING) protein, leading to activation of IRF3 and production of type I IFNs (64–67).

Type I IFNs are cytokines produced by the many signaling pathways activated by PRRs that sense DENV. Type I IFNs secreted by infected cells signal in an autocrine and paracrine fashion by binding to the type I IFN receptor (IFNAR) on infected or bystander cells and promote an antiviral state by inducing the production of antiviral IFN-stimulated genes (ISGs) (68). Binding of type I IFN to IFNAR triggers the phosphorylation and dimerization of signal transducer and activator of transcription proteins (STAT1/STAT2) by Janus kinases, leading to the formation and nuclear translocation of the STAT1/STAT2/IRF9 complex and inducing transcription of ISGs (69). Type I IFNs are a crucial component of the host response to DENV; cells pretreated with type I IFN *in vitro* are resistant to infection, and mice lacking the type I IFN receptor (*Ifnar1*$^{-/-}$) are more susceptible to disease compared to wild-type mice (70–72). ISGs induced by type I IFN antagonize multiple steps of the viral lifecycle, including viral entry and/or fusion (IFITM3 and CH25H), translation (IFIT1/2, PKR and C19orf66) and replication (RNASEL and RSAD2) (73,74). However, many of the anti-DENV ISGs and the mechanisms by which they restrict DENV infection remain to be determined.

The complement system is comprised of a set of soluble proteins that, upon activation, induce inflammation and opsonize pathogens, resulting in their removal by phagocytic cells or lysis of the infected cell/virion (75) Complement can be activated by antibodies that specifically recognize infected cells/virions or mannose-binding lectin (MBL), which recognizes specific carbohydrates present on the DENV E glycoprotein (76). Binding of antibodies or MBL to the surface of infected cells or virions leads to activation of C4bC2a, a serine protease that can cleave soluble C3 into C3a and C3b. C3a is a soluble effector that helps to induce vasodilation, vascular permeability,

and activate innate immune cells, whereas C3b binds to and opsonizes infected cells or virions. Complement receptors on the surface of macrophages and neutrophils promote phagocytosis of C3b-opsonized particles. C3b can also induce the formation of the membrane attack complex (MAC), composed of complement components C5b-C9, which disrupts the membranes of the opsonized cell/virion (75). MBL binding and antibody-mediated complement deposition have both been linked to protective responses against DENV (77–79).

DENV innate immune evasion

DENV employs multiple strategies to evade sensing by the innate immune system and antagonize innate immune effectors such as type I IFN. The formation of the viral replication complex in the ER shields nascent viral RNA from detection by the endosomal TLRs and cytoplasmic sensors RIG-I/MDA5. DENV also employs many of its NS proteins to inhibit the RIG-I/MAVS pathway at multiple levels. NS5-mediated 5' capping of the viral RNA prevents viral RNA from being sensed by RIG-I (80,81). Additionally, DENV NS3 binds to the mitochondrial-targeting chaperone protein 14-3-3ε, inhibiting RIG-I by preventing its translocation to the mitochondria (82). DENV NS4A inhibits the RIG-I/MAVS pathway by binding to MAVS and preventing its interaction with RIG-I (83). DENV blocks the cGAS-STING pathway by targeting cGAS for autophagy-lysosome-dependent degradation via NS2B and by cleaving both cGAS and STING using the N2B/NS3 protease, thereby inhibiting the production of type I IFN in response to DENV infection (65,84,85). In addition to evading innate immune sensing, DENV can also avoid type I IFN responses by blocking type I IFN signaling. The NS2A, NS4A, and NS4B complex blocks STAT1 signaling, and NS5 inhibits STAT2 by binding to the host ubiquitin protein ligase E3 and targeting STAT2 for proteasomal degradation (86–88). The ability of DENV NS proteins to inhibit the type I IFN response reflects DENV's adaptation to humans as a host species. Mice, for example, are not natural hosts of DENV and cannot be infected unless type I IFN responses are inhibited genetically or pharmacologically (89). Accordingly, DENV NS2B/3 can cleave human but not murine STING proteins, and DENV NS5 can only cleave human but not murine STAT2 (90,91). DENV's inability to antagonize the type I IFN response in mice in part explains why modeling DENV in animal models has been difficult. DENV NS1 plays a key role in inhibiting multiple steps of the complement pathway. DENV NS1 can bind to C4, recruiting C1 proteases to cleave C4 into C4b prematurely, reducing both the deposition of C4b on the surface of cells and C3 convertase activity. DENV NS1 can also bind to C4b binding protein, which leads to inactivation of C4b, bind to MBL, and prevent formation of the MAC, which together protect DENV from complement-mediated neutralization and protect DENV-infected cells from lysis (92–95).

Dengue immunology: Adaptive responses

The adaptative immune response to DENV is crucial for controlling and preventing infection, while also being associated with enhancement of viral infection and disease, complicating efforts to develop safe and efficacious DENV vaccines (96).

Protective humoral and B-cell responses to DENV

After a primary infection with DENV, individuals generate DENV-specific immunoglobulin M (IgM) that peaks early after infection, followed by a longer-lasting IgG response containing a mix of serotype-specific and cross-reactive antibodies that bind to serotypes other than the infecting

serotype. Most people are protected from reinfection by the primary infecting serotype, though secondary homotypic infections can occur (97). Serotype-specific monoclonal antibodies, such as 2D22 and 5J7, mediate homotypic protection by targeting quaternary epitopes across E homodimers as well as EDIII (98–103). In addition to neutralization, anti-DENV antibodies can also mediate protection against symptomatic infection through antibody-dependent effector functions such as antibody-mediated complement deposition (79). Recent work has shown that antibody responses after a primary DENV infection stabilize at ~8 months post-infection and have a half-life longer than a human life (104). Primary DENV infections also generate a cross-reactive antibody response to other serotypes, but this tends to be low avidity and weakly neutralizing (105,106). After a secondary infection with a heterologous serotype, high-avidity, highly neutralizing cross-reactive and type-specific neutralizing antibodies are generated (107–110). Anti-DENV neutralizing antibody titers after a secondary infection peak shortly after infection and display waning, with a rapid decline out to 8 months followed by gradual waning thereafter (104). Trends seen in the anti-DENV antibody response are reflected by the memory B-cell response to DENV. The initial memory B-cell (MBC) pool generated after a DENV infection is dominated by highly cross-reactive MBCs (111). Upon heterologous infection, these MBCs differentiate into a large pool of plasmablasts, the primary source of antibodies during the acute phase of secondary infection, which expand rapidly upon reinfection and contract quickly once the infection resolves (112–114).

T cell responses to DENV

Studies have established important roles for both $CD4^+$ and $CD8^+$ T cells in protective T cell responses to DENV (115,116). CD4 T-cells support the anti-viral response by boosting antibody responses through providing help to B-cells, sustaining $CD8^+$ T-cell responses (which enable viral clearance by lysing DENV-infected cells), and producing antiviral cytokines (117). Both CD4 and CD8 T-cells have been associated with protection, though studies in mice have suggested that CD8 T-cells may play a greater role (118–122). Additionally, cross-reactive CD8 T-cells in mice have been shown to contribute to protection against heterologous DENV infection (123–126). Low affinity, cross-reactive T cells have also been hypothesized to contribute to the pathogenesis of severe dengue; aberrant activation of these cells can lead to a dysfunctional cytokine response or increased programmed cell death, impeding T cell-mediated viral control, resulting in increased viral loads (127,128).

Antibody-dependent enhancement

Primary DENV infection also induces weakly neutralizing cross-reactive anti-DENV antibodies, which can mediate antibody-dependent enhancement (ADE) (129,130). ADE is a phenomenon wherein cross-reactive non-neutralizing or poorly neutralizing antibodies, mostly targeting the prM and the fusion loop on E as well as other epitopes, can promote entry of DENV into Fcγ receptor-expressing cells, activating the cells, increasing viremia, and initiating an immune cascade that can lead to increased vascular leakage and severe disease (131–133). ADE has been documented extensively *in vitro*, as well as in mouse models, and recent work in human populations has found strong evidence that severe dengue disease is highest within a narrow range of preexisting anti-DENV antibody titers (72,131,134–136). The currently licensed vaccine against DENV, Dengvaxia, is restricted to those who have had a previous laboratory-confirmed DENV infection due to the increased risk of disease in DENV-naïve individuals, limiting the effectiveness of the vaccine (137,138). The risk that incomplete vaccine immunity against all four

serotypes might paradoxically enhance pathogenesis in the setting of subsequent natural infection due to ADE remains a barrier for the development of safe, efficacious DENV vaccines.

Dengue NS1

DENV NS1 plays central roles in viral replication and pathogenesis (18). NS1 is a ~48-kDa glycoprotein, which is highly conserved across the flaviviruses genus, is secreted from infected cells at high levels. This makes NS1 a useful clinical biomarker for the diagnosis of DENV, as NS1 antigenemia in DENV-infected individuals correlates with both viraemia and disease severity (7,139,140). Beyond its clinical utility, NS1 is also a promising potential vaccine candidate, as vaccination of mice with adjuvanted NS1 alone is sufficient to protect against lethal DENV infection without the risk of generating ADE antibodies (141,142). Thus, understanding the role NS1 plays during DENV infection is essential for designing NS1-targeted vaccines and therapeutics.

NS1 structure

DENV NS1 is 352 amino acids (aa) in length, with a molecular mass between 40–50 kDa depending on its glycosylation states at asparagine (N) residues 130 and 207. NS1 has 3 contains three highly conserved domains – the β-roll (residues 1–29), wing (38–151), and β-ladder (181–352) domains (143). After translation, NS1 is cleaved from the DENV polyprotein by host proteases and quickly dimerizes, associating with host cell membranes, likely though interactions with many hydrophobic residues within the β-roll and wing domains (143–145). In the dimer form, the β-ladder domain makes up the central dimer structure with extensive β-sheets on the external-facing side termed "spaghetti loop" (143). The wing domain of each monomer extends out of the central structure in both directions; it encompasses a flexible loop at residues 108-129, which has not been successfully resolved in structures except for ZIKV NS1 (143,146). The β-roll is positioned at the membrane-facing side accompanied by the two connecting regions and the wing flexible loop, together forming the hydrophobic inner surface of the flavivirus NS1 dimer, which interacts with host membranes (143). Secreted NS1 consists of oligomers made of NS1 dimers, usually tetramers or hexamers, arranged in a barrel shape, with NS1 dimers surrounding a central lipid cargo reminiscent of a lipoprotein (147–149). The β-roll domains face the interior of the hexamer towards the lipid cargo, while the outer surface contains the spaghetti loops, disordered wing-domain loop, and C-terminal tip of the β-ladder (143). Recent developments in the field have begun to elucidate the function(s) of each domain as they pertain to NS1-mediated viral replication and pathogenesis and will be further detailed; however, many questions remain about the molecular details by which NS1 mediates its many functions.

NS1 secretion

The mechanism underlying NS1 secretion is also an open area of research. Studies have shown that endoplasmic reticulum-resident chaperones such as human glucose-regulated protein 78 (GRp78), calnexin, and calreticulin are required for proper folding of NS1, and antagonism of these proteins can impair the secretion of NS1 without any effect on viral replication (150,151). Another important post-translational modification linked to NS1 secretion is glycosylation of the two N-glycosylation sites at N130 and N207 (152). The N-linked glycan at position 130 has been found to be required for stabilization of the secreted form of NS1, whereas the N-linked glycan at residue 207 is required for the internalization of secreted NS1 into endothelial cells

(75,153). While it is clear that proper folding and post-translational modification is needed for optimal NS1 secretion, the process by which NS1 becomes secreted is less understood. Several amino acids (D136, W311, P319, E334 and R336), mostly residing at the C-terminal region of the β-ladder domain, have been identified as being essential for NS1 secretion, as mutating these amino acids inhibits NS1 secretion without affecting intracellular NS1 levels, arguing that impaired secretion is not due to improper folding of the mutated NS1 (29). Further mutagenesis studies have identified other amino acids within the C-terminus of the β-ladder and the wing domain that mediate NS1 secretion (154). Interrogating how these amino acids contribute to the translocation of NS1 from the ER into the extracellular milieu would advance our understanding the process of NS1 secretion.

Dengue NS1: Viral replication

Intracellular NS1 is largely localized within the ER, where it plays vital roles in coordinating viral replication and assembly of infectious DENV virions (155,156). Structure-guided mutagenesis studies have helped to highlight several key molecular determinants of NS1-dependent viral replication and infectious particle production (29,156). Residues within the *β-roll* (C4, W8), wing (Y32, C55, R62, D136, W150), and *β-ladder* domains (K189, D197, S252, C291, W331, C132, T317, P319, P320, E334, E336) that cluster on hydrophobic protrusions within the NS1 dimer structure were identified to be essential for viral RNA replication (156). Additionally, other mutations (S114A, W115A, D180A, T301A) were found to affect virus production independently of RNA replication (156). Interestingly, secretion of NS1 is dispensable for infectious DENV particle production, suggesting that NS1's ability to facilitate viral replication is independent of its secretory functions (156).

NS1 appears to have 2 distinct role in facilitating viral replication: assembly of the membranous replication organelle and RNA replication (29). Within the replication organelle, NS1 has been shown to interact with NS4A-2K-NS4B cleavage intermediates at amino acids G161 and W168 to facilitate DENV RNA replication, but this interaction is independent of NS1's ability to remodel membranes (26,29). The formation of DENV replication organelles has also been shown to be dependent on the interaction between NS1 and the host protein Receptor for Activated Protein C Kinase 1 (RACK1) (157,158). Despite these recent studies shedding more light on the various roles that NS1 plays intracellularly to support viral replication, the mechanistic basis by which NS1 engages host membranes, host proteins, and viral proteins to coordinate this step in the viral life cycle has yet to be determined.

Dengue NS1: Endothelial cell interactions

Extracellular NS1 can contribute to DENV pathogenesis through interactions with endothelial cells. Endothelial cells line the vascular system and play vital roles in maintaining vascular tone, nutrient exchange, and controlling vascular permeability (159). Two determinants of endothelial barrier function are cell-cell junctional complexes and the endothelial glycocalyx layer (EGL). Intercellular junctional complexes, composed of tight (TJ) and adherens (AJ) junction proteins, form the physical contact sites between adjacent cells and are involved in cell-cell adhesion, intercellular communication, and barrier function (160,161) TJ/AJ complexes are maintained and regulated by proteins such as occludin, claudin, and cadherin, which connect neighboring endothelial cells and physically regulate fluid passage into the underlying tissues (161,162).

These junctional proteins are dynamically regulated in response to stimuli like immune activation or angiogenesis (162,163). The EGL is a network of glycoproteins and proteoglycans that cover the luminal surface of endothelial cells and protect the endothelial cells from the shear force generated by the flow of blood (164,165). Elevated levels of major components of the EGL, such as sialic acid, heparan sulfate, chondroitin sulfate, and hyaluronic acid, have been found in dengue patients and in mouse models of DENV infection, and elevated levels of these components have been correlated with severe disease (166–171). Recent work in the field has found that DENV NS1 interacts with endothelial cells directly, disrupting endothelial barrier function and leading to endothelial hyperpermeability and vascular leak (18,172,173).

In order for NS1 to induce endothelial dysfunction, it must first bind to and be internalized into cells. Extracellular NS1 first attaches to glycosaminoglycans (GAGs) such as heparan sulfate and chondroitin sulfate found on the surface of endothelial cells (174). Compounds mimicking GAGs have been shown to inhibit DENV NS1-induced endothelial dysfunction, in part by preventing NS1 binding to cells (175,176). Modelling studies have suggested that GAGs and GAG mimetics associate with NS1 using charge-charge interactions on a stretch of positively charged amino acids within the β-ladder (175,177). Recent work from the Harris laboratory has also identified that the wing domain contributes to the binding of DENV NS1 to endothelial cells. Mutation of a flavivirus-conserved W115 W118 G119 motif (W115A W118A G119A; DENV NS1-WWG) or a DENV-specific motif at amino acids 91-93 (GDI->EKQ) inhibits DENV NS1's ability to bind to human pulmonary microvascular endothelial cells (HPMEC) (178,179).

In addition to GAG binding, it is thought that DENV NS1 must also interact with a proteinaceous receptor and be internalized. The identity of the proteinaceous receptor is a major question within the field. One study has proposed the scavenger receptor, class B type 1 (SRB1), as a possible NS1 receptor (180). Recent work in the Harris laboratory has identified the beta-2 adrenergic receptor (β2AR), as well as a receptor tyrosine kinase, epidermal growth factor receptor (EGFR), as putative NS1 receptors (S. Biering and E. Harris, unpublished). Ongoing studies in the laboratory are elucidating the exact roles that these receptors play in NS1-induced endothelial dysfunction. Once DENV NS1 interacts with its putative receptor, it must be internalized via clathrin-mediated endocytosis to trigger endothelial dysfunction (153). Endocytosis is dependent on glycosylation at N207, as a mutation at that site (DENV NS1 N207Q) blocks NS1-induced endothelial dysfunction without affecting the ability of DENV NS1 207Q to bind to endothelial cells (153).

Once internalized, DENV NS1 induces changes within endothelial cells resulting in EGL degradation and TJ/AJ mislocalization (172,181). The exact pathways activated by DENV NS1 and how NS1 induces these changes is a current area of study. What is known is that DENV NS1 induces the activation of several proteases, including cathepsin-L, heparanases, sialidases, and matrix metalloprotease 9 (MMP9), activation of the p38-mitogen activated protein kinase (MAPK) pathway, loss of the AJ protein VE-cadherin, and induction of secretion of macrophage inhibitory factor (MIF) (172,181–185). Ongoing work in the Harris laboratory has begun to define the hierarchy of these pathways and their relative contribution to NS1-endothelial dysfunction. Preliminary data suggest that several NS1-induced phenotypes such as EGL disruption and TJ/AJ mislocalization are distinct, separable outcomes branching from central signaling pathways (Tjang, Biering and Harris, unpublished data). Full elucidation of these

pathways, including how specific NS1 domains contribute to NS1-induced endothelial dysfunction, are crucial next steps in understanding NS1 biology.

Dengue NS1: Immune cell activation

In addition to interacting with endothelial cells, DENV NS1 has also been shown to interact with immune cells, including macrophages, dendritic cells, and platelets (186–188). Treatment of murine and human macrophages with DENV NS1 results is the production of pro-inflammatory cytokines such as TNF-α and IL-6 (186,189–191). DENV NS1 can also induce the secretion of IL-10 and other inflammatory mediators such as phospholipase A2 (PLA2), platelet activating factor, and leukotrienes in human monocytes (192,193). Studies in mice have proposed that DENV NS1 can activate TLR4, as antagonism of TLR4 by the TLR4 antagonist LPS-RS or anti-TLR4 antibodies in NS1-treated immune cells reduces pro-inflammatory cytokine production (186,189). In platelets, DENV NS1 can bind TLR4 to trigger platelet activation and aggregation (188,194,195). The impact of NS1-induced TLR4 activation in DENV pathogenesis is less clear. Studies have shown that DENV-induced thrombocytopenia and hemorrhage were attenuated in TLR4-deficient mice, and treatment of DENV-infected mice with LPS-RS reduced leak during infection (186,188). However, other studies using TLR4-deficient mice showed little-to-no impact of TLR4 deficiency on DENV NS1-induced vascular leak (173). Indeed, while it has been proposed that DENV NS1-induced endothelial dysfunction is a consequence of pro-inflammatory cytokine activation, Glasner and colleagues have experimentally shown that DENV NS1-induced endothelial dysfunction is intrinsic to endothelial cells and does not rely on TLR4 *in vitro* and *in vivo* (173). While it is evident that DENV NS1 can activate immune cells, much less is known about the mechanisms by which NS1 induces inflammation and how NS1-induced inflammation contributes to overall viral pathogenesis or protection.

Several recent studies have begun to investigate the role of secreted NS1's lipid cargo in the context of DENV NS1-induced inflammation. The composition of the lipid cargo within secreted NS1 is mostly triglycerides, bound at an equimolar ratio to the NS1 protomer, cholesteryl esters, and phospholipids (148). One study found that NS1 can associate with human high-density lipoproteins (HDL), and this complex was able to trigger the production of pro-inflammatory cytokines in human primary macrophages (191). Another study found that a T164S mutation in NS1 resulted in an increase in pro-inflammatory cytokine production and that this mutation was predicted to modulate the lipid classes with which NS1 associates (190). Lastly, one recent study found that human ApoA1, which is the major protein component of HDL, or the ApoA1 peptide mimetic 4F are able to block NS1-induced pro-inflammatory cytokine production (196). Taken together, the lipids associated with secreted NS1 seems to modulate NS1's inflammatory capacity. However, what this means for DENV pathogenesis writ large remains unknown.

Dengue NS1: Impact on dengue pathogenesis

While DENV NS1 has clear interactions with endothelial cells and immune cells *in vitro*, the contribution of these interactions to DENV pathogenesis writ large is still under investigation. DENV NS1 can enhance the lethality of DENV when co-administered with a sublethal dose of DENV in mice (142). When given alone, DENV NS1 can induce vascular leak in organs when given systemically or in the skin when administered intradermally (142,173,197) Intradermal leak is thought to be largely independent of DENV NS1-induced inflammation, as DENV NS1

can still induce leak in TLR4- or TNF-α-deficient mice, but dependent on NS1-induced endothelial dysfunction, as inhibitors of the EGL-degradation pathway inhibit NS1-induced vascular leak (173). In addition, Lo and colleagues found that the DENV NS1 wing domain and amino acids 91 to 93 (GDI), which are deficient in binding to human pulmonary microvascular endothelial cells (HPMECs), are required to trigger localized vascular leak, providing more evidence that NS1-induced vascular leak is dependent on the interactions between NS1 and endothelial cells (179). Mice doubly deficient in TLR4 and IFNAR (*Tlr4*$^{-/-}$ *x Ifnar*$^{-/-}$ mice) have similar levels of morbidity and mortality compared to IFNAR-deficient mice (*Ifnar*$^{-/-}$) when infected with DENV, arguing that the NS1-TLR4 pathway may not be involved in enhancing DENV pathogenesis in this mouse model (173). While it has been extensively hypothesized that DENV NS1-induced immune activation leads to a cytokine storm-like immunopathology, few studies have experimentally assessed whether NS1-induced inflammation contributes to overall viral pathogenesis or not.

Dengue NS1: Vaccination and antibodies

Immunization of mice with DENV1-4 NS1 is sufficient to protect them against lethal DENV2 challenge, arguing that immune responses to DENV are important for the prevention of severe dengue disease (142). Protective immunity to NS1 in this context is most likely mediated by antibodies, as transfer of NS1-immune polyclonal mouse serum or administration of anti-NS1 monoclonal antibodies were sufficient to confer protection (142,178,198). These anti-NS1 antibodies have been shown to prevent binding of NS1 to endothelial cells and inhibit NS1-induced endothelial hyperpermeability (142,178,198). In humans, people infected with DENV or vaccinated with a live-attenuated tetravalent dengue vaccine candidate (TAK-003) generate antibody responses to NS1, and sera from TAK-003 vaccinees were shown to block NS1-induced endothelial hyperpermeability and EGL degradation (199–201). A majority of anti-NS1-antibodies generated after natural infection in humans or after NS1 vaccination in mice target the wing (amino acids 101-130) and β-ladder domains (amino acids 296-330) (202,203). Despite clear evidence of the protective capacity of anti-NS1-antibodies, comparatively little is known about the mechanism by which protective anti-NS1 antibodies inhibit NS1-induced endothelial dysfunction. In addition, while it is clear that most people generate anti-NS1-antibodies after DENV infection, why these antibodies do not protect those experiencing severe dengue disease is unknown.

Despite evidence suggesting that immunity against DENV NS1 can be protective against DENV, some worries remain about NS1's use as a vaccine candidate. Murine anti-NS1 antibodies have been shown to cross-react with components of the human clotting cascade such as human platelets, thrombin, plasminogen, and data from mouse models suggested that cross-reactive antibodies to NS1 may contribute to pathogenesis (204–209) Host cross-reactive NS1 epitopes have been mapped to the C-terminus of NS1 (aa 300-352), and deleting this region of NS1 reduced the production of host cross-reactive antibodies (210). Though the role for NS1-derived autoantibodies has been implicated in DENV infection and NS1 immunization models, it has been difficult to demonstrate a direct role for these antibodies in human dengue disease. Several protective anti-NS1 monoclonal antibodies have not demonstrated any cross-reactivity to clotting cascade proteins, suggesting that it is possible to antagonize NS1 through antibodies without inducing potentially harmful, cross-reactive responses (178,198). Other questions remain about the universality of a protective anti-NS1 response. NS1-immunized mice are not protected from a non-mouse adapted, hyper-virulent DENV strain known as D2Y98P (211). The

virulence in this strain is thought to be through induction of key proinflammatory cytokines driven by the prM-E structural region (211). Thus, consideration of DENV NS1 as a vaccine candidate will require a deeper understanding of the various roles NS1 plays in mediating DENV pathogenesis and elucidating the protective determinants of anti-NS1-immunity.

The inflammasome pathway

One particular focus of this dissertation is that of inflammasomes, a class of innate immune sensors that surveil the cytosol for a broad range of pathogen or damage-associated molecular patterns (PAMPs/DAMPs) (207). Many viruses have been shown to activate inflammasomes during infection, including influenza A virus, HIV, SARS-CoV-2, picornaviruses, and DENV (208–212). Inflammasome activation by viruses can be protective and/or can contribute to pathogenic outcomes (210,212–215).

Mechanisms of inflammasome activation

Canonical inflammasomes recruit the cysteine protease caspase-1 via the apoptosis-associated speck-like protein containing CARD (ASC) protein (216). Certain inflammasomes respond to PAMPs such as viral double-stranded DNA in the case of the AIM2 inflammasome, or can be triggered by pathogenic effectors; examples include sensing of viral protease activity by the NLRP1B and CARD8 inflammasomes, sensing of ion fluxes and membrane damage by the NLRP3 inflammasome, or sensing of toxin-induced Rho guanosine triphosphatase (Rho GTPase) inactivation by the pyrin inflammasome (207,209,217–219). Further, caspase-11 in mice and caspases-4 and -5 in humans can activate the non-canonical inflammasome, in which caspase-11/4/5 binding to lipid A from bacterial lipopolysaccharide (LPS) leads to activation of the NLRP3 inflammasome (220,221). Inflammasome signaling typically comprises a two-step process in which inflammasome components and substrates are first transcriptionally upregulated and/or 'primed', usually in response to PAMPs/DAMPs and nuclear factor-κB (NF-κB) signaling (207). After priming, a second stimulus induces inflammasome oligomerization, leading to ASC recruitment and caspase-1 autoproteolytic processing into its active form (216). The active caspase-1 protease can then cleave pro-IL-1β, pro-IL-18 and gasdermin D (GSDMD) into their bioactive forms. Cleavage of GSDMD leads to insertion and oligomerization of the N-terminal domain (GSDMD-NT) to form pores in the plasma membrane (222). The formation of GSDMD pores canonically leads to pyroptosis, a form of inflammatory cell death; however, recent work has shown that GSDMD pore formation and pyroptosis are distinct events and that macrophages can release IL-1β from GSDMD pores without undergoing pyroptosis in response to certain stimuli (223–227). GSDMD pores also facilitate the release of cleaved IL-1β and IL-18, which then serve as major mediators of inflammation contributing to host defense as well as driving immunopathology (223,228).

Dengue and inflammasomes

Several studies have begun to investigate whether DENV infection triggers inflammasome activation and how this might impact DENV pathogenesis. Studies have shown that *in vitro* DENV infection of mouse and human macrophages, human skin endothelial cells, and platelets, as well as infection in mice can induce inflammasome activation (190,229–233). Clinically, IL-1β levels are also elevated in dengue patients, implicating a role for inflammasome activation in human DENV infections (232,234). Mechanistic studies have implicated both the membrane (M) and

NS2A/B proteins of DENV as viral triggers of the NLRP3 inflammasome (229,231). *In vivo* studies using an adeno-associated virus (AAV) vector to induce DENV M expression suggested that DENV M can cause NLRP3-dependent vascular leak, though the relevance of M-induced inflammasome activation in DENV infection is unknown (229). Another study showed that mice treated with an IL-1 receptor antagonist during DENV infection lost less weight and experienced less vascular leak compared to untreated control (232). Although it is established that DENV infection can induce inflammasome activation, the viral triggers and the contribution of inflammasome activation during infection remain open areas of investigation.

Summary and overview of dissertation

Recent work in the past decade has pushed DENV NS1 into the spotlight due to the central roles is plays in viral replication and pathogenesis. While NS1's role in driving endothelial dysfunction, vascular leak and immune activation is now well appreciated, many questions remain about the specific mechanisms by which NS1 mediates it's many functions. Despite structural and molecular advances in understanding how NS1 binds to cells, is internalized, and is blocked by anti-NS1-antibodies, many questions remain about how exactly NS1 induces endothelial dysfunction. In addition, the contribution of innate immune activation, both by DENV and by DENV NS1, to dengue pathogenesis has not been well established experimentally.

This dissertation aims to fill these gaps in our understanding. In chapter 2, I detail our findings implicating the inflammasome pathway as a protective innate immune response to DENV and identify a new role for DENV NS1 as a trigger of this pathway. In chapter 3, I detail our structure-guided interrogation of the mechanism behind a protective anti-NS1-monoclonalb antibody, 2B7, and identify molecular determinants of NS1 secretion and NS1-induced endothelial hyperpermeability. These studies combined detail new mechanistic insight into how immunity to NS1 can be protective during DENV infection and generate new tools for the study of innate immunity to DENV, the study of NS1: endothelial interactions, and the antibody response to NS1 in humans.

Severe acute respiratory syndrome coronavirus-2 (SARS-CoV-2) emerged in late 2019 during the course of study of my dissertation and went on to grow to the largest pandemic in the last century causing at least 770 million confirmed infections and 7 million deaths as of late November 2023. This pandemic severely upended societal function as social distancing restrictions aimed at controlling viral spread kept people in their homes and away from each other. Virologists and immunologists globally turned their research focus to the newly emerged virus in order to quickly understand the biology of SARS-CoV-2 to design countermeasures such as therapeutics and vaccines. In chapter 4 of this dissertation, I detail how I leveraged the skills acquired during over the course of study for my PhD to designing serological tools for measuring antibody responses to SARS-CoV-2 and how I used these tools in studies aimed at understanding asymptomatic spread and infection burden in migrant farmworkers.

References

1. Cattarino L, Rodriguez-Barraquer I, Imai N, Cummings DAT, Ferguson NM. Mapping global variation in dengue transmission intensity. Sci Transl Med [Internet]. 2020 Jan 29 [cited 2020 May 29];12(528).

2. Shepard DS, Undurraga EA, Halasa YA, Stanaway JD. The global economic burden of dengue: a systematic analysis. Lancet Infect Dis. 2016 Aug 1;16(8):935–41.

3. Zeng Z, Zhan J, Chen L, Chen H, Cheng S. Global, regional, and national dengue burden from 1990 to 2017: A systematic analysis based on the global burden of disease study 2017. eClinicalMedicine [Internet]. 2021 Feb 1 [cited 2023 Nov 20];32.

4. Bhatt S, Gething PW, Brady OJ, Messina JP, Farlow AW, Moyes CL, et al. The global distribution and burden of dengue. Nature. 2013 Apr;496(7446):504–7.

5. Messina JP, Brady OJ, Golding N, Kraemer MUG, Wint GRW, Ray SE, et al. The current and future global distribution and population at risk of dengue. Nat Microbiol. 2019;4(9):1508–15.

6. Kuhn RJ, Barrett ADT, Desilva AM, Harris E, Kramer LD, Montgomery RR, et al. A Prototype-Pathogen Approach for the Development of Flavivirus Countermeasures. J Infect Dis. 2023 Oct 15;228(Supplement_6):S398–413.

7. Muller DA, Depelsenaire ACI, Young PR. Clinical and Laboratory Diagnosis of Dengue Virus Infection. J Infect Dis. 2017 Mar 1;215(suppl_2):S89–95.

8. World Health Organization. Dengue guidelines for diagnosis, treatment, prevention and control : new edition [Internet]. World Health Organization; 2009 [cited 2023 May 30]. Report No.: WHO/HTM/NTD/DEN/2009.1. Available from: https://apps.who.int/iris/handle/10665/44188

9. Rathore AP, Farouk FS, St. John AL. Risk factors and biomarkers of severe dengue. Curr Opin Virol. 2020 Aug 1;43:1–8.

10. Leo YS, Gan VC, Ng EL, Hao Y, Ng LC, Pok KY, et al. Utility of warning signs in guiding admission and predicting severe disease in adult dengue. BMC Infect Dis. 2013 Oct 24;13(1):498.

11. Wong JM, Adams LE, Durbin AP, Muñoz-Jordán JL, Poehling KA, Sánchez-González LM, et al. Dengue: A Growing Problem With New Interventions. Pediatrics. 2022 May 11;149(6):e2021055522.

12. Guzman MG, Harris E. Dengue. Lancet Lond Engl. 2015 Jan 31;385(9966):453–65.

13. Chambers TJ, Hahn CS, Galler R, Rice CM. Flavivirus genome organization, expression, and replication. Annu Rev Microbiol. 1990;44:649–88.

14. Barrows NJ, Campos RK, Liao KC, Prasanth KR, Soto-Acosta R, Yeh SC, et al. Biochemistry and Molecular Biology of Flaviviruses. Chem Rev. 2018 Apr 4;118(8):4448.

15. Kuhn RJ, Zhang W, Rossmann MG, Pletnev SV, Corver J, Lenches E, et al. Structure of Dengue Virus: Implications for Flavivirus Organization, Maturation, and Fusion. Cell. 2002 Mar 8;108(5):717–25.

16. Zhang X, Ge P, Yu X, Brannan JM, Bi G, Zhang Q, et al. CryoEM structure of the mature dengue virus at 3.5-Å resolution. Nat Struct Mol Biol. 2013 Jan;20(1):105–10.

17. Byk LA, Gamarnik AV. Properties and Functions of the Dengue Virus Capsid Protein. Annu Rev Virol. 2016 Sep 29;3(1):263–81.

18. Glasner DR, Puerta-Guardo H, Beatty PR, Harris E. The Good, the Bad, and the Shocking: The Multiple Roles of Dengue Virus Nonstructural Protein 1 in Protection and Pathogenesis. Annu Rev Virol. 2018 Sep 29;5(1):227–53.

19. Xie X, Zou J, Zhang X, Zhou Y, Routh AL, Kang C, et al. Dengue NS2A Protein Orchestrates Virus Assembly. Cell Host Microbe. 2019 Nov 13;26(5):606-622.e8.

20. Falgout B, Pethel M, Zhang YM, Lai CJ. Both nonstructural proteins NS2B and NS3 are required for the proteolytic processing of dengue virus nonstructural proteins. J Virol. 1991 May;65(5):2467–75.

21. Yusof R, Clum S, Wetzel M, Murthy HM, Padmanabhan R. Purified NS2B/NS3 serine protease of dengue virus type 2 exhibits cofactor NS2B dependence for cleavage of substrates with dibasic amino acids in vitro. J Biol Chem. 2000 Apr 7;275(14):9963–9.

22. Wengler G, Wengler G. The NS 3 Nonstructural Protein of Flaviviruses Contains an RNA Triphosphatase Activity. Virology. 1993 Nov 1;197(1):265–73.

23. Matusan AE, Pryor MJ, Davidson AD, Wright PJ. Mutagenesis of the Dengue Virus Type 2 NS3 Protein within and outside Helicase Motifs: Effects on Enzyme Activity and Virus Replication. J Virol. 2001 Oct;75(20):9633–43.

24. Bartelma G, Padmanabhan R. Expression, Purification, and Characterization of the RNA 5′-Triphosphatase Activity of Dengue Virus Type 2 Nonstructural Protein 3. Virology. 2002 Jul 20;299(1):122–32.

25. Miller S, Kastner S, Krijnse-Locker J, Bühler S, Bartenschlager R. The Non-structural Protein 4A of Dengue Virus Is an Integral Membrane Protein Inducing Membrane Alterations in a 2K-regulated Manner *. J Biol Chem. 2007 Mar 23;282(12):8873–82.

26. Lindenbach BD, Rice CM. Genetic interaction of flavivirus nonstructural proteins NS1 and NS4A as a determinant of replicase function. J Virol. 1999 Jun;73(6):4611–21.

27. Umareddy I, Chao A, Sampath A, Gu F, Vasudevan SG. Dengue virus NS4B interacts with NS3 and dissociates it from single-stranded RNA. J Gen Virol. 2006 Sep;87(Pt 9):2605–14.

28. Miller S, Sparacio S, Bartenschlager R. Subcellular Localization and Membrane Topology of the Dengue Virus Type 2 Non-structural Protein 4B *. J Biol Chem. 2006 Mar 31;281(13):8854–63.

29. Płaszczyca A, Scaturro P, Neufeldt CJ, Cortese M, Cerikan B, Ferla S, et al. A novel interaction between dengue virus nonstructural protein 1 and the NS4A-2K-4B precursor is required for viral RNA replication but not for formation of the membranous replication organelle. PLoS Pathog. 2019 May 9;15(5):e1007736.

30. Tan BH, Fu J, Sugrue RJ, Yap EH, Chan YC, Tan YH. Recombinant Dengue Type 1 Virus NS5 Protein Expressed inEscherichia coliExhibits RNA-Dependent RNA Polymerase Activity. Virology. 1996 Feb 15;216(2):317–25.

31. Ray D, Shah A, Tilgner M, Guo Y, Zhao Y, Dong H, et al. West Nile virus 5'-cap structure is formed by sequential guanine N-7 and ribose 2'-O methylations by nonstructural protein 5. J Virol. 2006 Sep;80(17):8362–70.

32. Zhao Y, Soh TS, Lim SP, Chung KY, Swaminathan K, Vasudevan SG, et al. Molecular basis for specific viral RNA recognition and 2'-O-ribose methylation by the dengue virus nonstructural protein 5 (NS5). Proc Natl Acad Sci U S A. 2015 Dec 1;112(48):14834–9.

33. Kyle JL, Beatty PR, Harris E. Dengue virus infects macrophages and dendritic cells in a mouse model of infection. J Infect Dis. 2007 Jun 15;195(12):1808–17.

34. Aye KS, Charngkaew K, Win N, Wai KZ, Moe K, Punyadee N, et al. Pathologic highlights of dengue hemorrhagic fever in 13 autopsy cases from Myanmar. Hum Pathol. 2014 Jun;45(6):1221–33.

35. Cerny D, Haniffa M, Shin A, Bigliardi P, Tan BK, Lee B, et al. Selective Susceptibility of Human Skin Antigen Presenting Cells to Productive Dengue Virus Infection. PLoS Pathog. 2014 Dec 4;10(12):e1004548.

36. Prestwood TR, May MM, Plummer EM, Morar MM, Yauch LE, Shresta S. Trafficking and replication patterns reveal splenic macrophages as major targets of dengue virus in mice. J Virol. 2012 Nov;86(22):12138–47.

37. Schmid MA, Harris E. Monocyte Recruitment to the Dermis and Differentiation to Dendritic Cells Increases the Targets for Dengue Virus Replication. PLoS Pathog. 2014 Dec 4;10(12):e1004541.

38. Tassaneetrithep B, Burgess TH, Granelli-Piperno A, Trumpfheller C, Finke J, Sun W, et al. DC-SIGN (CD209) mediates dengue virus infection of human dendritic cells. J Exp Med. 2003 Apr 7;197(7):823–9.

39. Navarro-Sanchez E, Altmeyer R, Amara A, Schwartz O, Fieschi F, Virelizier JL, et al. Dendritic-cell-specific ICAM3-grabbing non-integrin is essential for the productive infection of human dendritic cells by mosquito-cell-derived dengue viruses. EMBO Rep. 2003 Jul;4(7):723–8.

40. Chen Y, Maguire T, Hileman RE, Fromm JR, Esko JD, Linhardt RJ, et al. Dengue virus infectivity depends on envelope protein binding to target cell heparan sulfate. Nat Med. 1997 Aug;3(8):866–71.

41. Meertens L, Carnec X, Lecoin MP, Ramdasi R, Guivel-Benhassine F, Lew E, et al. The TIM and TAM families of phosphatidylserine receptors mediate dengue virus entry. Cell Host Microbe. 2012 Oct 18;12(4):544–57.

42. Schaar HM van der, Rust MJ, Chen C, Ende-Metselaar H van der, Wilschut J, Zhuang X, et al. Dissecting the Cell Entry Pathway of Dengue Virus by Single-Particle Tracking in Living Cells. PLOS Pathog. 2008 Dec 19;4(12):e1000244.

43. Modis Y, Ogata S, Clements D, Harrison SC. Structure of the dengue virus envelope protein after membrane fusion. Nature. 2004 Jan;427(6972):313–9.

44. Mukhopadhyay S, Kuhn RJ, Rossmann MG. A structural perspective of the flavivirus life cycle. Nat Rev Microbiol. 2005 Jan;3(1):13–22.

45. Markoff L. In vitro processing of dengue virus structural proteins: cleavage of the pre-membrane protein. J Virol. 1989 Aug;63(8):3345–52.

46. Amberg SM, Rice CM. Mutagenesis of the NS2B-NS3-mediated cleavage site in the flavivirus capsid protein demonstrates a requirement for coordinated processing. J Virol. 1999 Oct;73(10):8083–94.

47. Welsch S, Miller S, Romero-Brey I, Merz A, Bleck CKE, Walther P, et al. Composition and Three-Dimensional Architecture of the Dengue Virus Replication and Assembly Sites. Cell Host Microbe. 2009 Apr 23;5(4):365–75.

48. Neufeldt CJ, Cortese M, Scaturro P, Cerikan B, Wideman JG, Tabata K, et al. ER-shaping atlastin proteins act as central hubs to promote flavivirus replication and virion assembly. Nat Microbiol. 2019 Dec;4(12):2416–29.

49. Aktepe TE, Liebscher S, Prier JE, Simmons CP, Mackenzie JM. The Host Protein Reticulon 3.1A Is Utilized by Flaviviruses to Facilitate Membrane Remodelling. Cell Rep. 2017 Nov 7;21(6):1639–54.

50. Stadler K, Allison SL, Schalich J, Heinz FX. Proteolytic activation of tick-borne encephalitis virus by furin. J Virol. 1997 Nov;71(11):8475–81.

51. Mukherjee S, Sirohi D, Dowd KA, Chen Z, Diamond MS, Kuhn RJ, et al. Enhancing dengue virus maturation using a stable furin over-expressing cell line. Virology. 2016 Oct;497:33–40.

52. Junjhon J, Edwards TJ, Utaipat U, Bowman VD, Holdaway HA, Zhang W, et al. Influence of pr-M Cleavage on the Heterogeneity of Extracellular Dengue Virus Particles. J Virol. 2010 Aug 15;84(16):8353–8.

53. Kaptein SJF, Goethals O, Kiemel D, Marchand A, Kesteleyn B, Bonfanti JF, et al. A pan-serotype dengue virus inhibitor targeting the NS3-NS4B interaction. Nature. 2021 Oct;598(7881):504–9.

54. Janeway CA. Approaching the Asymptote? Evolution and Revolution in Immunology. Cold Spring Harb Symp Quant Biol. 1989 Jan 1;54:1–13.

55. Tsai YT, Chang SY, Lee CN, Kao CL. Human TLR3 recognizes dengue virus and modulates viral replication in vitro. Cell Microbiol. 2009 Apr;11(4):604–15.

56. Wang JP, Liu P, Latz E, Golenbock DT, Finberg RW, Libraty DH. Flavivirus activation of plasmacytoid dendritic cells delineates key elements of TLR7 signaling beyond endosomal recognition. J Immunol Baltim Md 1950. 2006 Nov 15;177(10):7114–21.

57. Nasirudeen AMA, Wong HH, Thien P, Xu S, Lam KP, Liu DX. RIG-I, MDA5 and TLR3 Synergistically Play an Important Role in Restriction of Dengue Virus Infection. PLoS Negl Trop Dis. 2011 Jan 4;5(1):e926.

58. Majer O, Liu B, Barton GM. Nucleic acid-sensing TLRs: trafficking and regulation. Curr Opin Immunol. 2017 Feb 1;44:26–33.

59. Kawai T, Akira S. The role of pattern-recognition receptors in innate immunity: update on Toll-like receptors. Nat Immunol. 2010 May;11(5):373–84.

60. Loo YM, Fornek J, Crochet N, Bajwa G, Perwitasari O, Martinez-Sobrido L, et al. Distinct RIG-I and MDA5 Signaling by RNA Viruses in Innate Immunity. J Virol. 2008 Jan;82(1):335–45.

61. Loo YM, Gale M. Immune signaling by RIG-I-like receptors. Immunity. 2011 May 27;34(5):680–92.

62. Chazal M, Beauclair G, Gracias S, Najburg V, Simon-Lorière E, Tangy F, et al. RIG-I Recognizes the 5’ Region of Dengue and Zika Virus Genomes. Cell Rep. 2018 Jul 10;24(2):320–8.

63. Seth RB, Sun L, Ea CK, Chen ZJ. Identification and characterization of MAVS, a mitochondrial antiviral signaling protein that activates NF-kappaB and IRF 3. Cell. 2005 Sep 9;122(5):669–82.

64. Sun B, Sundström KB, Chew JJ, Bist P, Gan ES, Tan HC, et al. Dengue virus activates cGAS through the release of mitochondrial DNA. Sci Rep. 2017 Jun 15;7:3594.

65. Aguirre S, Luthra P, Sanchez-Aparicio MT, Maestre AM, Patel J, Lamothe F, et al. Dengue virus NS2B protein targets cGAS for degradation and prevents mitochondrial DNA sensing during infection. Nat Microbiol. 2017 Mar 27;2:17037.

66. Wu J, Sun L, Chen X, Du F, Shi H, Chen C, et al. Cyclic-GMP-AMP Is An Endogenous Second Messenger in Innate Immune Signaling by Cytosolic DNA. Science. 2013 Feb 15;339(6121):10.1126/science.1229963.

67. Burdette DL, Monroe KM, Sotelo-Troha K, Iwig JS, Eckert B, Hyodo M, et al. STING is a direct innate immune sensor of cyclic di-GMP. Nature. 2011 Sep 25;478(7370):515–8.

68. McNab F, Mayer-Barber K, Sher A, Wack A, O'Garra A. Type I interferons in infectious disease. Nat Rev Immunol. 2015 Feb;15(2):87–103.

69. Ivashkiv LB, Donlin LT. Regulation of type I interferon responses. Nat Rev Immunol. 2014 Jan;14(1):36–49.

70. Diamond MS, Roberts TG, Edgil D, Lu B, Ernst J, Harris E. Modulation of Dengue Virus Infection in Human Cells by Alpha, Beta, and Gamma Interferons. J Virol. 2000 Jun;74(11):4957–66.

71. Shresta S, Sharar KL, Prigozhin DM, Beatty PR, Harris E. Murine Model for Dengue Virus-Induced Lethal Disease with Increased Vascular Permeability. J Virol. 2006 Oct;80(20):10208–17.

72. Orozco S, Schmid MA, Parameswaran P, Lachica R, Henn MR, Beatty R, et al. Characterization of a model of lethal dengue virus 2 infection in C57BL/6 mice deficient in the alpha/beta interferon receptor. J Gen Virol. 2012 Oct;93(Pt 10):2152–7.

73. Schoggins JW. Recent advances in antiviral interferon-stimulated gene biology [Internet]. F1000Research; 2018 [cited 2023 Nov 24]. Available from: https://f1000research.com/articles/7-309

74. Diamond MS, Farzan M. The broad-spectrum antiviral functions of IFIT and IFITM proteins. Nat Rev Immunol. 2013 Jan;13(1):46–57.

75. Somnuke P, Hauhart RE, Atkinson JP, Diamond MS, Avirutnan P. N-linked glycosylation of Dengue virus NS1 protein modulates secretion, cell-surface expression, hexamer stability, and interactions with human complement. Virology. 2011 May 10;413(2):253–64.

76. Avirutnan P, Mehlhop E, Diamond MS. Complement and its role in protection and pathogenesis of flavivirus infections. Vaccine. 2008 Dec 30;26:I100–7.

77. Avirutnan P, Hauhart RE, Marovich MA, Garred P, Atkinson JP, Diamond MS. Complement-mediated neutralization of dengue virus requires mannose-binding lectin. mBio. 2011;2(6):e00276-11.

78. Mehlhop E, Ansarah-Sobrinho C, Johnson S, Engle M, Fremont DH, Pierson TC, et al. C1q Inhibits Antibody-Dependent Enhancement of Flavivirus Infection In Vitro and In Vivo in an IgG Subclass Specific Manner. Cell Host Microbe. 2007 Dec 13;2(6):417–26.

79. Dias AG, Atyeo C, Loos C, Montoya M, Roy V, Bos S, et al. Antibody Fc characteristics and effector functions correlate with protection from symptomatic dengue virus type 3 infection. Sci Transl Med. 2022 Jun 29;14(651):eabm3151.

80. Chang DC, Hoang LT, Mohamed Naim AN, Dong H, Schreiber MJ, Hibberd ML, et al. Evasion of early innate immune response by 2′-O-methylation of dengue genomic RNA. Virology. 2016 Dec;499:259–66.

81. Dong H, Chang DC, Hua MHC, Lim SP, Chionh YH, Hia F, et al. 2′-O Methylation of Internal Adenosine by Flavivirus NS5 Methyltransferase. PLoS Pathog. 2012 Apr 5;8(4):e1002642.

82. Chan YK, Gack MU. A phosphomimetic-based mechanism of dengue virus to antagonize innate immunity. Nat Immunol. 2016 May;17(5):523–30.

83. He Z, Zhu X, Wen W, Yuan J, Hu Y, Chen J, et al. Dengue Virus Subverts Host Innate Immunity by Targeting Adaptor Protein MAVS. J Virol. 2016 Jul 27;90(16):7219–30.

84. Aguirre S, Maestre AM, Pagni S, Patel JR, Savage T, Gutman D, et al. DENV Inhibits Type I IFN Production in Infected Cells by Cleaving Human STING. PLoS Pathog. 2012 Oct 4;8(10):e1002934.

85. Bhattacharya M, Bhowmik D, Tian Y, He H, Zhu F, Yin Q. The Dengue virus protease NS2B3 cleaves cyclic GMP-AMP synthase to suppress cGAS activation. J Biol Chem. 2023 Mar;299(3):102986.

86. Muñoz-Jordán JL, Sánchez-Burgos GG, Laurent-Rolle M, García-Sastre A. Inhibition of interferon signaling by dengue virus. Proc Natl Acad Sci U S A. 2003 Nov 25;100(24):14333–8.

87. Ashour J, Laurent-Rolle M, Shi PY, García-Sastre A. NS5 of Dengue Virus Mediates STAT2 Binding and Degradation. J Virol. 2009 Jun;83(11):5408–18.

88. Morrison J, Laurent-Rolle M, Maestre AM, Rajsbaum R, Pisanelli G, Simon V, et al. Dengue Virus Co-opts UBR4 to Degrade STAT2 and Antagonize Type I Interferon Signaling. PLoS Pathog. 2013 Mar 28;9(3):e1003265.

89. Chen RE, Diamond MS. Dengue mouse models for evaluating pathogenesis and countermeasures. Curr Opin Virol. 2020 Aug;43:50.

90. Stabell AC, Meyerson NR, Gullberg RC, Gilchrist AR, Webb KJ, Old WM, et al. Dengue viruses cleave STING in humans but not in nonhuman primates, their presumed natural reservoir. eLife. 2018 Mar 20;7:e31919.

91. Ashour J, Morrison J, Laurent-Rolle M, Belicha-Villanueva A, Plumlee CR, Bernal-Rubio D, et al. Mouse STAT2 Restricts Early Dengue Virus Replication. Cell Host Microbe. 2010 Nov 18;8(5):410–21.

92. Avirutnan P, Fuchs A, Hauhart RE, Somnuke P, Youn S, Diamond MS, et al. Antagonism of the complement component C4 by flavivirus nonstructural protein NS1. J Exp Med. 2010 Apr 12;207(4):793–806.

93. Avirutnan P, Hauhart RE, Somnuke P, Blom AM, Diamond MS, Atkinson JP. Binding of flavivirus nonstructural protein NS1 to C4b binding protein modulates complement activation. J Immunol Baltim Md 1950. 2011 Jul 1;187(1):424–33.

94. Conde JN, da Silva EM, Allonso D, Coelho DR, Andrade I da S, de Medeiros LN, et al. Inhibition of the Membrane Attack Complex by Dengue Virus NS1 through Interaction with Vitronectin and Terminal Complement Proteins. J Virol. 2016 Nov 1;90(21):9570–81.

95. Thiemmeca S, Tamdej C, Punyadee N, Prommool T, Songjaeng A, Noisakran S, et al. Secreted NS1 protects dengue virus from mannose binding lectin-mediated neutralization. J Immunol Baltim Md 1950. 2016 Nov 15;197(10):4053–65.

96. Slon Campos JL, Mongkolsapaya J, Screaton GR. The immune response against flaviviruses. Nat Immunol. 2018 Nov;19(11):1189–98.

97. Waggoner JJ, Balmaseda A, Gresh L, Sahoo MK, Montoya M, Wang C, et al. Homotypic Dengue Virus Reinfections in Nicaraguan Children. J Infect Dis. 2016 Oct 1;214(7):986–93.

98. Teoh EP, Kukkaro P, Teo EW, Lim APC, Tan TT, Yip A, et al. The Structural Basis for Serotype-Specific Neutralization of Dengue Virus by a Human Antibody. Sci Transl Med. 2012 Jun 20;4(139):139ra83-139ra83.

99. Fibriansah G, Tan JL, Smith SA, de Alwis R, Ng TS, Kostyuchenko VA, et al. A highly potent human antibody neutralizes dengue virus serotype 3 by binding across three surface proteins. Nat Commun. 2015 Feb 20;6(1):6341.

100. Fibriansah G, Ibarra KD, Ng TS, Smith SA, Tan JL, Lim XN, et al. Cryo-EM structure of an antibody that neutralizes dengue virus type 2 by locking E protein dimers. Science. 2015 Jul 3;349(6243):88–91.

101. Gallichotte EN, Baric TJ, Jr BLY, Widman DG, Durbin A, Whitehead S, et al. Human dengue virus serotype 2 neutralizing antibodies target two distinct quaternary epitopes. PLOS Pathog. 2018 Feb 26;14(2):e1006934.

102. Gallichotte EN, Widman DG, Yount BL, Wahala WM, Durbin A, Whitehead S, et al. A New Quaternary Structure Epitope on Dengue Virus Serotype 2 Is the Target of Durable Type-Specific Neutralizing Antibodies. mBio. 2015 Oct 13;6(5):10.1128/mbio.01461-15.

103. Young E, Carnahan RH, Andrade DV, Kose N, Nargi RS, Fritch EJ, et al. Identification of Dengue Virus Serotype 3 Specific Antigenic Sites Targeted by Neutralizing Human Antibodies. Cell Host Microbe. 2020 May 13;27(5):710-724.e7.

104. Katzelnick LC, Zambrana JV, Elizondo D, Collado D, Garcia N, Arguello S, et al. Dengue and Zika virus infections in children elicit cross-reactive protective and enhancing antibodies that persist long term. Sci Transl Med. 2021 Oct 6;13(614):eabg9478.

105. Lai CY, Tsai WY, Lin SR, Kao CL, Hu HP, King CC, et al. Antibodies to Envelope Glycoprotein of Dengue Virus during the Natural Course of Infection Are Predominantly Cross-Reactive and Recognize Epitopes Containing Highly Conserved Residues at the Fusion Loop of Domain II. J Virol. 2008 Jul;82(13):6631–43.

106. Schieffelin JS, Costin JM, Nicholson CO, Orgeron NM, Fontaine KA, Isern S, et al. Neutralizing and non-neutralizing monoclonal antibodies against dengue virus E protein derived from a naturally infected patient. Virol J. 2010 Feb 4;7:28.

107. Tsai WY, Lai CY, Wu YC, Lin HE, Edwards C, Jumnainsong A, et al. High-Avidity and Potently Neutralizing Cross-Reactive Human Monoclonal Antibodies Derived from Secondary Dengue Virus Infection. J Virol. 2013 Dec;87(23):12562–75.

108. Tsai WY, Durbin A, Tsai JJ, Hsieh SC, Whitehead S, Wang WK. Complexity of Neutralizing Antibodies against Multiple Dengue Virus Serotypes after Heterotypic Immunization and Secondary Infection Revealed by In-Depth Analysis of Cross-Reactive Antibodies. J Virol. 2015 May 13;89(14):7348–62.

109. Patel B, Longo P, Miley MJ, Montoya M, Harris E, Silva AM de. Dissecting the human serum antibody response to secondary dengue virus infections. PLoS Negl Trop Dis. 2017 May 15;11(5):e0005554.

110. Dejnirattisai W, Wongwiwat W, Supasa S, Zhang X, Dai X, Rouvinski A, et al. A new class of highly potent, broadly neutralizing antibodies isolated from viremic patients infected with dengue virus. Nat Immunol. 2015 Feb;16(2):170–7.

111. Beltramello M, Williams KL, Simmons CP, Macagno A, Simonelli L, Quyen NTH, et al. The Human Immune Response to Dengue Virus Is Dominated by Highly Cross-Reactive Antibodies Endowed with Neutralizing and Enhancing Activity. Cell Host Microbe. 2010 Sep 16;8(3):271–83.

112. Wrammert J, Onlamoon N, Akondy RS, Perng GC, Polsrila K, Chandele A, et al. Rapid and Massive Virus-Specific Plasmablast Responses during Acute Dengue Virus Infection in Humans. J Virol. 2012 Mar;86(6):2911–8.

113. Xu M, Hadinoto V, Appanna R, Joensson K, Toh YX, Balakrishnan T, et al. Plasmablasts Generated during Repeated Dengue Infection Are Virus Glycoprotein–Specific and Bind to Multiple Virus Serotypes. J Immunol. 2012 Dec 15;189(12):5877–85.

114. Priyamvada L, Cho A, Onlamoon N, Zheng NY, Huang M, Kovalenkov Y, et al. B Cell Responses during Secondary Dengue Virus Infection Are Dominated by Highly Cross-Reactive, Memory-Derived Plasmablasts. J Virol. 2016 May 27;90(12):5574–85.

115. Ngono AE, Shresta S. Immune Response to Dengue and Zika. Annu Rev Immunol. 2018 Apr 26;36:279–308.

116. Tian Y, Grifoni A, Sette A, Weiskopf D. Human T Cell Response to Dengue Virus Infection. Front Immunol. 2019 Sep 4;10:2125.

117. Swain SL, McKinstry KK, Strutt TM. Expanding roles for CD4+ T cells in immunity to viruses. Nat Rev Immunol. 2012;12(2):136–48.

118. Weiskopf D, Angelo MA, de Azeredo EL, Sidney J, Greenbaum JA, Fernando AN, et al. Comprehensive analysis of dengue virus-specific responses supports an HLA-linked protective role for CD8+ T cells. Proc Natl Acad Sci U S A. 2013 May 28;110(22):E2046–53.

119. de Alwis R, Bangs DJ, Angelo MA, Cerpas C, Fernando A, Sidney J, et al. Immunodominant Dengue Virus-Specific CD8+ T Cell Responses Are Associated with a Memory PD-1+ Phenotype. J Virol. 2016 Apr 14;90(9):4771–9.

120. Hatch S, Endy TP, Thomas S, Mathew A, Potts J, Pazoles P, et al. Intracellular Cytokine Production by Dengue Virus–specific T cells Correlates with Subclinical Secondary Infection. J Infect Dis. 2011 May 1;203(9):1282–91.

121. Yauch LE, Zellweger RM, Kotturi MF, Qutubuddin A, Sidney J, Peters B, et al. A Protective Role for Dengue Virus-Specific CD8+ T Cells. J Immunol Baltim Md 1950. 2009 Apr 15;182(8):4865–73.

122. Yauch LE, Prestwood TR, May MM, Morar MM, Zellweger RM, Peters B, et al. CD4+ T cells Are Not Required for the Induction of Dengue Virus-Specific CD8+ T cell or Antibody Responses but Contribute to Protection After Vaccination. J Immunol Baltim Md 1950. 2010 Nov 11;185(9):5405.

123. Zompi S, Santich BH, Beatty PR, Harris E. Protection from Secondary Dengue Virus Infection in a Mouse Model Reveals the Role of Serotype Cross-reactive B and T cells,. J Immunol Baltim Md 1950. 2012 Jan 1;188(1):404–16.

124. Zellweger RM, Tang WW, Eddy WE, King K, Sanchez MC, Shresta S. CD8+ T Cells Can Mediate Short-Term Protection against Heterotypic Dengue Virus Reinfection in Mice. J Virol. 2015 Apr 8;89(12):6494–505.

125. Elong Ngono A, Chen HW, Tang WW, Joo Y, King K, Weiskopf D, et al. Protective Role of Cross-Reactive CD8 T Cells Against Dengue Virus Infection. EBioMedicine. 2016 Oct 7;13:284–93.

126. Beaumier CM, Mathew A, Bashyam HS, Rothman AL. Cross-reactive memory CD8(+) T cells alter the immune response to heterologous secondary dengue virus infections in mice in a sequence-specific manner. J Infect Dis. 2008 Feb 15;197(4):608–17.

127. Beaumier CM, Rothman AL. Cross-Reactive Memory CD4+ T Cells Alter the CD8+ T-Cell Response to Heterologous Secondary Dengue Virus Infections in Mice in a Sequence-Specific Manner. Viral Immunol. 2009 Jun;22(3):215–9.

128. Mongkolsapaya J, Dejnirattisai W, Xu X ning, Vasanawathana S, Tangthawornchaikul N, Chairunsri A, et al. Original antigenic sin and apoptosis in the pathogenesis of dengue hemorrhagic fever. Nat Med. 2003 Jul;9(7):921–7.

129. Dejnirattisai W, Jumnainsong A, Onsirisakul N, Fitton P, Vasanawathana S, Limpitikul W, et al. Enhancing cross-reactive anti-prM dominates the human antibody response in dengue infection. Science. 2010 May 7;328(5979):10.1126/science.1185181.

130. de Alwis R, Williams KL, Schmid MA, Lai CY, Patel B, Smith SA, et al. Dengue Viruses Are Enhanced by Distinct Populations of Serotype Cross-Reactive Antibodies in Human Immune Sera. PLoS Pathog. 2014 Oct 2;10(10):e1004386.

131. Halstead SB. Neutralization and antibody-dependent enhancement of dengue viruses. Adv Virus Res. 2003;60:421–67.

132. Waggoner JJ, Katzelnick LC, Burger-Calderon R, Gallini J, Moore RH, Kuan G, et al. Antibody-Dependent Enhancement of Severe Disease Is Mediated by Serum Viral Load in Pediatric Dengue Virus Infections. J Infect Dis. 2020 Jun 1;221(11):1846–54.

133. Gallichotte EN, Baric RS, de Silva AM. The Molecular Specificity of the Human Antibody Response to Dengue Virus Infections. Adv Exp Med Biol. 2018;1062:63–76.

134. Balsitis SJ, Williams KL, Lachica R, Flores D, Kyle JL, Mehlhop E, et al. Lethal antibody enhancement of dengue disease in mice is prevented by Fc modification. PLoS Pathog. 2010 Feb 12;6(2):e1000790.

135. Zellweger RM, Prestwood TR, Shresta S. Enhanced infection of liver sinusoidal endothelial cells in a mouse model of antibody-induced severe dengue disease. Cell Host Microbe. 2010 Feb 18;7(2):128–39.

136. Katzelnick LC, Gresh L, Halloran ME, Mercado JC, Kuan G, Gordon A, et al. Antibody-dependent enhancement of severe dengue disease in humans. Science. 2017 Nov 17;358(6365):929–32.

137. Halstead SB. Dengvaxia sensitizes seronegatives to vaccine enhanced disease regardless of age. Vaccine. 2017 Nov 7;35(47):6355–8.

138. Sridhar S, Luedtke A, Langevin E, Zhu M, Bonaparte M, Machabert T, et al. Effect of Dengue Serostatus on Dengue Vaccine Safety and Efficacy. N Engl J Med. 2018 Jul 26;379(4):327–40.

139. Paranavitane SA, Gomes L, Kamaladasa A, Adikari TN, Wickramasinghe N, Jeewandara C, et al. Dengue NS1 antigen as a marker of severe clinical disease. BMC Infect Dis. 2014 Oct 31;14:570.

140. Libraty DH, Young PR, Pickering D, Endy TP, Kalayanarooj S, Green S, et al. High circulating levels of the dengue virus nonstructural protein NS1 early in dengue illness correlate with the development of dengue hemorrhagic fever. J Infect Dis. 2002 Oct 15;186(8):1165–8.

141. Amorim JH, Diniz MO, Cariri FAMO, Rodrigues JF, Bizerra RSP, Gonçalves AJS, et al. Protective immunity to DENV2 after immunization with a recombinant NS1 protein using a genetically detoxified heat-labile toxin as an adjuvant. Vaccine. 2012 Jan 20;30(5):837–45.

142. Beatty PR, Puerta-Guardo H, Killingbeck SS, Glasner DR, Hopkins K, Harris E. Dengue virus NS1 triggers endothelial permeability and vascular leak that is prevented by NS1 vaccination. Sci Transl Med. 2015 Sep 9;7(304):304ra141-304ra141.

143. Akey DL, Brown WC, Dutta S, Konwerski J, Jose J, Jurkiw TJ, et al. Flavivirus NS1 crystal structures reveal a surface for membrane association and regions of interaction with the immune system. Science. 2014 Feb 21;343(6173):881–5.

144. Falgout B, Markoff L. Evidence that flavivirus NS1-NS2A cleavage is mediated by a membrane-bound host protease in the endoplasmic reticulum. J Virol. 1995 Nov;69(11):7232–43.

145. Winkler G, Randolph VB, Cleaves GR, Ryan TE, Stollar V. Evidence that the mature form of the flavivirus nonstructural protein NS1 is a dimer. Virology. 1988 Jan;162(1):187–96.

146. Brown WC, Akey DL, Konwerski JR, Tarrasch JT, Skiniotis G, Kuhn RJ, et al. Extended surface for membrane association in Zika virus NS1 structure. Nat Struct Mol Biol. 2016 Sep;23(9):865–7.

147. Flamand M, Megret F, Mathieu M, Lepault J, Rey FA, Deubel V. Dengue virus type 1 nonstructural glycoprotein NS1 is secreted from mammalian cells as a soluble hexamer in a glycosylation-dependent fashion. J Virol. 1999 Jul;73(7):6104–10.

148. Gutsche I, Coulibaly F, Voss JE, Salmon J, d'Alayer J, Ermonval M, et al. Secreted dengue virus nonstructural protein NS1 is an atypical barrel-shaped high-density lipoprotein. Proc Natl Acad Sci U S A. 2011 May 10;108(19):8003–8.

149. Shu B, Ooi JSG, Tan AWK, Ng TS, Dejnirattisai W, Mongkolsapaya J, et al. CryoEM structures of the multimeric secreted NS1, a major factor for dengue hemorrhagic fever. Nat Commun. 2022 Nov 9;13(1):6756.

150. Songprakhon P, Limjindaporn T, Perng GC, Puttikhunt C, Thaingtamtanha T, Dechtawewat T, et al. Human glucose-regulated protein 78 modulates intracellular production and secretion of nonstructural protein 1 of dengue virus. J Gen Virol. 2018 Oct;99(10):1391–406.

151. Denolly S, Guo H, Martens M, Płaszczyca A, Scaturro P, Prasad V, et al. Dengue virus NS1 secretion is regulated via importin-subunit β1 controlling expression of the chaperone GRp78 and targeted by the clinical drug ivermectin. mBio. 14(5):e01441-23.

152. Pryor MJ, Wright PJ. Glycosylation mutants of dengue virus NS1 protein. J Gen Virol. 1994;75(5):1183–7.

153. Wang C, Puerta-Guardo H, Biering SB, Glasner DR, Tran EB, Patana M, et al. Endocytosis of flavivirus NS1 is required for NS1-mediated endothelial hyperpermeability and is abolished by a single N-glycosylation site mutation. PLOS Pathog. 2019 Jul 29;15(7):e1007938.

154. Tan BEK, Beard MR, Eyre NS. Identification of Key Residues in Dengue Virus NS1 Protein That Are Essential for Its Secretion. Viruses. 2023 Apr 30;15(5):1102.

155. Mackenzie JM, Jones MK, Young PR. Immunolocalization of the dengue virus nonstructural glycoprotein NS1 suggests a role in viral RNA replication. Virology. 1996 Jun 1;220(1):232–40.

156. Scaturro P, Cortese M, Chatel-Chaix L, Fischl W, Bartenschlager R. Dengue Virus Non-structural Protein 1 Modulates Infectious Particle Production via Interaction with the Structural Proteins. PLOS Pathog. 2015 Nov 12;11(11):e1005277.

157. Shue B, Chiramel AI, Cerikan B, To TH, Frölich S, Pederson SM, et al. Genome-Wide CRISPR Screen Identifies RACK1 as a Critical Host Factor for Flavivirus Replication. J Virol. 95(24):e00596-21.

158. Hafirassou ML, Meertens L, Umaña-Diaz C, Labeau A, Dejarnac O, Bonnet-Madin L, et al. A Global Interactome Map of the Dengue Virus NS1 Identifies Virus Restriction and Dependency Host Factors. Cell Rep. 2017 Dec 26;21(13):3900–13.

159. Sturtzel C. Endothelial Cells. In: Sattler S, Kennedy-Lydon T, editors. The Immunology of Cardiovascular Homeostasis and Pathology [Internet]. Cham: Springer International Publishing; 2017 [cited 2023 Nov 28]. p. 71–91. (Advances in Experimental Medicine and Biology). Available from: https://doi.org/10.1007/978-3-319-57613-8_4

160. Dejana E. Endothelial cell–cell junctions: happy together. Nat Rev Mol Cell Biol. 2004 Apr;5(4):261–70.

161. Cerutti C, Ridley AJ. Endothelial cell-cell adhesion and signaling. Exp Cell Res. 2017 Sep 1;358(1):31–8.

162. Otani T, Furuse M. Tight Junction Structure and Function Revisited. Trends Cell Biol. 2020 Oct;30(10):805–17.

163. Steed E, Balda MS, Matter K. Dynamics and functions of tight junctions. Trends Cell Biol. 2010 Mar;20(3):142–9.

164. Reitsma S, Slaaf DW, Vink H, van Zandvoort MAMJ, oude Egbrink MGA. The endothelial glycocalyx: composition, functions, and visualization. Pflugers Arch. 2007 Jun;454(3):345–59.

165. Weinbaum S, Tarbell JM, Damiano ER. The structure and function of the endothelial glycocalyx layer. Annu Rev Biomed Eng. 2007;9:121–67.

166. Lin CY, Kolliopoulos C, Huang CH, Tenhunen J, Heldin CH, Chen YH, et al. High levels of serum hyaluronan is an early predictor of dengue warning signs and perturbs vascular integrity. EBioMedicine. 2019 Oct;48:425.

167. Tang THC, Alonso S, Ng LFP, Thein TL, Pang VJX, Leo YS, et al. Increased Serum Hyaluronic Acid and Heparan Sulfate in Dengue Fever: Association with Plasma Leakage and Disease Severity. Sci Rep. 2017 Apr 10;7:46191.

168. Honsawek S, Kongtawelert P, Pothacharoen P, Khongphatthanayothin A, Chongsrisawat V, Poovorawan Y. Increased levels of serum hyaluronan in patients with dengue infection. J Infect. 2007 Mar;54(3):225–9.

169. Suwarto S, Sasmono RT, Sinto R, Ibrahim E, Suryamin M. Association of Endothelial Glycocalyx and Tight and Adherens Junctions With Severity of Plasma Leakage in Dengue Infection. J Infect Dis. 2017 Mar 15;215(6):992–9.

170. Buijsers B, Garishah FM, Riswari SF, van Ast RM, Pramudo SG, Tunjungputri RN, et al. Increased Plasma Heparanase Activity and Endothelial Glycocalyx Degradation in Dengue Patients Is Associated With Plasma Leakage. Front Immunol. 2021;12:759570.

171. Espinosa DA, Beatty PR, Puerta-Guardo H, Islam MN, Belisle JT, Perera R, et al. Increased serum sialic acid is associated with morbidity and mortality in a murine model of dengue disease. J Gen Virol. 2019 Nov;100(11):1515–22.

172. Puerta-Guardo H, Glasner DR, Harris E. Dengue Virus NS1 Disrupts the Endothelial Glycocalyx, Leading to Hyperpermeability. PLoS Pathog. 2016;12(7):e1005738.

173. Glasner DR, Ratnasiri K, Puerta-Guardo H, Espinosa DA, Beatty PR, Harris E. Dengue virus NS1 cytokine-independent vascular leak is dependent on endothelial glycocalyx components. PLOS Pathog. 2017 Nov 9;13(11):e1006673.

174. Avirutnan P, Zhang L, Punyadee N, Manuyakorn A, Puttikhunt C, Kasinrerk W, et al. Secreted NS1 of dengue virus attaches to the surface of cells via interactions with heparan sulfate and chondroitin sulfate E. PLoS Pathog. 2007 Nov;3(11):e183.

175. Modhiran N, Gandhi NS, Wimmer N, Cheung S, Stacey K, Young PR, et al. Dual targeting of dengue virus virions and NS1 protein with the heparan sulfate mimic PG545. Antiviral Res. 2019 Aug;168:121–7.

176. Sousa FTG de, Biering SB, Patel TS, Blanc SF, Camelini CM, Venzke D, et al. Sulfated β-glucan from Agaricus subrufescens inhibits flavivirus infection and nonstructural protein 1-mediated pathogenesis. Antiviral Res. 2022 Jul 1;203:105330.

177. Edeling MA, Diamond MS, Fremont DH. Structural basis of Flavivirus NS1 assembly and antibody recognition. Proc Natl Acad Sci. 2014 Mar 18;111(11):4285–90.

178. Biering SB, Akey DL, Wong MP, Brown WC, Lo NTN, Puerta-Guardo H, et al. Structural basis for antibody inhibition of flavivirus NS1–triggered endothelial dysfunction. Science. 2021 Jan 8;371(6525):194–200.

179. Lo NTN, Roodsari SZ, Tin NL, Wong MP, Biering SB, Harris E. Molecular Determinants of Tissue Specificity of Flavivirus Nonstructural Protein 1 Interaction with Endothelial Cells. J Virol. 2022 Sep 15;96(19):e00661-22.

180. Alcalá AC, Maravillas JL, Meza D, Ramirez OT, Ludert JE, Palomares LA. Dengue Virus NS1 Uses Scavenger Receptor B1 as a Cell Receptor in Cultured Cells. J Virol. 96(5):e01664-21.

181. Puerta-Guardo H, Biering SB, Sousa FTG de, Shu J, Glasner DR, Li J, et al. Flavivirus NS1 Triggers Tissue-Specific Disassembly of Intercellular Junctions Leading to Barrier Dysfunction and Vascular Leak in a GSK-3β-Dependent Manner. Pathogens [Internet]. 2022 Jun

[cited 2023 Nov 9];11(6). Available from:
https://www.ncbi.nlm.nih.gov/pmc/articles/PMC9228372/

182. Barbachano-Guerrero A, Endy TP, King CA. Dengue virus non-structural protein 1 activates the p38 MAPK pathway to decrease barrier integrity in primary human endothelial cells. J Gen Virol. 2020 May;101(5):484–96.

183. Pan P, Li G, Shen M, Yu Z, Ge W, Lao Z, et al. DENV NS1 and MMP-9 cooperate to induce vascular leakage by altering endothelial cell adhesion and tight junction. PLOS Pathog. 2021 Jul 26;17(7):e1008603.

184. Chen HR, Chuang YC, Lin YS, Liu HS, Liu CC, Perng GC, et al. Dengue Virus Nonstructural Protein 1 Induces Vascular Leakage through Macrophage Migration Inhibitory Factor and Autophagy. PLoS Negl Trop Dis. 2016 Jul 13;10(7):e0004828.

185. Singh S, Anupriya MG, Modak A, Sreekumar E. Dengue virus or NS1 protein induces trans-endothelial cell permeability associated with VE-Cadherin and RhoA phosphorylation in HMEC-1 cells preventable by Angiopoietin-1. J Gen Virol. 2018 Dec;99(12):1658–70.

186. Modhiran N, Watterson D, Muller DA, Panetta AK, Sester DP, Liu L, et al. Dengue virus NS1 protein activates cells via Toll-like receptor 4 and disrupts endothelial cell monolayer integrity. Sci Transl Med. 2015 Sep 9;7(304):304ra142.

187. Alayli F, Scholle F. Dengue virus NS1 enhances viral replication and pro-inflammatory cytokine production in human dendritic cells. Virology. 2016 Sep;496:227–36.

188. Chao CH, Wu WC, Lai YC, Tsai PJ, Perng GC, Lin YS, et al. Dengue virus nonstructural protein 1 activates platelets via Toll-like receptor 4, leading to thrombocytopenia and hemorrhage. PLoS Pathog. 2019 Apr;15(4):e1007625.

189. Modhiran N, Watterson D, Blumenthal A, Baxter AG, Young PR, Stacey KJ. Dengue virus NS1 protein activates immune cells via TLR4 but not TLR2 or TLR6. Immunol Cell Biol. 2017 May;95(5):491–5.

190. Chan KWK, Watanabe S, Jin JY, Pompon J, Teng D, Alonso S, et al. A T164S mutation in the dengue virus NS1 protein is associated with greater disease severity in mice. Sci Transl Med. 2019 Jun 26;11(498):eaat7726.

191. Benfrid S, Park KH, Dellarole M, Voss JE, Tamietti C, Pehau-Arnaudet G, et al. Dengue virus NS1 protein conveys pro-inflammatory signals by docking onto high-density lipoproteins. EMBO Rep. 2022 Jul 5;23(7):e53600.

192. Adikari TN, Gomes L, Wickramasinghe N, Salimi M, Wijesiriwardana N, Kamaladasa A, et al. Dengue NS1 antigen contributes to disease severity by inducing interleukin (IL)-10 by monocytes. Clin Exp Immunol. 2016 Apr;184(1):90–100.

193. Silva T, Gomes L, Jeewandara C, Ogg GS, Malavige GN. Dengue NS1 induces phospholipase A2 enzyme activity, prostaglandins, and inflammatory cytokines in monocytes. Antiviral Res. 2022 Jun;202:105312.

194. García-Larragoiti N, Kim YC, López-Camacho C, Cano-Méndez A, López-Castaneda S, Hernández-Hernández D, et al. Platelet activation and aggregation response to dengue virus nonstructural protein 1 and domains. J Thromb Haemost JTH. 2021 Oct;19(10):2572–82.

195. Hottz ED, Lopes JF, Freitas C, Valls-de-Souza R, Oliveira MF, Bozza MT, et al. Platelets mediate increased endothelium permeability in dengue through NLRP3-inflammasome activation. Blood. 2013 Nov 14;122(20):3405–14.

196. Coelho DR, Carneiro PH, Mendes-Monteiro L, Conde JN, Andrade I, Cao T, et al. ApoA1 Neutralizes Proinflammatory Effects of Dengue Virus NS1 Protein and Modulates Viral Immune Evasion. J Virol. 2021 Jun 10;95(13):e0197420.

197. Puerta-Guardo H, Glasner DR, Espinosa DA, Biering SB, Patana M, Ratnasiri K, et al. Flavivirus NS1 Triggers Tissue-Specific Vascular Endothelial Dysfunction Reflecting Disease Tropism. Cell Rep. 2019 Feb;26(6):1598-1613.e8.

198. Modhiran N, Song H, Liu L, Bletchly C, Brillault L, Amarilla AA, et al. A broadly protective antibody that targets the flavivirus NS1 protein. Science. 2021 Jan 8;371(6525):190–4.

199. Churdboonchart V, Bhamarapravati N, Peampramprecha S, Sirinavin S. Antibodies against dengue viral proteins in primary and secondary dengue hemorrhagic fever. Am J Trop Med Hyg. 1991 May;44(5):481–93.

200. Shu PY, Chen LK, Chang SF, Yueh YY, Chow L, Chien LJ, et al. Dengue NS1-specific antibody responses: isotype distribution and serotyping in patients with Dengue fever and Dengue hemorrhagic fever. J Med Virol. 2000 Oct;62(2):224–32.

201. Sharma M, Glasner DR, Watkins H, Puerta-Guardo H, Kassa Y, Egan MA, et al. Magnitude and Functionality of the NS1-Specific Antibody Response Elicited by a Live-Attenuated Tetravalent Dengue Vaccine Candidate. J Infect Dis. 2020 Mar 2;221(6):867–77.

202. Hertz T, Beatty PR, MacMillen Z, Killingbeck SS, Wang C, Harris E. Antibody epitopes identified in critical regions of dengue virus nonstructural 1 protein in mouse vaccination and natural human infections. J Immunol Baltim Md 1950. 2017 May 15;198(10):4025–35.

203. Jayathilaka D, Gomes L, Jeewandara C, Jayarathna GeethalSB, Herath D, Perera PA, et al. Role of NS1 antibodies in the pathogenesis of acute secondary dengue infection. Nat Commun. 2018 Dec 7;9:5242.

204. Falconar AK. The dengue virus nonstructural-1 protein (NS1) generates antibodies to common epitopes on human blood clotting, integrin/adhesin proteins and binds to human endothelial cells: potential implications in haemorrhagic fever pathogenesis. Arch Virol. 1997;142(5):897–916.

205. Lin CF, Wan SW, Chen MC, Lin SC, Cheng CC, Chiu SC, et al. Liver injury caused by antibodies against dengue virus nonstructural protein 1 in a murine model. Lab Investig J Tech Methods Pathol. 2008 Oct;88(10):1079–89.

206. Lin YS, Yeh TM, Lin CF, Wan SW, Chuang YC, Hsu TK, et al. Molecular mimicry between virus and host and its implications for dengue disease pathogenesis. Exp Biol Med Maywood NJ. 2011 May 1;236(5):515–23.

207. Sun DS, King CC, Huang HS, Shih YL, Lee CC, Tsai WJ, et al. Antiplatelet autoantibodies elicited by dengue virus non-structural protein 1 cause thrombocytopenia and mortality in mice. J Thromb Haemost JTH. 2007 Nov;5(11):2291–9.

208. Chuang YC, Lei HY, Lin YS, Liu HS, Wu HL, Yeh TM. Dengue virus-induced autoantibodies bind to plasminogen and enhance its activation. J Immunol Baltim Md 1950. 2011 Dec 15;187(12):6483–90.

209. Cheng HJ, Lei HY, Lin CF, Luo YH, Wan SW, Liu HS, et al. Anti-dengue virus nonstructural protein 1 antibodies recognize protein disulfide isomerase on platelets and inhibit platelet aggregation. Mol Immunol. 2009 Dec;47(2–3):398–406.

210. Chen MC, Lin CF, Lei HY, Lin SC, Liu HS, Yeh TM, et al. Deletion of the C-terminal region of dengue virus nonstructural protein 1 (NS1) abolishes anti-NS1-mediated platelet dysfunction and bleeding tendency. J Immunol Baltim Md 1950. 2009 Aug 1;183(3):1797–803.

211. Lee PX, Ting DHR, Boey CPH, Tan ETX, Chia JZH, Idris F, et al. Relative contribution of nonstructural protein 1 in dengue pathogenesis. J Exp Med. 2020 Sep 7;217(9):e20191548.

212. Barnett KC, Li S, Liang K, Ting JPY. A 360° view of the inflammasome: Mechanisms of activation, cell death, and diseases. Cell. 2023 May 25;186(11):2288–312.

213. Shrivastava G, Valenzuela Leon PC, Calvo E. Inflammasome Fuels Dengue Severity. Front Cell Infect Microbiol. 2020 Sep 10;10:489.

214. Tsu BV, Beierschmitt C, Ryan AP, Agarwal R, Mitchell PS, Daugherty MD. Diverse viral proteases activate the NLRP1 inflammasome. Schoggins JW, Rothlin CV, editors. eLife. 2021 Jan 7;10:e60609.

215. Sarvestani ST, McAuley JL. The role of the NLRP3 inflammasome in regulation of antiviral responses to influenza A virus infection. Antiviral Res. 2017 Dec 1;148:32–42.

216. Wang Q, Gao H, Clark KM, Mugisha CS, Davis K, Tang JP, et al. CARD8 is an inflammasome sensor for HIV-1 protease activity. Science. 2021 Mar 19;371(6535):eabe1707.

217. Diamond MS, Kanneganti TD. Innate immunity: the first line of defense against SARS-CoV-2. Nat Immunol. 2022 Feb;23(2):165–76.

218. Thomas PG, Dash P, Aldridge JR, Ellebedy AH, Reynolds C, Funk AJ, et al. NLRP3 (NALP3/CIAS1/Cryopyrin) mediates key innate and healing responses to influenza A virus via the regulation of caspase-1. Immunity. 2009 Apr 17;30(4):566–75.

219. Ramos HJ, Lanteri MC, Blahnik G, Negash A, Suthar MS, Brassil MM, et al. IL-1β Signaling Promotes CNS-Intrinsic Immune Control of West Nile Virus Infection. PLoS Pathog. 2012 Nov 29;8(11):e1003039.

220. Tate MD, Ong JDH, Dowling JK, McAuley JL, Robertson AB, Latz E, et al. Reassessing the role of the NLRP3 inflammasome during pathogenic influenza A virus infection via temporal inhibition. Sci Rep. 2016 Jun 10;6(1):27912.

221. Lu A, Magupalli VG, Ruan J, Yin Q, Atianand MK, Vos MR, et al. Unified Polymerization Mechanism for the Assembly of ASC-Dependent Inflammasomes. Cell. 2014 Mar 13;156(6):1193–206.

222. Zhao Y, Yang J, Shi J, Gong YN, Lu Q, Xu H, et al. The NLRC4 inflammasome receptors for bacterial flagellin and type III secretion apparatus. Nature. 2011 Sep;477(7366):596–600.

223. Hornung V, Ablasser A, Charrel-Dennis M, Bauernfeind F, Horvath G, Caffrey DR, et al. AIM2 recognizes cytosolic dsDNA and forms a caspase-1-activating inflammasome with ASC. Nature. 2009 Mar;458(7237):514–8.

224. Sandstrom A, Mitchell PS, Goers L, Mu EW, Lesser CF, Vance RE. Functional degradation: A mechanism of NLRP1 inflammasome activation by diverse pathogen enzymes. Science. 2019 Apr 5;364(6435):eaau1330.

225. Hagar JA, Powell DA, Aachoui Y, Ernst RK, Miao EA. Cytoplasmic LPS activates caspase-11: implications in TLR4-independent endotoxic shock. Science. 2013 Sep 13;341(6151):1250–3.

226. Kayagaki N, Wong MT, Stowe IB, Ramani SR, Gonzalez LC, Akashi-Takamura S, et al. Noncanonical inflammasome activation by intracellular LPS independent of TLR4. Science. 2013 Sep 13;341(6151):1246–9.

227. Sims JE, Smith DE. The IL-1 family: regulators of immunity. Nat Rev Immunol. 2010 Feb;10(2):89–102.

228. Liu X, Zhang Z, Ruan J, Pan Y, Magupalli VG, Wu H, et al. Inflammasome-activated gasdermin D causes pyroptosis by forming membrane pores. Nature. 2016 Jul;535(7610):153–8.

229. Kayagaki N, Kornfeld OS, Lee BL, Stowe IB, O'Rourke K, Li Q, et al. NINJ1 mediates plasma membrane rupture during lytic cell death. Nature. 2021 Mar;591(7848):131–6.

230. Evavold CL, Ruan J, Tan Y, Xia S, Wu H, Kagan JC. The Pore-Forming Protein Gasdermin D Regulates Interleukin-1 Secretion from Living Macrophages. Immunity. 2018 Jan 16;48(1):35-44.e6.

231. Zanoni I, Tan Y, Di Gioia M, Broggi A, Ruan J, Shi J, et al. An endogenous caspase-11 ligand elicits interleukin-1 release from living dendritic cells. Science. 2016 Jun 3;352(6290):1232–6.

232. de Sá KSG, Amaral LA, Rodrigues TS, Ishimoto AY, de Andrade WAC, de Almeida L, et al. Gasdermin-D activation promotes NLRP3 activation and host resistance to Leishmania infection. Nat Commun. 2023 Feb 24;14:1049.

233. Heilig R, Dick MS, Sborgi L, Meunier E, Hiller S, Broz P. The Gasdermin-D pore acts as a conduit for IL-1β secretion in mice. Eur J Immunol. 2018;48(4):584–92.

234. Pan P, Zhang Q, Liu W, Wang W, Lao Z, Zhang W, et al. Dengue Virus M Protein Promotes NLRP3 Inflammasome Activation To Induce Vascular Leakage in Mice. J Virol. 2019 01;93(21).

235. Wu MF, Chen ST, Yang AH, Lin WW, Lin YL, Chen NJ, et al. CLEC5A is critical for dengue virus–induced inflammasome activation in human macrophages. Blood. 2013 Jan 3;121(1):95–106.

236. Shrivastava G, Visoso-Carvajal G, Garcia-Cordero J, Leon-Juarez M, Chavez-Munguia B, Lopez T, et al. Dengue Virus Serotype 2 and Its Non-Structural Proteins 2A and 2B Activate NLRP3 Inflammasome. Front Immunol. 2020;11:352.

237. Pan P, Zhang Q, Liu W, Wang W, Yu Z, Lao Z, et al. Dengue Virus Infection Activates Interleukin-1β to Induce Tissue Injury and Vascular Leakage. Front Microbiol [Internet]. 2019 [cited 2020 Jun 28];10. Available from: https://www.frontiersin.org/articles/10.3389/fmicb.2019.02637/full

238. Tan TY, Chu JJH. Dengue virus-infected human monocytes trigger late activation of caspase-1, which mediates pro-inflammatory IL-1β secretion and pyroptosis. J Gen Virol. 2013 Oct;94(Pt 10):2215–20.

239. Yong YK, Tan HY, Jen SH, Shankar EM, Natkunam SK, Sathar J, et al. Aberrant monocyte responses predict and characterize dengue virus infection in individuals with severe disease. J Transl Med. 2017 May 31;15:121.

Chapter 2

The Inflammasome Pathway is Activated by Dengue Virus Non-structural Protein 1 and is Protective During Dengue Virus Infection

This chapter was submitted as:

Wong MP, Juan EYW, Chelluri SS, Wang P, Pahmeier F, Castillo-Rojas B, Blanc SF, Biering SB, Vance RE, Harris E. The Inflammasome Pathway is Activated by Dengue Virus Non-structural Protein 1 and is Protective During Dengue Virus Infection. *bioRxiv [Preprint].* 2023 Sep 21:2023.09.21.558875. doi: 10.1101/2023.09.21.558875.

Abstract

Dengue virus (DENV) is a medically important flavivirus causing an estimated 50-100 million dengue cases annually, some of whom progress to severe disease. DENV non-structural protein 1 (NS1) is secreted from infected cells and has been implicated as a major driver of dengue pathogenesis by inducing endothelial barrier dysfunction. However, less is known about how DENV NS1 interacts with immune cells and what role these interactions play. Here we report that DENV NS1 can trigger activation of inflammasomes, a family of cytosolic innate immune sensors that respond to infectious and noxious stimuli, in mouse and human macrophages. DENV NS1 induces the release of IL-1β in a caspase-1 dependent manner. Additionally, we find that DENV NS1-induced inflammasome activation is independent of the NLRP3, Pyrin, and AIM2 inflammasome pathways, but requires CD14. Intriguingly, DENV NS1-induced inflammasome activation does not induce pyroptosis and rapid cell death; instead, macrophages maintain cellular viability while releasing IL-1β. Lastly, we show that caspase-1/11-deficient, but not NLRP3-deficient, mice are more susceptible to lethal DENV infection. Together, these results indicate that the inflammasome pathway acts as a sensor of DENV NS1 and plays a protective role during infection.

Introduction

Dengue virus (DENV) is a mosquito-borne flavivirus consisting of 4 serotypes (DENV1-4) that represents a growing burden on global public health, with cases increasing 10-fold over the past 20 years. Over 3.8 billion people are at risk of infection with DENV, estimated to reach 6.1 billion by 2080 as urban populations grow and climate change increases the suitable range for *Aedes* mosquitoes, the transmission vectors for DENV.(1) Of the estimated 105 million people infected by DENV annually, up to 51 million develop dengue; symptoms span a wide range of clinical outcomes from an acute febrile illness accompanied by joint and muscle pain to severe disease characterized by vascular leakage and thrombocytopenia, hemorrhagic manifestations, pulmonary edema, and hypovolemic shock.(2,3) The causes of endothelial dysfunction and vascular leak seen in severe dengue disease are likely multifactorial, but some studies suggest a "cytokine storm" triggered by uncontrolled viral replication and immune activation.(4,5) There are no current treatment options for severe dengue disease other than supportive care, due in part to an incomplete understanding of dengue pathogenesis.(6) This underscores a need to better understand both protective and pathogenic host pathways to develop future therapeutics for dengue.

DENV non-structural protein 1 (NS1) has drawn recent interest as a vaccine and therapeutic target for the prevention of severe dengue. DENV NS1 is an approximately 45-kDa protein that dimerizes after translation in infected cells.(7) Dimeric, intracellular NS1 associates with the lumen of the endoplasmic reticulum and participates in the formation of the viral replication complex.[9–11] NS1 is also secreted from infected cells as a tetramer and/or hexamer, with NS1 dimers oligomerizing around a lipid cargo enriched in triglycerides, cholesteryl esters and phospholipids.(7,11,12) Secreted NS1 plays multiple roles during infection, including binding and inactivating complement components and interacting directly with endothelial cells to induce endothelial hyperpermeability and pathogenic vascular leak.(13–17) Mice vaccinated with DENV NS1 are protected from lethal systemic DENV challenge in mouse models of infection, and blockade of NS1-induced endothelial hyperpermeability by glycan therapeutics or by NS1-specific monoclonal antibodies also reduces DENV-induced disease, emphasizing the pivotal roles NS1 plays in DENV replication and pathogenesis.(14,18–21) DENV NS1 has also been shown to induce the activation of pro-inflammatory cytokines such as TNF-α and IL-6 in both murine and human macrophages.(22–25) Studies in mice have identified a TLR4-dependent axis for pro-inflammatory cytokine induction, and it has been hypothesized that NS1-induced macrophage activation leads to cytokine storm and immunopathology; however, few studies have experimentally assessed the mechanisms by which NS1 induces inflammation and whether NS1-induced inflammation contributes to overall viral pathogenesis.

DENV has been shown to trigger multiple innate immune pathways that contribute to both host defense and pathogenesis.(26,27) Among these pathways are the inflammasomes, a class of innate immune sensors that surveil the cytosol for a broad range of pathogen or damage-associated molecular patterns (PAMPs/DAMPs).(28) Canonical inflammasomes recruit the cysteine protease caspase-1 via the apoptosis-associated speck-like protein containing CARD (ASC) protein.(29) Certain inflammasomes respond to PAMPs such as viral double-stranded DNA in the case of the AIM2 inflammasome, or can be triggered by pathogenic effectors; examples include sensing of viral protease activity by the NLRP1B and CARD8 inflammasomes, sensing of ion fluxes and membrane damage by the NLRP3 inflammasome, or sensing of toxin-induced Rho guanosine

triphosphatase (Rho GTPase) inactivation by the pyrin inflammasome.(28,30–33) Further, caspase-11 in mice and caspases-4 and -5 in humans can activate the non-canonical inflammasome, in which caspase-11/4/5 binding to lipid A from bacterial lipopolysaccharide (LPS) leads to activation of the NLRP3 inflammasome.(34,35)

Inflammasome signaling typically comprises a two-step process in which inflammasome components and substrates are first transcriptionally upregulated and/or 'primed', usually in response to PAMPs/DAMPs and nuclear factor-κB (NF-κB) signaling.(28) After priming, a second stimulus induces inflammasome oligomerization, leading to ASC recruitment and caspase-1 autoproteolytic processing into its active form.(29) The active caspase-1 protease can then cleave pro-IL-1β, pro-IL-18 and gasdermin D (GSDMD) into their bioactive forms. Cleavage of GSDMD leads to insertion and oligomerization of the N-terminal domain (GSDMD-NT) to form pores in the plasma membrane.(36) The formation of GSDMD pores canonically leads to pyroptosis, a form of inflammatory cell death; however, recent work has shown that GSDMD pore formation and pyroptosis are distinct events and that macrophages can release IL-1β from GSDMD pores without undergoing pyroptosis in response to certain stimuli.(37–41) GSDMD pores also facilitate the release of cleaved IL-1β and IL-18, which then serve as major mediators of inflammation contributing to host defense as well as driving immunopathology.(37,42) Many viruses have been shown to activate inflammasomes during infection, including influenza A virus, HIV, SARS-CoV-2, picornaviruses, and DENV.(27,33,43–45) Inflammasome activation by viruses can be protective and/or can contribute to pathogenic outcomes.(43,45–48) Ultimately, the impact of inflammasome activation depends on the context and timing of the infection; thus, understanding these complexities is crucial for designing inflammasome-targeted therapies as potential treatments for viral disease.

Several studies have begun to investigate whether DENV infection triggers inflammasome activation and how this might impact DENV pathogenesis. Studies have shown that *in vitro* DENV infection of mouse and human macrophages, human skin endothelial cells, and platelets, as well as infection in mice can induce inflammasome activation.(49–54) Clinically, IL-1β levels are also elevated in dengue patients, implicating a role for inflammasome activation in human DENV infections.(53,55) Mechanistic studies have implicated both the membrane (M) and NS2A/B proteins of DENV as viral triggers of the NLRP3 inflammasome.(49,52) *In vivo* studies using an adeno-associated virus (AAV) vector to induce DENV M expression suggested that DENV M can cause NLRP3-dependent vascular leak, though the relevance of M-induced inflammasome activation in DENV infection is unknown.(49) Another study showed that mice treated with an IL-1 receptor antagonist during DENV infection lost less weight and experienced less vascular leak compared to untreated controls.(53) Although it is established that DENV infection can induce inflammasome activation, the viral triggers and the contribution of inflammasome activation during infection remain open areas of investigation. In this study, we identify secreted NS1 as a trigger of the inflammasome pathway in a caspase-1-dependent manner that is independent of the NLRP3, pyrin, and AIM2 inflammasomes but dependent on CD14. Further, we demonstrate that caspase-1/11 deficiency, but not NLRP3 deficiency, makes mice more susceptible to DENV infection, indicating that inflammasome activation can be protective during DENV infection.

Results

DENV NS1 can activate the inflammasome pathway

Since DENV NS1 is secreted from infected cells and can activate macrophages to induce a pro-inflammatory response, we hypothesized that DENV NS1 could be a viral trigger of the inflammasome pathway in macrophages.(22) To test this hypothesis, we assessed whether DENV NS1 could activate the inflammasome pathway in mouse bone marrow-derived macrophages (BMDMs). BMDMs were first primed with PAM_3CSK_4, a synthetic triacylated lipopeptide TLR1/TLR2 agonist, and then treated with DENV NS1. Cell supernatants were assessed 24 hours (h) post-treatment for the presence of IL-1β as a readout of inflammasome activation. We found that DENV NS1 induced the release of IL-1β in BMDMs in a dose-dependent manner **(Figure 1A)**. Additionally, DENV NS1 induced the cleavage of pro-IL-1β, GSDMD, and pro-caspase-1 into their cleaved, bioactive components (IL-1β p17, GSDMD-N p31, and caspase-1 p20, respectively), confirming activation of the inflammasome pathway **(Figure 1B)**. Next, we obtained BMDMs from mice genetically deficient in caspase-1 and -11, required for canonical and non-canonical inflammasome signaling, respectively, and compared them to BMDMs from WT caspase-1/11-sufficient littermates and found that NS1-induced IL-1β release was abolished in BMDMs derived from caspase-1/11 knockout mice **(Figure 1C)**. Similarly, nigericin, a NLRP3 inflammasome agonist, was unable to induce IL-1β release in caspase-1/1-deficient macrophages **(Figure 1C)**. Consistent with these findings, the caspase-1-specific inhibitor AC-YVAD-cmk inhibited both DENV NS1 and nigericin-induced IL-1β release in a dose-dependent manner (**Figure 1D).**(56) Additionally, DENV NS1 was also able to induce cleavage of caspase-1 and the release of bioactive IL-1β in human THP-1-derived macrophages in a caspase-1 dependent manner **(Figure 1E-F).** Collectively, these data suggest that DENV NS1 induces inflammasome activation in a caspase-1-dependent manner in macrophages.

DENV NS1-mediated inflammasome activation is NLRP3-independent.

Since the NLRP3 inflammasome has previously been shown to be activated by other DENV proteins as well as by NS1 from the closely related Zika virus, we hypothesized that DENV NS1 might also activate the NLRP3 inflammasome. (49,52,57) Surprisingly, we found that DENV NS1 was still able to induce IL-1β cleavage and release in BMDMs derived from *Nlrp3*$^{-/-}$ mice, whereas IL-1β release was severely reduced in BMDMs derived from *Nlrp3*$^{-/-}$ mice treated with the NLRP3 inflammasome activator nigericin (**Figure 2A-B)**. Likewise, treatment of WT BMDMs with the NLRP3-specific inhibitor MCC950 inhibited nigericin-mediated IL-1β release in a dose-dependent manner, whereas DENV NS1-induced IL-1β release was unaffected by MCC950 treatment **(Figure 2C).**(58) These data suggest that DENV NS1-mediated inflammasome activation is independent of the NLRP3 inflammasome. Since IL-1β release downstream of the non-canonical inflammasome and the lipopolysaccharide (LPS)-triggered inflammasome pathway requires NLRP3, these results further suggest that NS1-induced inflammasome activation is not via caspase-11 or due to LPS contamination.(59) We then utilized CRISPR-Cas9 gene editing to knock out additional components in the inflammasome pathway via nucleofection of Cas9-guide RNA (gRNA) ribonucleoprotein complexes in WT BMDMs to attempt to identify the inflammasome pathway activated by DENV NS1. We targeted *Nlrp3* (encoding Nlrp3), *Aim2* (encoding Aim2), *Mefv* (encoding Pyrin) and *Casp1* in C57BL/6 mice using 2 guide RNAs per gene and used a non-targeting guide (NTG) as an experimental control. This approach achieved robust deletion of the target proteins, as assessed by Western blot (**Figure 2D).** We then treated

gene-edited BMDMs with DENV NS1 for 48h and assessed inflammasome activation by IL-1β release, as measured by ELISA. Corroborating the results from *Nlrp3*$^{-/-}$ mice, CRISPR-Cas9 knockout of *Nlrp3* did not affect DENV NS1-mediated inflammasome activation **(Figure 2E).** CRISPR-Cas9 knockout of the AIM2 and Pyrin inflammasomes also had no effect on DENV NS1-induced inflammasome activation. Thus, DENV NS1-mediated inflammasome activation in BMDMs is independent of the NLRP3, AIM2, and Pyrin inflammasomes.

DENV NS1-induced inflammasome activation is dependent on CD14 and does not lead to cell death

We observed that DENV NS1-treated BMDMs maintain their morphology and do not undergo detectable cell death, in contrast to nigericin-treated cells, despite evidence of cleavage of GSDMD (**Figure 1B)**. Measurement of lactase dehydrogenase (LDH) is often used as a proxy for pyroptotic cell death; consistent with this, we found that PAM_3CSK_4-primed BMDMs treated with nigericin rapidly released near maximum amounts of LDH 2h post-treatment.(60–62) In contrast, PAM_3CSK_4-primed, NS1-treated BMDMs released LDH at similar levels to the BMDMs primed with PAM_3CSK_4 alone, up to 24h post-treatment **(Figure 3A).** In addition**,** at 24h post-treatment, nigericin-treated macrophages displayed high levels of staining by an amine-reactive dye used to fluorescently label dead cells, whereas DENV NS1-treated macrophages were labeled at similar levels to the untreated controls **(Figure 3B)**. These lines of evidence indicate that DENV NS1 induces inflammasome activation without inducing cell death. Previous studies have shown that pyroptosis and inflammasome activation are separable processes and that myeloid cells can release IL-1β over time without undergoing pyroptosis.(38,39,41) One such study showed that oxidized phospholipids can enhance IL-1β release without inducing cell death through engagement of CD14 in macrophages and dendritic cells.(63) Since DENV NS1 is secreted from infected cells as an oligomer surrounding a lipid cargo, we hypothesized that DENV NS1 might also enhance IL-1β release by delivering lipids to cells in a CD14-dependent manner. Indeed, we found that DENV NS1 was able to deplete surface levels of CD14 on BMDMs, as was LPS, a canonical CD14 ligand, suggesting that DENV NS1 can induce endocytosis of CD14 similar to other characterized CD14 ligands **(Figure 3C).** We next generated CD14-deficient BMDMs by nucleofection **(Figure 3D)** and treated these cells with DENV NS1. We found that IL-1β release was abrogated in DENV NS1-treated CD14-deficient BMDMs compared to NTG control cells, suggesting that CD14 is required for DENV NS1 inflammasome activation **(Figure 3E)**. Nigericin-treated CD14 knockout BMDMs still induced IL-1β release at similar levels to NTG controls **(Figure 3F),** and CD14-deficient BMDMs were able to secrete TNF-α in response to PAM_3CSK_4 **(Figure 3G)**, showing that NF-κB responses needed for inflammasome priming were intact, leading us to conclude that the lack of NS1-triggered inflammasome activation in CD14-deficient macrophages was not a consequence of off-target effects in other inflammasome pathways. These findings suggest that DENV NS1 inflammasome activation is CD14-dependent and induces Il-1β release without pyroptosis.

Caspase-1/11 mediates a protective response during DENV infection

We have previously characterized a lethal mouse model of DENV infection and disease consisting of interferon α/β receptor-deficient (*Ifnar*$^{-/-}$) mice infected with a mouse-adapted DENV2 strain (D220).(64) To determine how inflammasome activation impacts DENV pathogenesis upon viral infection, we crossed *Casp1/11*$^{-/-}$ or *Nlrp3*$^{-/-}$ separately with *Ifnar*$^{-/-}$ mice to generate *Casp1/11*$^{-/-}$ *x Ifnar*$^{-/-}$ and *Nlrp3*$^{-/-}$ *x Ifnar*$^{-/-}$ double-deficient mice and infected them with DENV2 D220. We

found that *Casp1/11* $^{-/-}$*x Ifnar* $^{-/-}$ mice were significantly more susceptible to lethal DENV2 infection and showed greater morbidity compared to littermate controls with functional *Casp1/11* alleles **(Figure 4A-B)**, indicating that inflammasome activation plays a protective role during DENV2 infection in mice. Previous studies have implicated the NLRP3 inflammasome as playing a pathogenic role during DENV infection; thus, mice deficient in NLRP3 would be predicted to exhibit less severe disease compared to NLRP3-functional mice. However, we found that *Nlrp3* $^{-/-}$*x Ifnar* $^{-/-}$ mice displayed similar outcomes after lethal DENV2 challenge as littermate controls with functional *Nlrp3* alleles across both high and low doses of DENV2 D220 **(Figure 4C-D)**. Thus, these data suggest that while inflammasomes can play a protective role during DENV infection, this protection is independent of the NLRP3 inflammasome, consistent with NS1-triggered inflammasome activation patterns that we measured *in vitro*.

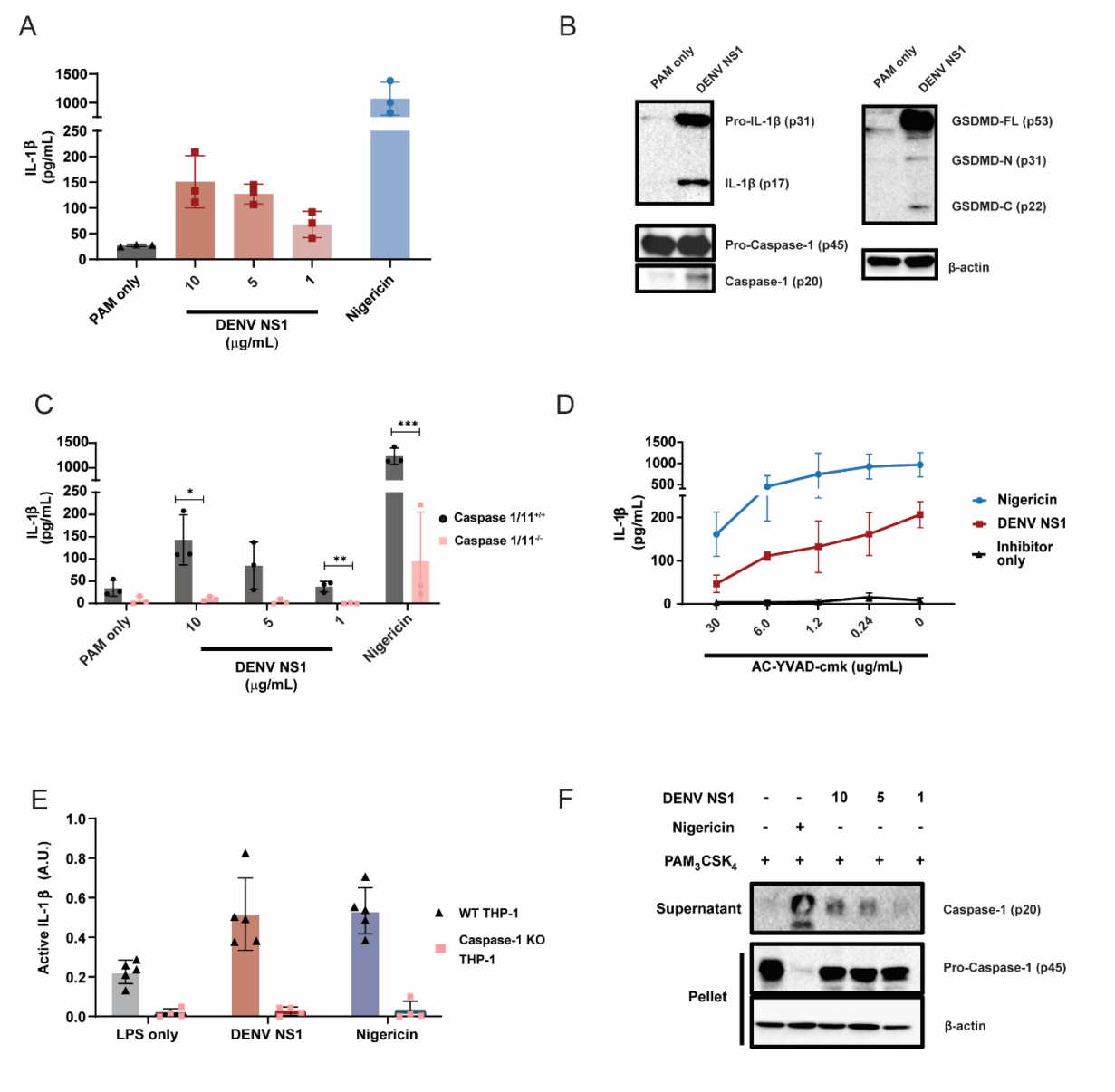

Figure 1. DENV NS1 can activate the inflammasome. (A) BMDMs were primed with PAM_3CSK_4 (1μg/mL) for 17 h and then treated with DENV2 NS1 at indicated concentrations, treated with 5μM nigericin, or left untreated (PAM only). IL-1β levels in the supernatant after 2h (nigericin) or 24h (NS1 and PAM only) were measured by ELISA. *p<0.05 as determined by one-way ANOVA with Dunn's multiple comparison correction. **(B)** Representative Western blots of BMDM cell lysates after priming with PAM_3CSK_4 (1μg/mL) for 17h and treatment with 10ug/mL DENV2 NS1 (DENV NS1) or PAM_3CSK_4 treatment for 24h without NS1 treatment (PAM only). **(C)** WT and *Casp1/11*$^{-/-}$ BMDMs were primed with PAM_3CSK_4 (1μg/mL) for 17h and then treated with DENV2 NS1 at the indicated concentrations, nigericin (5μM), or medium (PAM only). IL-1β levels in the supernatant after 2h (Nigericin) or 24h (NS1 and PAM only) were measured by ELISA. *p<0.05, **p<0.01. Statistical significance was determined using two-way ANOVA followed by multiple t-tests using Holm-Sidak correction. **(D)** BMDMs were primed with PAM_3CSK_4 (1μg/mL)

for 17h and then pre-treated with Ac-YVAD-cmk at the indicated concentrations before addition of DENV2 NS1 (10μg/mL), nigericin (5μM), or medium (Inhibitor only). IL-1β levels in supernatant 2h (Nigericin) or 24h (NS1 and PAM only) were measured by ELISA. **(E)** WT or *Casp-1*$^{-/-}$ THP-1 human monocytes were differentiated into macrophages in 10ng/mL PMA and primed with medium or LPS for 4h. Primed macrophages were treated with DENV NS1 (10μg/mL) or left untreated (LPS only). Eighteen hours later, supernatants were collected. Cells were stimulated with 5μM nigericin for 2h as a positive control. Bioactive IL-1β in supernatants was measured using HEK-Blue IL-1R reporter cells. **(F)** Representative Western blots of THP-1 macrophage cell lysates after priming with PAM_3CSK_4 (100ng/mL) for 17h and treatment with DENV2 NS1 at indicated concentrations (μg/mL), treatment with 5μM nigericin, or no treatment for 24h. The data are shown as the mean ± standard deviation (SD) of 3 independent experiments (A, C-D) or 4-6 independent experiments (E) or a representative image taken from 2 biological replicates (B,F).

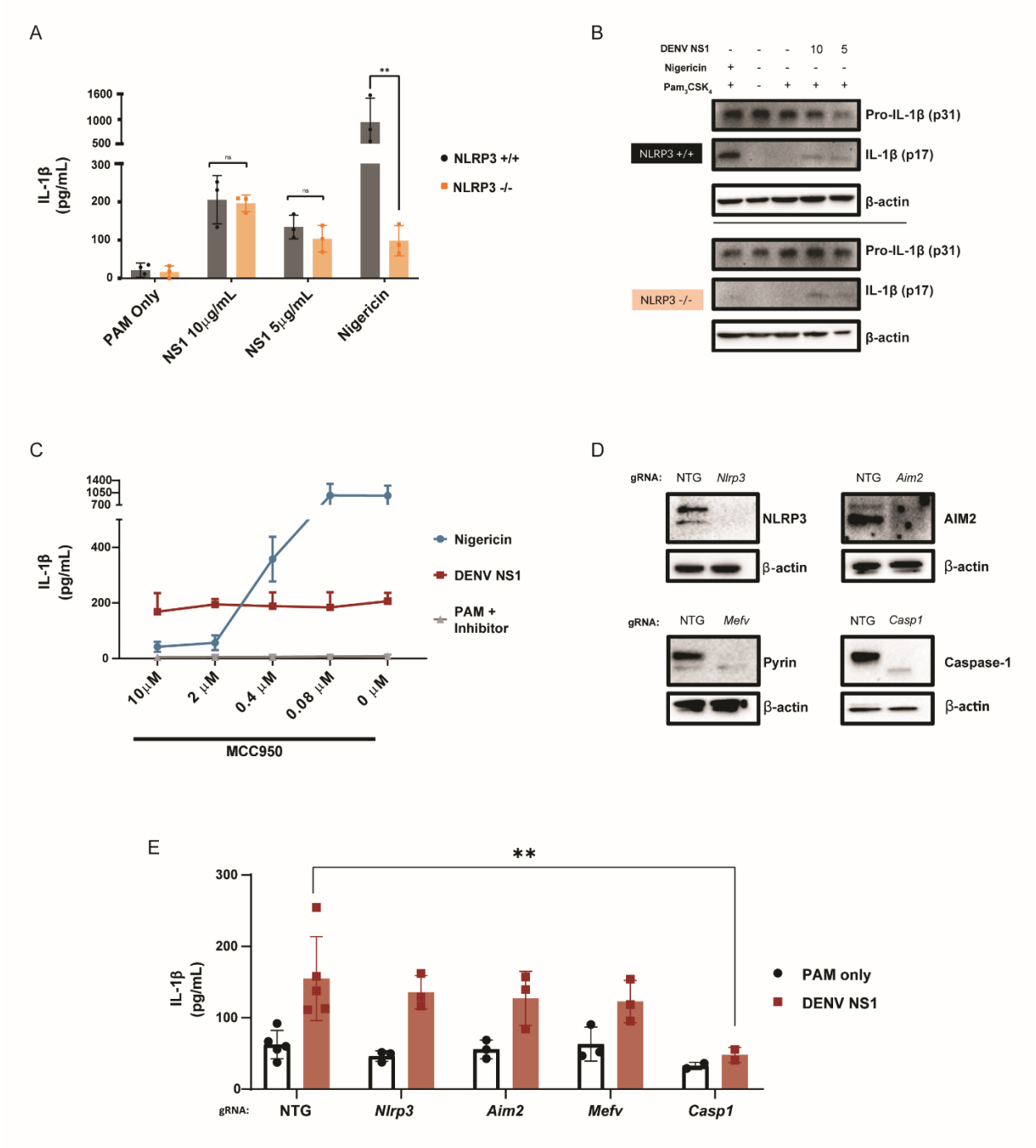

Figure 2. DENV NS1-induced inflammasome activation is NLPR3-independent. **(A)** WT and *Nlrp3* $^{-/-}$ BMDMs were primed with PAM_3CSK_4 (1μg/mL) for 17h and then treated with DENV2 NS1 at indicated concentrations, nigericin (5μM), or medium (PAM only). IL-1β levels in supernatant 2h (nigericin) or 24h (NS1 and PAM only) were measured by ELISA. *p<0.05, **p<0.01. Statistical significance was determined using two-way ANOVA followed by multiple t-tests with Holm-Sidak correction. **(B)** Representative Western blots of cell lysates from WT and *Nlrp3*$^{-/-}$ BMDMs after priming with PAM_3CSK_4 (1μg/mL) for 17h and treatment with

DENV2 NS1 (10 or 5 μg/mL), treatment with nigericin (5μM), or no treatment for 24h. **(C)** BMDMs were primed with PAM_3CSK_4 (1μg/mL) for 17h and then pre-treated with MCC950 at the indicated concentrations before addition of DENV2 NS1 (10μg/mL), nigericin (5μM), or medium (Inhibitor only). IL-1β levels in the supernatant after 2h (Nigericin) or 24h (NS1 and PAM only) were measured by ELISA. **(D)** Representative Western blots of cell lysates from BMDMs nucleofected with Cas9-gRNA ribonuclear protein complexes to knock out the indicated genes. Two gRNAs per gene were used per nucleofection. NTG = non-targeting guide. (**E)** Knockout BMDMs from **(D)** were primed with PAM_3CSK_4 (1μg/mL) for 17h and treated with DENV2 NS1 (10μg/mL) or left untreated for 48h. *$p<0.05$. Statistical significance was determined using two-way ANOVA followed by multiple t-tests with Holm-Sidak correction. The data are shown as the mean ± SD of 3 biological replicates (A,C), a representative image taken from 2 biological replicates (B,D), or data pooled from 5 independent experiments with 3 biological replicates per guide (E).

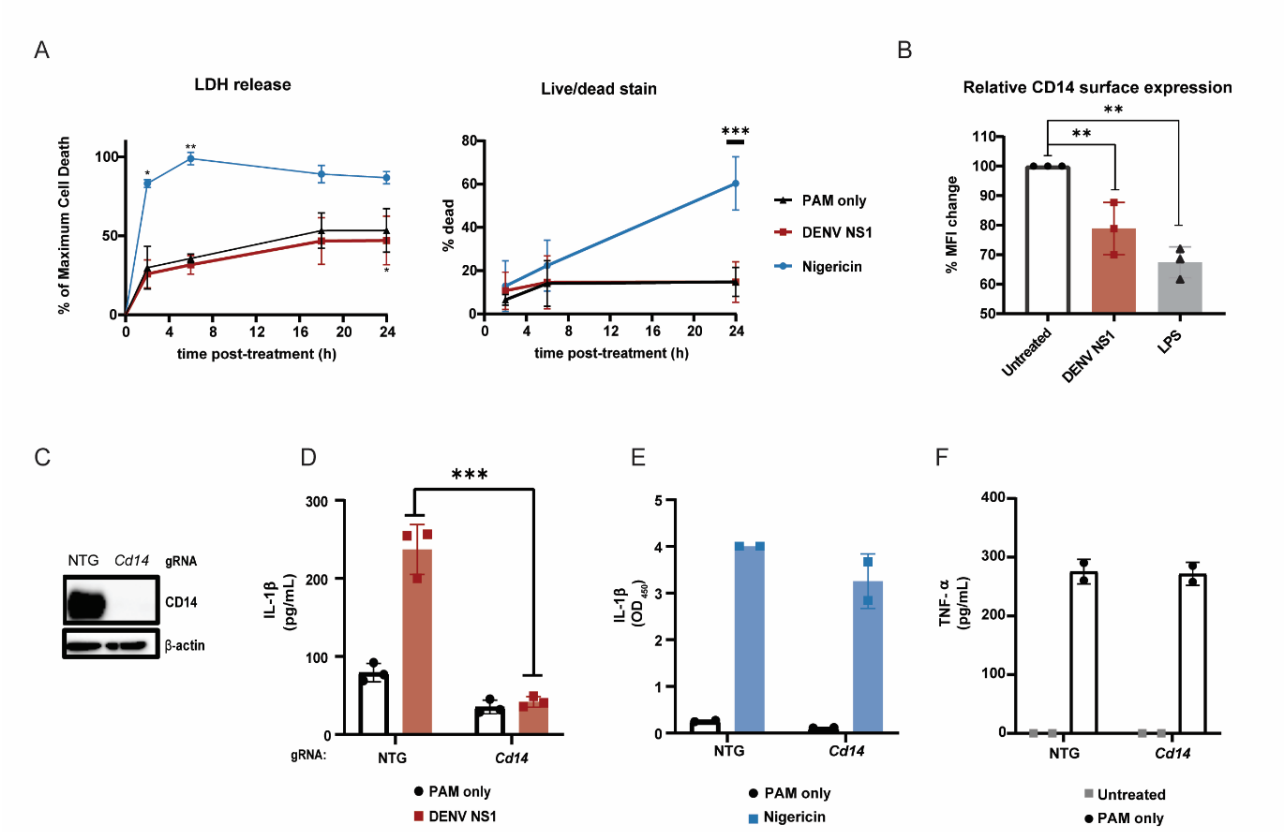

Figure 3. DENV NS1 induces inflammasome activation in macrophages in a CD14-dependent manner without inducing cell death. (A-B) BMDMs were primed with PAM_3CSK_4 (1µg/mL) for 17h and then treated with DENV2 NS1 (10µg/mL), nigericin (5µM), or medium (PAM only). **(A)** At the indicated timepoints, supernatants were assessed for lactase dehydrogenase (LDH) levels as a proxy for cell death. LDH levels were calculated as a percentage of maximum LDH release. **(B)** Cells were stained using a LIVE/DEAD Fixable Far Red stain and analyzed by flow cytometry. *p<0.05 **p<0.01 ***p<0.001. Statistical significance was determined using two-way ANOVA with Dunnetts's multiple comparison test. **(C)** BMDMs were primed with PAM_3CSK_4 (1µg/mL) for 17h and then treated with DENV2 NS1 (10µg/mL), LPS (5µg/mL) or no treatment (Untreated). After 30 min, cells were stained for surface CD14 expression and analyzed by flow cytometry. Data are normalized as a percentage of the median fluorescence intensity of the treatment groups divided by the untreated control. **p<0.01. Statistical significance was determined using one-way ANOVA with Holm-Sidak's multiple comparisons test. **(D)** Representative Western blots of cell lysates from BMDMs nucleofected with either NTG or CD14 Cas9-gRNA ribonuclear protein complexes. **(E-G)** BMDMs from **(D)** were primed with PAM_3CSK_4 (1µg/mL) for 17h and treated with DENV2 NS1 (10µg/mL), nigericin (5µM) or no treatment for 48h. IL-1β levels in supernatant after 24h (Nigericin) or 48h (NS1 and PAM only) were measured by ELISA **(E-F)**. TNF-α levels were measured in supernatants 17h post-priming with PAM_3CSK_4 **(G).** ***p<0.001. Statistical significance was determined using two-way ANOVA with Sidak's multiple comparison test. The data are shown as the mean ± SD of 3 biological replicates (A,C,E), 5 biological replicates (B), or 2 biological replicates (F-G) or a representative image taken from 2 biological replicates (D).

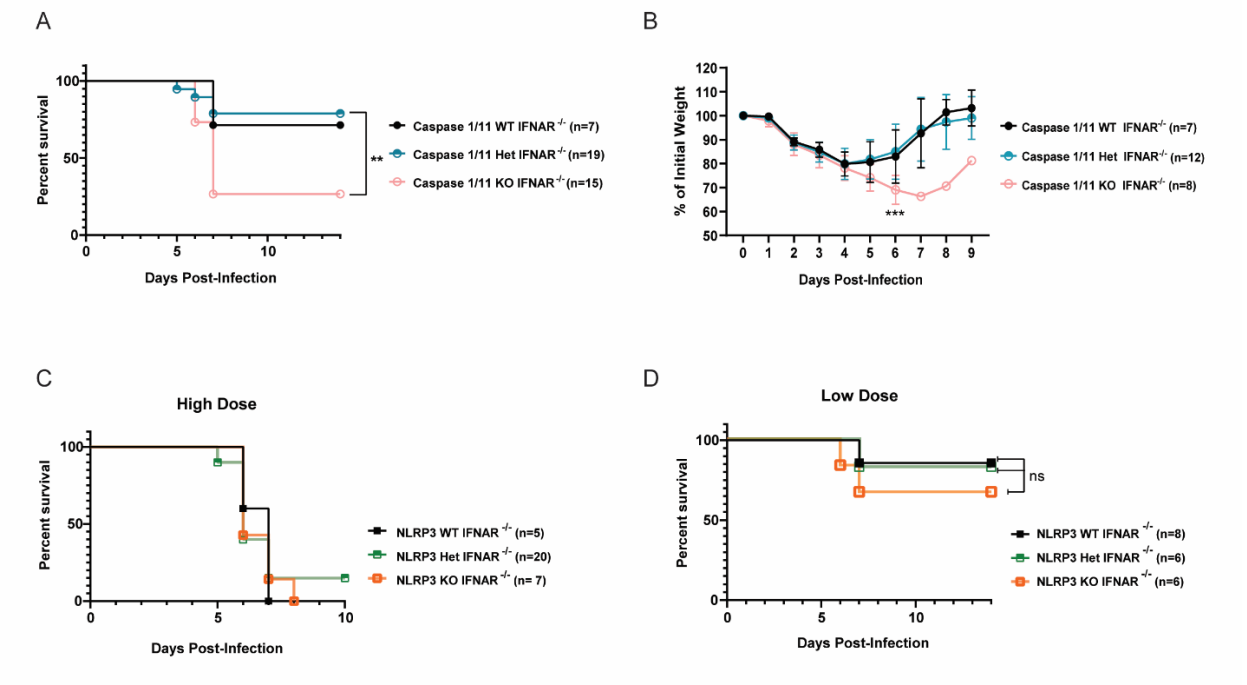

Figure 4. The inflammasome is protective during DENV infection. (A-B) Survival curves **(A)** and weight loss over time **(B)** of *Casp1/11*$^{+/+}$*Ifnar* $^{-/-}$ (Caspase 1/11 WT), *Casp1/11* $^{+/-}$*Ifnar* $^{-/-}$ (Caspase 1/11 Het), or *Casp1/11* $^{-/-}$*Ifnar* $^{-/-}$ (Caspase 1/11 KO) littermates infected intravenously with 3 x 10^5 PFU of DENV2 D220. Survival was monitored over 14 days. Weight loss was monitored over 9 days. Numbers in parentheses indicate the numbers of mice in each group. **p<0.01. Statistical significance was determined by Mantel–Cox log-rank test **(A)** or two-way ANOVA with Holm-Sidak's multiple comparisons test **(B)**. **(C-D)** Survival curves of *Nlrp3* $^{+/+}$*Ifnar* $^{-/-}$ (NLRP3 WT), *Nlrp3* $^{+/-}$*Ifnar* $^{-/-}$ (NLRP3 Het), or *Nlrp3* $^{-/-}$*Ifnar* $^{-/-}$ (NLRP3 KO) littermates infected intravenously with a 5 x 10^5 PFU **(**High Dose**)** **(C)** or 7.5 x 10^4 PFU **(**Low Dose**)** **(D)** of DENV2 D220 and monitored over 10 days. Numbers in parentheses indicate the numbers of mice in each group.

Discussion

In this study, we demonstrate that the inflammasome pathway is activated by DENV NS1 in mouse BMDMs and human THP-1 macrophages. Interestingly, we find that DENV NS1-induced inflammasome activation is independent of the NLRP3, AIM2 and Pyrin inflammasomes in BMDMs and that NLRP3 deficiency in mice does not affect the outcome of DENV infection, in contrast to previous reports ascribing a pathogenic role to the NLRP3 inflammasome during DENV infection.(49,52) Instead, we find that inflammasome activation may play a protective role during DENV infection, as caspase-1/11-deficient mice are more susceptible to DENV infection compared to their caspsase-1/11-functional littermates.

Our study experimentally assessed the contribution of inflammasome activation to DENV infection *in vivo* using genetically deficient mice, in contrast to previous studies. In one study, investigators sought to define the contribution of DENV M to DENV pathogenesis and found that NLRP3-deficient mice infected with an adeno-associated virus expressing DENV M showed less pathology than WT controls.(49) However, it is not clear how generalizable this model is to DENV pathogenesis, as the study relied on expression of DENV M protein by an adeno-associated virus rather than by infection with DENV. Our study differs in that we use a DENV2 strain (D220) in a well-characterized IFNAR-deficient mouse model, which has been previously shown to more readily model features of DENV pathogenesis observed in severe disease in humans, such as vascular leak.(64,65) Using this model, we found that caspase-1/11-deficient mice are more susceptible to DENV infection than their caspase-1/11 functional littermates, implicating the inflammasome pathway as a protective pathway during DENV infection. Further, we find that NLRP3-deficient, IFNAR-deficient mice are not protected from lethal DENV infection and succumb to infection at similar rates as NLRP3-sufficient IFNAR-deficient mice, thus suggesting that the NLRP3 inflammasome does not contribute to pathogenesis in the context of DENV infection, at least in our DENV D220 mouse model of vascular leak syndrome. Another study showed that treatment of mice with IL-1 receptor antagonist can reduce pathology during DENV infection in IFNAR-deficient mice.(53) Our results do not necessarily conflict with this prior study since there can be IL-1β-independent effects of inflammasome activation.(66) Further studies are needed to understand the mechanistic basis of caspase-1/11-mediated protection during DENV infection.

The timing and magnitude of inflammasome activation are key factors in determining whether activation is protective or detrimental to the host. Administration of the NLRP3 inhibitor MCC950 at days 1 and 3 after influenza A virus (IAV) infection led to hyper-susceptibility to lethality, whereas treatment on days 3 and 5 post-infection protected mice against IAV-induced disease.(48) Thus, in this context, the NLRP3 inflammasome plays both a protective role early in infection and a pathogenic role later in infection. The use of genetic models in our study implicates a protective role for inflammasome activation early in DENV infection as well, though our data does not preclude the possibility of inflammasome activation being pathogenic in later stages of infection.

In addition, increased inflammasome activation was observed under antibody-dependent enhancement (ADE) conditions during a secondary DENV infection.(67,68) ADE is a phenomenon whereby cross-reactive non-neutralizing anti-DENV antibodies elicited from a primary DENV infection facilitate Fcγ receptor-mediated viral entry and replication in immune cells during a secondary DENV infection with a different serotype, resulting in higher viremia and

increased immune activation.(69,70) Thus, the altered viremic and immune context of ADE may also determine whether inflammasome activation still plays a protective role or contributes to DENV disease. While our study ascribes a protective role for inflammasome activation during DENV infection, more investigation is needed to understand whether targeting the inflammasome pathway at specific times and under ADE conditions can lead to therapeutic benefit during severe dengue.

Our data raises some interesting questions regarding the mechanism of DENV NS1-induced inflammasome activation. While we establish that DENV NS1 induces inflammasome activation independently of the NLRP3 inflammasome using multiple orthogonal genetic and chemical approaches, the identity of the inflammasome activated by DENV NS1 is unknown. CRISPR-Cas9-mediated knockout of other, well-studied inflammasomes such as Pyrin and AIM2 had no effect on DENV NS1-induced inflammasome activation, suggesting that these inflammasomes may not be involved or may be redundant with each other. Further work is needed to establish whether DENV NS1 may activate other inflammasomes such as NLRP1B, CARD8, NLRP6 and NLRP10 inflammasomes, as well as to provide deeper insight into the mechanisms behind inflammasome sensing of DENV NS1 in macrophages.(71,72)

Interestingly, we find here that NS1 can activate the inflammasome pathway through a CD14-dependent pathway without triggering detectable cell death. It has become increasingly appreciated that inflammasome activation and the formation of GSDMD pores in cell membranes do not necessarily lead to pyroptotic cell death, but it is unknown how different inflammasome stimuli induce different cell fates(39). Previous studies have implicated CD14 as a receptor for oxidized phospholipids such as 1-palmitoyl-2-glutaryl-sn-glycero-3-phosphocholine (PGPC) and 1-palmitoyl-2-(5′-oxo-valeroyl)-sn-glycero-3-phosphocholine (POV-PC); these phospholipids engage CD14 to promote the release of IL-1β from living macrophages via a pathway dependent on caspase-11, caspase-1 and NLRP3.(40,63,73) We found that, similar to POV-PC and PGPC, DENV NS1 can deplete CD14 from the surface of macrophages and is dependent on CD14 to activate the inflammasome pathway. Since LPS is a canonical ligand of CD14 and cytosolic LPS can activate the non-canonical inflammasome pathway, it was critical to eliminate the potential role of LPS in our studies. We primed cells with PAM_3CSK_4 and regularly tested DENV NS1 stocks for LPS contamination to ensure that LPS exposure was not driving IL-1β release in our experiments. Importantly, non-canonical inflammasome activation by cytosolic LPS is dependent on the NLRP3 inflammasome, whereas our studies indicate that DENV NS1 activates an inflammasome pathway that is independent of NLRP3. Thus, it is likely that DENV NS1-induced inflammasome activation is not due to contaminating LPS; rather, we propose that, like oxidized phospholipids, DENV NS1 utilizes CD14 to induce IL-1β release in macrophages. However, the mechanism by which oxidized phospholipids enhance IL-1β release remains poorly understood, and further work will be required to determine whether DENV NS1 operates via a similar or distinct mechanism.

A previous study reported that NS1-associated lipid cargo is enriched in triglycerides, cholesterol, and phospholipids, lipids commonly found in cell membranes.(11) We speculate that NS1 could act as a carrier of oxidized phospholipids generated from infected cells and subsequently be detected by macrophages at sites distal from infection, activating an inflammasome and cytokine response. We were unable to determine whether oxidized phospholipids were present within the

lipid cargo of our NS1 in this study; however, it would be interesting to explore whether the inflammatory capacity of NS1 is ultimately modulated by the lipids within the lipid cargo.

Overall, our results provide insight into interactions between DENV NS1 and macrophages and the role of NS1 in protection. Our current study suggests that NS1-myeloid cell interactions can be protective during DENV infection and that activation of pro-inflammatory circuits during DENV infection can be beneficial. Thus, we find that the activation of pro-inflammatory immune responses does not always lead to detrimental outcomes during DENV infection, contrary to many studies in the field.(22,27,74) Instead, a more nuanced view accounting for the timing and magnitude of the inflammatory response may be a crucial aspect of understanding both the beneficial and detrimental aspects of inflammation in DENV infection. Our data suggest that further investigation into understanding the delicate balance and precise contexts in which cytokines can be protective and/or pathogenesis during DENV infection will be crucial for developing novel therapeutics and identifying the best biomarkers to assess risk of progression to severe disease.

Materials and Methods

Mice

All mice were bred in-house in compliance with Federal and University regulations. All experiments involving animals were pre-approved by the Animal Care and Use Committee (ACUC) of UC Berkeley under protocol AUP-2014-08-6638-2 and maintained under specific pathogen-free conditions. Wildtype (WT) C57BL/6 mice were obtained from Jackson Labs and used for preparation of bone marrow-derived macrophage (BMDMs) . *Nlrp3*$^{-/-}$ and *Casp-1/11*$^{-/-}$ C57BL/6 mice were provided by Dr. Russell Vance and maintained in the Harris lab mouse colony. *Nlrp3*$^{+/-}$ and *Casp 1/11*$^{+/-}$ mice were bred to generate the corresponding WT $^{(+/+)}$ or deficient ($^{-/-}$) litermates mice the corresponding $^{(+/+)}$ or deficient ($^{-/-}$) litermates mice for all experiments. For *in vivo* experiments involving DENV2 infection, *Nlrp3*$^{-/-}$ and *Casp 1/11*$^{-/-}$ were bred with C57BL/6 mice deficient in the interferon α/β receptor (*Ifnar*$^{-/-}$) to generate doubly-deficient *Nlrp3*$^{+/-}$ x *Ifnar*$^{-/-}$ or *Casp-1/11*$^{+/-}$ x *Ifnar*$^{-/-}$ mice by backcrossing *Nlrp3*$^{-/-}$ and *Casp-1/11*$^{-/-}$ mice with *Ifnar*$^{-/-}$ mice over 6 generations. The genotypes of mice used for breeding were tracked via PCR and gel electrophoresis. *Nlrp3*$^{+/-}$ x *Ifnar*$^{-/-}$ or *Casp-1/11*$^{+/-}$ x *Ifnar*$^{-/-}$ mice were bred to generate littermate WT, heterozygous, or KO mice at the *Nlrp3*$^{-/-}$ or *Casp-1/11*$^{-/-}$ allele.

Individual PCR reactions were utilized to confirm the WT genotype and genetically deficient genotype for *Casp-1/11* and *Nlrp3*. The primers for each of these reactions were as follows: *Caspase 1/11* WT (*CATGCCTGAATAATGATCACC* and *GAAGAGATGTTACAGAAGCC*), *Caspase 1/11*-deficient(*GCGCCTCCCCTACCCGG* and *CTGTGGTGACTAACCGATAA*), *Nlrp3* WT (*CCACCTGTCTTTCTCTCTCTGGGC* and *CCTAAGGTAAGCTTTTGTCACCCAGG*), *Nlrp3*-deficient (*TTCCATTACAGTCACTCCAGATGT* and *TGCCTGCTCTTTACTGAAGG*). To determine the IFNAR genotype of the mice, a multiplex PCR protocol consisting of three primers was used (*CGAGGCGAAGTGGTTAAAAG*, *ACGGATCAACCTCATTCCAC*, and *AATTCGCCAATGACAAGACG*).

Viral stocks and proteins

A mouse-attenuated strain of DENV2, D220, was utilized for infection of *Ifnar*$^{-/-}$ mice.(64) The D220 strain was derived from the Taiwanese DENV2DENV2 isolate PL046 and is a further modification of the D2S10 strain, as described previously.(64) Viral stocks were titered using focus-forming assays on Vero cells. All virus stocks were confirmed to be mycoplasma-free. Recombinant DENV2 NS1 (Thailand/16681/84) was produced in mammalian HEK293 cells or purchased from The Native Antigen Company (Oxford, UK). All NS1 stocks were certified to be endotoxin-free and >95% purity.

DENV mouse model

Six- to eight-week-old littermate mice of either gender were challenged with DENV via retroorbital intravenous (IV) injection of the indicated plaque-forming units (PFU) of the DENV2 D220 strain. Mice were observed for morbidity and mortality over a 2-week period. Morbidity of mice was assessed utilizing a standardized 1-5 scoring system as follows: 1 = no signs of lethargy, mice are considered healthy; 2 = mild signs of lethargy and fur ruffling; 3 = hunched posture, further fur ruffling, failure to groom, and intermediate level of lethargy; 4 = hunched posture with severe lethargy and limited mobility, while still being able to cross the cage upon stimulation; and 5 = moribund with limited to no mobility and inability to reach food or water. Mice scored as 4

were monitored twice per day until recovery or until reaching moribund status. Moribund mice were euthanized immediately. Mice were also weighed to measure weight changes throughout the infection period.

BMDM generation

BMDMs were generated from 8-13-week-old WT C57BL/6 mice purchased from Jackson Laboratories or 8-13-week-old C57BL/6 littermate mice of the following genotypes: *Casp-1/11*$^{-/-}$, *Casp-1/11*$^{+/+}$, *Nlrp3*$^{-/-}$, and *NLRP3*$^{+/+}$. Additionally, BMDMs were generated from 8-13-week-old WT C57BL/6 mice purchased from Jackson Laboratories.*Nlrp3*$^{+/+}$. Bone marrow was extracted from the femur and tibia of dissected mice and plated on non-tissue culture-treated 15-cm Petri dishes at a density of 1 x 10^7 cells per plate in macrophage differentiation medium (DMEM, Gibco) supplemented with 2mM L-glutamine, 10% fetal bovine serum (FBS; Corning), 1% penicillin/streptomycin (Pen/Strep, Gibco), and 10% macrophage colony-stimulating factor (M-CSF) containing supernatant solution harvested from 3T3-CSF cells and cultured at 37°C with 5% CO_2 for 7 days. On day 3 of incubation, cells were supplemented with additional macrophage differentiation medium. On day 7, differentiated BMDM cells were harvested by incubating the plated cells in phosphate-buffered saline without calcium and magnesium (PBS) at 4°C for 20 minutes (min). The BMDM cells were then removed from the plate by gentle spraying with PBS, resuspended in DMEM supplemented with 1% Pen-Strep, 40% FBS, and 10% DMSO and frozen in liquid nitrogen until future use.

BMDM inflammasome activation assay

A macrophage-based assay was adapted from previously described protocols to assess inflammasome activation in BMDMs.(60) Frozen BMDMs were thawed and plated in 24-well or 96-well tissue culture-treated, flat-bottom plates in complete DMEM (DMEM + 2mM L-glutamine + 10% FBS + 1% Pen/Strep) at a density of 1x10^6 or 2x10^5 cells per well, respectively. After plating, cells were left to rest at 37°C and 5% CO_2 overnight. BMDMs were then primed using 1μg/mL Pam_3CSK_4 (InvivoGen) for 17 hours (h) or left untreated. Primed BMDMs were stimulated with DENV NS1, 5μM nigericin (InvivoGen), or left untreated. After 24h, supernatants were spun down at 10,600 x g for 10 minutes, and the cell-free supernatant was collected. BMDM layers were washed twice with PBS and then lysed in RIPA buffer (150mM NaCl, 1% Nonidet P-40, 0.5% sodium deoxycholate, 0.1% sodium dodecyl sulfate (SDS), 50mM Tris pH 7.4) supplemented with protease inhibitor (Roche). Supernatants and cell lysates were stored at -80°C until further analysis. For experiments involving inhibitors, the NLRP3 inhibitor MCC950 (InvivoGen) or caspase-1 inhibitor Ac-YVAD-cmk (InvivoGen) were added at indicated concentrations 30 min prior to treatment with DENV2 NS1 or nigericin.

Cell culture

HEK-Blue-IL-1β cells were obtained from InvivoGen (catalog # hkb-il1b) and grown in complete medium containing DMEM, 10% FBS, 1% Pen/Strep, 100μg/mL Zeocin (Invivogen), and 200μg/mL Hygromycin B Gold (InvivioGen). WT THP-1 cells or *casp-1*$^{-/-}$ THP-1 were purchased from InvivoGen and grown in complete medium containing RPMI (Gibco), 10% FBS, and 1% Pen/Strep. HEK-Blue IL-1β reporter cells were grown and assayed in 96-well plates.
All cell lines were routinely tested for mycoplasma by PCR kit (ATCC, Manassas, VA).

THP-1 inflammasome activation assay

To assess inflammasome activation in THP-1 macrophages, WT or *casp-1*$^{-/-}$ THP-1 human monocytes were differentiated into macrophages in 10ng/mL phorbol 12-myristate 13-acetate (PMA) and primed with medium or 1μg/mL LPS for 4h. Primed macrophages were treated with 10μg/mL DENV NS1 or left untreated (LPS only). 18h later, supernatants were collected. Cells were stimulated with 5μM nigericin for 2h as a positive control. Supernatants were then assessed for bioactive IL-1β using a HEK-Blue IL-1β reporter assay. To assess cleavage of caspase-1 in THP-1 macrophages, WT THP-1 human monocytes were differentiated into macrophages in 10ng/mL PMA and primed with medium or 100 ng/mL Pam_3CSK_4 for 17h. Primed macrophages were then treated with DENV NS1 or 5μM nigericin in RPMI + 2% FBS + 1% Pen/Strep for 24h. Supernatants were collected, and cells were lysed with RIPA buffer. Proteins in supernatant were precipitated by methanol/chloroform precipitation and resuspended in 50uL of 1X SDS-PAGE sample buffer (0.1% β-mercaptoethanol, 0.0005% bromophenol blue, 10% glycerol, 2% SDS, 63mM Tris-HCl pH 6.8).

HEK-Blue IL-1β reporter assay

To quantify the levels of bioactive IL-1β released from cells, we employed HEK-Blue IL-1β reporter cells. In these cells, binding of IL-1β to the surface receptor IL-1R1 results in the downstream activation of NF-κB and subsequent production of secreted embryonic alkaline phosphatase (SEAP) in a dose-dependent manner. SEAP levels were detected using a colorimetric substrate assay, QUANTI-Blue (InvivoGen) by measuring an increase in absorbance at OD655. Culture supernatant from THP-1 cells was added to HEK-Blue IL-1β reporter cells plated in 96-well format in a total volume of 200 μl per well. After 24h, SEAP levels were assayed by adding 20 μl of the supernatant from HEK-Blue IL-1β reporter cells to 180 μl of QUANTI-Blue colorimetric substrate following the manufacturer's protocol. After incubation at 37°C for 30-60 min, absorbance at OD_{655} was measured on a microplate reader.

CRISPR-Cas9-mediated gene editing in primary BMDMs

CRISPR-Cas9 gene editing was performed in WT BMDMs to knock out specified genes using a nucleofection-based approach.(75) Bone marrow from WT B6 mice was isolated, and cells were differentiated as previously described. On day 5 of macrophage differentiation, BMDMs were harvested and resuspended in P3 Primary Cell Nucleofector Solution with Supplement (Lonza). Separately, Cas9-ribonuclear protein (RNP) complexes were made by incubating *S. pyogenes* Cas9 with 2 nuclear localization signals (SpCas9-2NLS, Synthego) and 2 guide RNAs per gene (Synthego), together with Alt-R™ Cas9 Electroporation Enhancer (IDT) at room temperature for 25 min. BMDMs ($4x10^6$ per gene target) were mixed with RNP complex, and cells were nucleofected in 16-well Nucleocuvette strips (Lonza) using a 4D-Nucelofector® (Lonza). Nucleofected cells were then seeded in non-tissue culture-treated 15-cm Petri dishes in macrophage differentiation medium and differentiated for an additional 5 days, with medium changes every 2 days. After differentiation, gene-edited macrophages were harvested and used in the previously described inflammasome activation assay. Gene-edited macrophages were stimulated with inflammasome activators for 48h before supernatants were assessed for IL-1β. Additionally, primed, gene-edited macrophages were lysed in RIPA buffer, and cell lysates were frozen for validation of efficient gene knockout by Western blot.

Cytokine and lactase dehydrogenase (LDH) quantification

Cytokine levels in cell supernatants were assessed using the mouse IL-1β/IL-1F2 DuoSet ELISA kit (R&D Systems) and mouse TNF-α DuoSet ELISA kit (R&D Systems) according to the manufacturer's instructions. ELISA plates were measured at OD_{450} using a microplate reader, and cytokine levels were quantified by interpolation using a standard curve. Supernatants were assayed for LDH release immediately after stimulation time courses per the manufacturer's protocol from the CytoTox 96® Non-Radioactive Cytotoxicity Assay (Promega). Measurements of absorbance readings were performed on a microplate reader at wavelengths of 490 nm and 680 nm. LDH release was assessed as a percentage of background-subtracted maximum LDH values from lysed cells.

SDS-PAGE and Western blot

Cell supernatants and lysates were diluted in 6X SDS-PAGE protein sample buffer (360mM Tris pH 6.8, 12% SDS, 18% β-mercaptoethanol, 60% glycerol, 0.015% bromophenol blue), boiled for 10 min at 95°C, and resolved using SDS-PAGE. The proteins were then transferred onto a nitrocellulose membrane, washed 3 times with Tris-buffered saline with 0.1% Tween20 (TBS-T) and probed with primary antibodies diluted in 5% non-fat dry milk in TBS-T at 4°C overnight. The membrane was then washed 3 times with TBS-T and probed with secondary antibodies in 5% non-fat dry milk in TBS-T rocking at room temperature for 2 hours. The membrane was then washed 3 times with TBS-T and 2 times in TBS and developed using SuperSignal West Pico PLUS Chemiluminescence reagent (ThermoFisher). The resulting membrane was imaged on a BioRad ChemiDoc system and visualized using Image Lab software (BioRad). The antibodies and working dilutions used were as follows: goat-α-mouse IL-1β, 1:1000 (R&D Systems, AF-401-NA); rabbit-α-NLRP3, 1:1000 (Cell Signaling, D4D8T); rabbit-α-mouse AIM2, 1:500 (Cell Signaling, 63660), α-mouse Caspase-1 (p20) 1:1000 (Adipogen, Casper-1), α-human Caspase-1 (p20), 1:1000 (Adipogen, Bally-1); α-Pyrin, 1:1000 (Abcam, EPR18676); goat-α-mouse IgG HRP, 1:5000 (Biolegend, 405306); donkey-α-rabbit IgG HRP, 1:5000 (Biolegend, 405306);α-actin HRP, 1:2000 (Santa Cruz Biotechnologies, sc-8432).

Flow Cytometry

BMDMs were primed with 1μg/mL Pam_3CSK_4 for 17h, then stimulated with 5μg/mL *E. coli* LPS, 10μg/mL DENV NS1, or 5μM nigericin for the indicated time periods at 37°C. Cells were washed twice with PBS, then incubated in PBS at 4°C for 10 min and scraped to suspend cells. Suspended cells were stained with either Live/Dead Fixable Far-Red Stain (ThermoFisher) or APC-α-mouse CD14 primary antibody (clone Sa2-8; Thermo Scientific) on ice in the dark for 30 minutes. Purified rat α-mouse CD16/CD32 (Mouse FcBlock; Becton Dickenson) was used as the blocking reagent to reduce non-specific binding of the antibodies. The stained cells were then washed twice with 1ml cold FACS buffer (1% Bovine Serum Albumin [Sigma] and 1% Purified Mouse IgG [Invitrogen] in PBS) and fixed in 500μL of 4% paraformaldehyde at room temperature. Cells were washed once in PBS and kept in 500μL PBS at 4°C in the dark until analysis with an Intellicyt iQue3 Screener (Sartorius). For viability analysis, a dead-cell gate was set based on unstained cell controls, and the percentage of singlet cells in the dead-cell gate compared to all singlet cells was calculated. For CD14 expression, the mean fluorescence intensity (MFI) of CD14 from unstimulated or stimulated cells was recorded. The percentage of surface receptor staining at 30 min, which is the ratio of the MFI values measured from the stimulated cells to those measured

from the unstimulated cells, was plotted to reflect the efficiency of receptor endocytosis. At least 10,000 events were acquired per sample for analysis.

Statistics

All quantitative analyses were conducted and all data were plotted using GraphPad Prism 8 Software. Data with error bars are represented as mean ± SEM. Statistical significance for experiments with more than two groups was tested with two-way ANOVA with multiple comparison test correction as indicated.

Acknowledgments

We thank Dr. Patrick Mitchell at the University of Washington and Elizabeth Turcotte from Dr. Russell Vance's laboratory for provision of key reagents and helpful discussions about inflammasome biology. Additionally, we thank Kristen Witt, Dr. Sarah Stanley, and Marietta Ravesloot-Chavez for training on CRISPR-Cas9 genetic editing in macrophages and access to their nucleofectors. We also thank Xinyi Feng, Elin Lee, Eduarda Lopes, Pedro Henrique Nascimento Carneiro da Saliva for assistance with animal colony maintenance and experiments; Samantha Hernandez, Maria Jose Andrade, Marco Chapa, and Claudia Sanchez San Martin for administrative and lab management support; and Nicholas Tzuning Lo, Elias Duarte, Sandra Bos, and P. Robert Beatty for their many helpful discussions.

References

1. Messina JP, Brady OJ, Golding N, Kraemer MUG, Wint GRW, Ray SE, et al. The current and future global distribution and population at risk of dengue. Nat Microbiol. 2019;4(9):1508–15.

2. Cattarino L, Rodriguez-Barraquer I, Imai N, Cummings DAT, Ferguson NM. Mapping global variation in dengue transmission intensity. Sci Transl Med [Internet]. 2020 Jan 29 [cited 2020 May 29];12(528). Available from: https://stm.sciencemag.org/content/12/528/eaax4144

3. World Health Organization. Dengue guidelines for diagnosis, treatment, prevention and control : new edition [Internet]. World Health Organization; 2009 [cited 2023 May 30]. Report No.: WHO/HTM/NTD/DEN/2009.1. Available from: https://apps.who.int/iris/handle/10665/44188

4. Aguilar-Briseño JA, Moser J, Rodenhuis-Zybert IA. Understanding immunopathology of severe dengue: lessons learnt from sepsis. Curr Opin Virol. 2020 Aug 1;43:41–9.

5. Srikiatkhachorn A, Mathew A, Rothman AL. Immune Mediated Cytokine Storm and Its Role in Severe Dengue. Semin Immunopathol. 2017 Jul;39(5):563–74.

6. Wong JM, Adams LE, Durbin AP, Muñoz-Jordán JL, Poehling KA, Sánchez-González LM, et al. Dengue: A Growing Problem With New Interventions. Pediatrics. 2022 May 11;149(6):e2021055522.

7. Flamand M, Megret F, Mathieu M, Lepault J, Rey FA, Deubel V. Dengue virus type 1 nonstructural glycoprotein NS1 is secreted from mammalian cells as a soluble hexamer in a glycosylation-dependent fashion. J Virol. 1999 Jul;73(7):6104–10.

8. Welsch S, Miller S, Romero-Brey I, Merz A, Bleck CKE, Walther P, et al. Composition and Three-Dimensional Architecture of the Dengue Virus Replication and Assembly Sites. Cell Host Microbe. 2009 Apr 23;5(4):365–75.

9. Płaszczyca A, Scaturro P, Neufeldt CJ, Cortese M, Cerikan B, Ferla S, et al. A novel interaction between dengue virus nonstructural protein 1 and the NS4A-2K-4B precursor is required for viral RNA replication but not for formation of the membranous replication organelle. PLoS Pathog. 2019 May 9;15(5):e1007736.

10. Glasner DR, Puerta-Guardo H, Beatty PR, Harris E. The Good, the Bad, and the Shocking: The Multiple Roles of Dengue Virus Nonstructural Protein 1 in Protection and Pathogenesis. Annu Rev Virol. 2018 Sep 29;5(1):227–53.

11. Gutsche I, Coulibaly F, Voss JE, Salmon J, d'Alayer J, Ermonval M, et al. Secreted dengue virus nonstructural protein NS1 is an atypical barrel-shaped high-density lipoprotein. Proc Natl Acad Sci U S A. 2011 May 10;108(19):8003–8.

12. Shu B, Ooi JSG, Tan AWK, Ng TS, Dejnirattisai W, Mongkolsapaya J, et al. CryoEM structures of the multimeric secreted NS1, a major factor for dengue hemorrhagic fever. Nat Commun. 2022 Nov 9;13(1):6756.

13. Avirutnan P, Fuchs A, Hauhart RE, Somnuke P, Youn S, Diamond MS, et al. Antagonism of the complement component C4 by flavivirus nonstructural protein NS1. J Exp Med. 2010 Apr 12;207(4):793–806.

14. Beatty PR, Puerta-Guardo H, Killingbeck SS, Glasner DR, Hopkins K, Harris E. Dengue virus NS1 triggers endothelial permeability and vascular leak that is prevented by NS1 vaccination. Sci Transl Med. 2015 Sep 9;7(304):304ra141-304ra141.

15. Puerta-Guardo H, Glasner DR, Harris E. Dengue Virus NS1 Disrupts the Endothelial Glycocalyx, Leading to Hyperpermeability. PLoS Pathog. 2016;12(7):e1005738.

16. Glasner DR, Ratnasiri K, Puerta-Guardo H, Espinosa DA, Beatty PR, Harris E. Dengue virus NS1 cytokine-independent vascular leak is dependent on endothelial glycocalyx components. PLOS Pathog. 2017 Nov 9;13(11):e1006673.

17. Barbachano-Guerrero A, Endy TP, King CA. Dengue virus non-structural protein 1 activates the p38 MAPK pathway to decrease barrier integrity in primary human endothelial cells. J Gen Virol. 2020 May;101(5):484–96.

18. Modhiran N, Gandhi NS, Wimmer N, Cheung S, Stacey K, Young PR, et al. Dual targeting of dengue virus virions and NS1 protein with the heparan sulfate mimic PG545. Antiviral Res. 2019 Aug;168:121–7.

19. Sousa FTG de, Biering SB, Patel TS, Blanc SF, Camelini CM, Venzke D, et al. Sulfated β-glucan from Agaricus subrufescens inhibits flavivirus infection and nonstructural protein 1-mediated pathogenesis. Antiviral Res. 2022 Jul 1;203:105330.

20. Biering SB, Akey DL, Wong MP, Brown WC, Lo NTN, Puerta-Guardo H, et al. Structural basis for antibody inhibition of flavivirus NS1–triggered endothelial dysfunction. Science. 2021 Jan 8;371(6525):194–200.

21. Modhiran N, Song H, Liu L, Bletchly C, Brillault L, Amarilla AA, et al. A broadly protective antibody that targets the flavivirus NS1 protein. Science. 2021 Jan 8;371(6525):190–4.

22. Modhiran N, Watterson D, Muller DA, Panetta AK, Sester DP, Liu L, et al. Dengue virus NS1 protein activates cells via Toll-like receptor 4 and disrupts endothelial cell monolayer integrity. Sci Transl Med. 2015 Sep 9;7(304):304ra142.

23. Modhiran N, Watterson D, Blumenthal A, Baxter AG, Young PR, Stacey KJ. Dengue virus NS1 protein activates immune cells via TLR4 but not TLR2 or TLR6. Immunol Cell Biol. 2017 May;95(5):491–5.

24. Chan KWK, Watanabe S, Jin JY, Pompon J, Teng D, Alonso S, et al. A T164S mutation in the dengue virus NS1 protein is associated with greater disease severity in mice. Sci Transl Med. 2019 Jun 26;11(498):eaat7726.

25. Benfrid S, Park KH, Dellarole M, Voss JE, Tamietti C, Pehau-Arnaudet G, et al. Dengue virus NS1 protein conveys pro-inflammatory signals by docking onto high-density lipoproteins. EMBO Rep. 2022 Jul 5;23(7):e53600.

26. Uno N, Ross TM. Dengue virus and the host innate immune response. Emerg Microbes Infect. 2018 Oct 10;7:167.

27. Shrivastava G, Valenzuela Leon PC, Calvo E. Inflammasome Fuels Dengue Severity. Front Cell Infect Microbiol. 2020 Sep 10;10:489.

28. Barnett KC, Li S, Liang K, Ting JPY. A 360° view of the inflammasome: Mechanisms of activation, cell death, and diseases. Cell. 2023 May 25;186(11):2288–312.

29. Lu A, Magupalli VG, Ruan J, Yin Q, Atianand MK, Vos MR, et al. Unified Polymerization Mechanism for the Assembly of ASC-Dependent Inflammasomes. Cell. 2014 Mar 13;156(6):1193–206.

30. Zhao Y, Yang J, Shi J, Gong YN, Lu Q, Xu H, et al. The NLRC4 inflammasome receptors for bacterial flagellin and type III secretion apparatus. Nature. 2011 Sep;477(7366):596–600.

31. Hornung V, Ablasser A, Charrel-Dennis M, Bauernfeind F, Horvath G, Caffrey DR, et al. AIM2 recognizes cytosolic dsDNA and forms a caspase-1-activating inflammasome with ASC. Nature. 2009 Mar;458(7237):514–8.

32. Sandstrom A, Mitchell PS, Goers L, Mu EW, Lesser CF, Vance RE. Functional degradation: A mechanism of NLRP1 inflammasome activation by diverse pathogen enzymes. Science. 2019 Apr 5;364(6435):eaau1330.

33. Tsu BV, Beierschmitt C, Ryan AP, Agarwal R, Mitchell PS, Daugherty MD. Diverse viral proteases activate the NLRP1 inflammasome. Schoggins JW, Rothlin CV, editors. eLife. 2021 Jan 7;10:e60609.

34. Hagar JA, Powell DA, Aachoui Y, Ernst RK, Miao EA. Cytoplasmic LPS activates caspase-11: implications in TLR4-independent endotoxic shock. Science. 2013 Sep 13;341(6151):1250–3.

35. Kayagaki N, Wong MT, Stowe IB, Ramani SR, Gonzalez LC, Akashi-Takamura S, et al. Noncanonical inflammasome activation by intracellular LPS independent of TLR4. Science. 2013 Sep 13;341(6151):1246–9.

36. Sims JE, Smith DE. The IL-1 family: regulators of immunity. Nat Rev Immunol. 2010 Feb;10(2):89–102.

37. Liu X, Zhang Z, Ruan J, Pan Y, Magupalli VG, Wu H, et al. Inflammasome-activated gasdermin D causes pyroptosis by forming membrane pores. Nature. 2016 Jul;535(7610):153–8.

38. Kayagaki N, Kornfeld OS, Lee BL, Stowe IB, O'Rourke K, Li Q, et al. NINJ1 mediates plasma membrane rupture during lytic cell death. Nature. 2021 Mar;591(7848):131–6.

39. Evavold CL, Ruan J, Tan Y, Xia S, Wu H, Kagan JC. The Pore-Forming Protein Gasdermin D Regulates Interleukin-1 Secretion from Living Macrophages. Immunity. 2018 Jan 16;48(1):35-44.e6.

40. Zanoni I, Tan Y, Di Gioia M, Broggi A, Ruan J, Shi J, et al. An endogenous caspase-11 ligand elicits interleukin-1 release from living dendritic cells. Science. 2016 Jun 3;352(6290):1232–6.

41. de Sá KSG, Amaral LA, Rodrigues TS, Ishimoto AY, de Andrade WAC, de Almeida L, et al. Gasdermin-D activation promotes NLRP3 activation and host resistance to Leishmania infection. Nat Commun. 2023 Feb 24;14:1049.

42. Heilig R, Dick MS, Sborgi L, Meunier E, Hiller S, Broz P. The Gasdermin-D pore acts as a conduit for IL-1β secretion in mice. Eur J Immunol. 2018;48(4):584–92.

43. Sarvestani ST, McAuley JL. The role of the NLRP3 inflammasome in regulation of antiviral responses to influenza A virus infection. Antiviral Res. 2017 Dec 1;148:32–42.

44. Wang Q, Gao H, Clark KM, Mugisha CS, Davis K, Tang JP, et al. CARD8 is an inflammasome sensor for HIV-1 protease activity. Science. 2021 Mar 19;371(6535):eabe1707.

45. Diamond MS, Kanneganti TD. Innate immunity: the first line of defense against SARS-CoV-2. Nat Immunol. 2022 Feb;23(2):165–76.

46. Thomas PG, Dash P, Aldridge JR, Ellebedy AH, Reynolds C, Funk AJ, et al. NLRP3 (NALP3/CIAS1/Cryopyrin) mediates key innate and healing responses to influenza A virus via the regulation of caspase-1. Immunity. 2009 Apr 17;30(4):566–75.

47. Ramos HJ, Lanteri MC, Blahnik G, Negash A, Suthar MS, Brassil MM, et al. IL-1β Signaling Promotes CNS-Intrinsic Immune Control of West Nile Virus Infection. PLoS Pathog. 2012 Nov 29;8(11):e1003039.

48. Tate MD, Ong JDH, Dowling JK, McAuley JL, Robertson AB, Latz E, et al. Reassessing the role of the NLRP3 inflammasome during pathogenic influenza A virus infection via temporal inhibition. Sci Rep. 2016 Jun 10;6(1):27912.

49. Pan P, Zhang Q, Liu W, Wang W, Lao Z, Zhang W, et al. Dengue Virus M Protein Promotes NLRP3 Inflammasome Activation To Induce Vascular Leakage in Mice. J Virol. 2019 01;93(21).

50. Hottz ED, Lopes JF, Freitas C, Valls-de-Souza R, Oliveira MF, Bozza MT, et al. Platelets mediate increased endothelium permeability in dengue through NLRP3-inflammasome activation. Blood. 2013 Nov 14;122(20):3405–14.

51. Wu MF, Chen ST, Yang AH, Lin WW, Lin YL, Chen NJ, et al. CLEC5A is critical for dengue virus–induced inflammasome activation in human macrophages. Blood. 2013 Jan 3;121(1):95–106.

52. Shrivastava G, Visoso-Carvajal G, Garcia-Cordero J, Leon-Juarez M, Chavez-Munguia B, Lopez T, et al. Dengue Virus Serotype 2 and Its Non-Structural Proteins 2A and 2B Activate NLRP3 Inflammasome. Front Immunol. 2020;11:352.

53. Pan P, Zhang Q, Liu W, Wang W, Yu Z, Lao Z, et al. Dengue Virus Infection Activates Interleukin-1β to Induce Tissue Injury and Vascular Leakage. Front Microbiol [Internet]. 2019 [cited 2020 Jun 28];10. Available from: https://www.frontiersin.org/articles/10.3389/fmicb.2019.02637/full

54. Tan TY, Chu JJH. Dengue virus-infected human monocytes trigger late activation of caspase-1, which mediates pro-inflammatory IL-1β secretion and pyroptosis. J Gen Virol. 2013 Oct;94(Pt 10):2215–20.

55. Yong YK, Tan HY, Jen SH, Shankar EM, Natkunam SK, Sathar J, et al. Aberrant monocyte responses predict and characterize dengue virus infection in individuals with severe disease. J Transl Med. 2017 May 31;15:121.

56. Garcia-Calvo M, Peterson EP, Leiting B, Ruel R, Nicholson DW, Thornberry NA. Inhibition of human caspases by peptide-based and macromolecular inhibitors. J Biol Chem. 1998 Dec 4;273(49):32608–13.

57. Zheng Y, Liu Q, Wu Y, Ma L, Zhang Z, Liu T, et al. Zika virus elicits inflammation to evade antiviral response by cleaving cGAS via NS1-caspase-1 axis. EMBO J. 2018 Sep 14;37(18):e99347.

58. Coll RC, Robertson AAB, Chae JJ, Higgins SC, Muñoz-Planillo R, Inserra MC, et al. A small-molecule inhibitor of the NLRP3 inflammasome for the treatment of inflammatory diseases. Nat Med. 2015 Mar;21(3):248–55.

59. Kayagaki N, Warming S, Lamkanfi M, Vande Walle L, Louie S, Dong J, et al. Non-canonical inflammasome activation targets caspase-11. Nature. 2011 Oct 16;479(7371):117–21.

60. Inflammasome Assays In Vitro and in Mouse Models - Guo - 2020 - Current Protocols in Immunology - Wiley Online Library [Internet]. [cited 2020 Oct 19]. Available from: https://currentprotocols.onlinelibrary.wiley.com/doi/10.1002/cpim.107

61. den Hartigh AB, Fink SL. Detection of Inflammasome Activation and Pyroptotic Cell Death in Murine Bone Marrow-derived Macrophages. J Vis Exp JoVE. 2018 May 21;(135):57463.

62. Russo HM, Rathkey J, Boyd-Tressler A, Katsnelson MA, Abbott DW, Dubyak GR. Active Caspase-1 Induces Plasma Membrane Pores That Precede Pyroptotic Lysis and Are Blocked by Lanthanides. J Immunol. 2016 Aug 15;197(4):1353–67.

63. Zanoni I, Tan Y, Di Gioia M, Springstead JR, Kagan JC. By Capturing Inflammatory Lipids Released from Dying Cells, the Receptor CD14 Induces Inflammasome-Dependent Phagocyte Hyperactivation. Immunity. 2017 Oct 17;47(4):697-709.e3.

64. Orozco S, Schmid MA, Parameswaran P, Lachica R, Henn MR, Beatty R, et al. Characterization of a model of lethal dengue virus 2 infection in C57BL/6 mice deficient in the alpha/beta interferon receptor. J Gen Virol. 2012 Oct;93(Pt 10):2152–7.

65. Chen RE, Diamond MS. Dengue mouse models for evaluating pathogenesis and countermeasures. Curr Opin Virol. 2020 Aug;43:50.

66. Dinarello CA. Overview of the IL-1 family in innate inflammation and acquired immunity. Immunol Rev. 2018;281(1):8–27.

67. Callaway JB, Smith SA, McKinnon KP, de Silva AM, Crowe JE, Ting JPY. Spleen Tyrosine Kinase (Syk) Mediates IL-1β Induction by Primary Human Monocytes during Antibody-enhanced Dengue Virus Infection. J Biol Chem. 2015 Jul 10;290(28):17306–20.

68. Callaway JB, Smith SA, Widman DG, McKinnon KP, Scholle F, Sempowski GD, et al. Source and Purity of Dengue-Viral Preparations Impact Requirement for Enhancing Antibody to Induce Elevated IL-1β Secretion: A Primary Human Monocyte Model. PLoS ONE [Internet]. 2015 Aug 24 [cited 2021 Mar 26];10(8). Available from: https://www.ncbi.nlm.nih.gov/pmc/articles/PMC4547738/

69. Katzelnick LC, Gresh L, Halloran ME, Mercado JC, Kuan G, Gordon A, et al. Antibody-dependent enhancement of severe dengue disease in humans. Science. 2017 Nov 17;358(6365):929–32.

70. Waggoner JJ, Katzelnick LC, Burger-Calderon R, Gallini J, Moore RH, Kuan G, et al. Antibody-Dependent Enhancement of Severe Disease Is Mediated by Serum Viral Load in Pediatric Dengue Virus Infections. J Infect Dis. 2020 Jun 1;221(11):1846–54.

71. Shen C, Li R, Negro R, Cheng J, Vora SM, Fu TM, et al. Phase separation drives RNA virus-induced activation of the NLRP6 inflammasome. Cell. 2021 Nov;184(23):5759-5774.e20.

72. Próchnicki T, Vasconcelos MB, Robinson KS, Mangan MSJ, De Graaf D, Shkarina K, et al. Mitochondrial damage activates the NLRP10 inflammasome. Nat Immunol. 2023 Apr;24(4):595–603.

73. Kayagaki N, Stowe IB, Lee BL, O'Rourke K, Anderson K, Warming S, et al. Caspase-11 cleaves gasdermin D for non-canonical inflammasome signalling. Nature. 2015 Oct;526(7575):666–71.

74. Malavige GN, Jeewandara C, Ogg GS. Dysfunctional Innate Immune Responses and Severe Dengue. Front Cell Infect Microbiol. 2020;10:590004.

75. Freund EC, Lock JY, Oh J, Maculins T, Delamarre L, Bohlen CJ, et al. Efficient gene knockout in primary human and murine myeloid cells by non-viral delivery of CRISPR-Cas9. J Exp Med. 2020 Jul 6;217(7):e20191692.

Chapter 3

Characterization of a protective antibody response against dengue virus non-structural protein 1 (NS1) reveals critical domains required for NS1-triggered pathogenesis

Portions of work presented in this chapter have been published in:

Biering SB, Akey DL, Wong MP, Brown WC, Lo NTN, Puerta-Guardo H, Tramontini Gomes de Sousa F, Wang C, Konwerski JR, Espinosa DA, Bockhaus NJ, Glasner DR, Li J, Blanc SF, Juan EY, Elledge SJ, Mina MJ, Beatty PR, Smith JL, Harris E. Structural basis for antibody inhibition of flavivirus NS1-triggered endothelial dysfunction. *Science*. 2021 Jan 8;371(6525):194-200. doi: 10.1126/science.abc0476.

Abstract

Dengue virus (DENV) is a medically important, mosquito-borne flavivirus that infects up to 100 million people annually. A signature of severe DENV infection is vascular leak, which can lead to shock and organ failure. We and others have shown that secreted DENV non-structural protein 1 (NS1) triggers endothelial cell (EC) hyperpermeability and vascular leak. Antibodies (Abs) targeting NS1 prevent NS1-induced EC hyperpermeability *in vitro* and are protective against lethal DENV challenge, as shown by vaccination of mice against NS1 and passive transfer of α-NS1 polyclonal serum. How α-NS1 Abs protect against pathogenesis, however, remains obscure. Here we characterize possible mechanisms behind the protective ability of an NS1-specific monoclonal Ab, 2B7, which abrogates NS1 binding to ECs and EC hyperpermeability *in vitro* and inhibits vascular leak and mortality *in vivo*. Guided by crystal structures of NS1 complexed to a 2B7 Fab fragment, we mutated the amino acids on NS1 that comprise the NS1:2B7 interface. We found that 2B7 has pan-flavivirus NS1 cross-reactivity due to the conservation of the residues in the core epitope targeted by 2B7. The mutagenesis also identified key residues on NS1 with the 2B7 epitope that are necessary for inducing EC hyperpermeability without affecting NS1:EC binding, suggesting that 2B7 can block additional step in NS1 pathogenesis downstream of binding. Lastly, we find that humans infected with DENV generate antibody responses towards residues within the 2B7 epitope. This work provides mechanistic insight into the blockade of DENV NS1-mediated pathogenesis by α-NS1 Abs and identifies critical domains that serve as targets for drugs and vaccine-induced α-NS1 Ab responses.

Introduction

Dengue virus (DENV) is the most prevalent member of the *Flavivirus* family which includes other flaviviruses of medical importance like Zika virus (ZIKV) and West Nile virus (WNV). An estimated 100 million people are infected with any of the four DENV serotypes (DENV1-4) annually (1). Infection leads to a range of outcomes, from inapparent infection to classic dengue fever to severe dengue, which includes dengue hemorrhagic fever (DHF) and dengue shock syndrome (DSS). Severe dengue is characterized by increased vascular leak, where fluids extravasating from the vasculature and accumulate in tissues, leading to complication such as severe bleeding, pulmonary edema, and hypovolemic shock, which can be fatal if left untreated (2). No current treatments currently exist for the treatment of dengue other than supportive care and currently licensed vaccines against DENV are restricted to those who have had a previous laboratory-confirmed DENV infection due to the increased risk of disease in DENV-naïve individuals, limiting the effectiveness of the vaccine (3,4). This is likely due the ability of cross-reactive, weakly neutralizing antibodies (Abs) targeting the prM and envelope (E) proteins mediating enhanced entry of DENV into infected cells, a phenomenon known antibody-dependent enhancement (ADE) (5,6). The risk that incomplete vaccine immunity against all four serotypes might paradoxically enhance pathogenesis in the setting of subsequent natural infection due to ADE remains a barrier for the development of safe, efficacious DENV vaccines.

DENV non-structural protein 1 (NS1) has emerged as a promising vaccine candidate because vaccination of mice with NS1 protects them against lethal DENV infection and NS1 does not generate disease-enhancing antibodies (7,8). DENV NS1 is a viral toxin secreted from infected cells and circulates in the body, where it plays key roles in promoting viral dissemination and pathogenesis (9,10). Extracellular NS1 has been shown to inhibit complement, activate platelets and immune cells, and directly interacts with endothelial cells (8,9,11–14). The interaction between NS1 and endothelial cell leads to the disruption of the endothelial glycocalyx and modulation of intercellular junctional complexes, ultimately resulting in endothelial dysfunction, hyperpermeability and vascular leak (14–16). Though NS1's role in DENV pathogenesis is clear, many questions remain about the exact mechanisms by which NS1 induces endothelial dysfunction. Understanding these mechanisms is key for designing NS1-targetted vaccines and therapeutics.

DENV NS1 is a ~48 kDa glycoprotein containing three domains: the β-roll (residues 1–29), wing (residues 30–180), and β-ladder (residues 181–352) and is highly conserved across flaviviruses (17). After translation, NS1 quickly dimerizes, associating with host cell membranes likely though interactions with many hydrophobic residues within the β-roll and wing domains (17,18). ER-associated NS1 is essential for the assembly of the viral replication complex, viral RNA replication and infectious particle production (19,20). Extracellular NS1 is barrel-shaped, with NS1 tetramers or hexamers surrounding a central lipid cargo reminiscent of a lipoprotein (21–23). Despite our understanding of the structural forms of NS1, the molecular function of each domain with respect to DENV pathogenesis remains unclear. This information is crucial for the design of therapeutics like monoclonal antibodies (mAbs) aimed at disrupting NS1's pathogenic functions and for deepening our understanding of how α-NS1-Abs work to protect against severe dengue.

α-NS1 Abs are a central component of protective anti-NS1 immunity. Immune sera from DENV NS1-vaccinated mice and α-NS1 mAbs are sufficient prevent mice from succumbing lethal DENV infection through multiple mechanisms (7,8,24–27). α-NS1 Abs have been shown to mediate antibody-dependent complement deposition on infected cells expressing cell surface NS1 and prevent NS1-induced endothelial dysfunction *in vitro* and *in vivo* (8,26,28). People infected with DENV and those vaccinated with a live-attenuated tetravalent dengue vaccine candidate (TAK-003) generate antibody responses to NS1 and sera from TAK-003 vaccinees were also shown to be able to block NS1-induced endothelial hyperpermeability and EGL degradation (29–31). Despite clear evidence of the protective capacity of α-NS1 Abs, comparatively little is known about which epitopes are targeted by protective α-NS1 Abs. A majority of α-NS1 Abs generated after natural infection in humans or after NS1 vaccination in mice target the wing (amino acids 101-130) and β-ladder domains (amino acids 296-330) (32,33). One mAb, 33D2, targets the wing domain and can reduce DENV-induced hemorrhage, vascular leakage, and mortality in mice, in part due tothe ability of mAb 33D2 to induce complement-dependent cytolysis and antibody-dependent cellular cytotoxicity (ADCC) (27,28). While protective α-NS1 Abs can also prevent DENV mortality by blocking NS1-induced endothelial dysfunction, the molecular mechanisms underlying this inhibition have not yet been fully elucidated.

The Harris laboratory has isolated 2B7, an α-DENV NS1 mouse monoclonal antibody (mAb) that prevents NS1 from binding to endothelial cells, inhibits NS1-induced endothelial dysfunction and vascular leak, and is protective against lethal dengue virus infection in mice (34). Understanding the mechanisms by which 2B7 prevents NS1-induced endothelial dysfunction and vascular leak will provide crucial insight into vaccine development and therapeutics targeting NS1-induced pathology. Thus, we sought to elucidate the structural basis of 2B7-mediated inhibition of NS1-induced endothelial dysfunction through mutagenesis of the 2B7 binding epitope on NS1. The work described in this chapter includes data published in (34) as well as several pilot experiments leveraging NS1 mutants generated from this work to characterize the α-NS1 response in humans which will form parts of more complete stories in the future.

Results

Crystal structures of the 2B7 Fab: NS1 complex reveal the 2B7 binding epitope

In order to elucidate the structural basis of 2B7-mediated inhibition of NS1-triggered endothelial dysfunction, Janet Smith and colleagues at the University of Michigan resolved crystal structures of the 2B7 F'ab fragment or 2B7 single-chain variable fragment (scFv) in complex with NS1. These structures mapped the 2B7 epitope to the β-ladder region of DENV2 NS1 and identified specific amino acid residues recognized by 2B7 **(Figure 1A)**. The amino acid residues in the 2B7 epitope can be divided into two classes: the epitope core region, composed of residues that are highly conserved across flaviviruses, and the epitope periphery, displaying varying levels of divergence among flaviviruses but are relatively conserved across DENV 1-4; these classes are referred to as pan-flavivirus or DENV-conserved respectively (34) **(Figure 1B-C)**.

Mutagenesis screening of the 2B7 epitope identifies molecular determinants of NS1 secretion and 2B7 binding

To determine the relative contribution of each amino acid to 2B7 binding, we generated mutant DENV2 NS1 constructs containing single, double, triple, or quadruple substitutions within the 2B7 epitope using site-directed mutagenesis **(Table 1)**. Each amino acid had 2 possible substitutions; one designed to negate the functional side chain (e.g. E->A) and another designed to maximally disrupt the interaction between that residue and the 2B7 complementarity-determining region (CDR) (i.e reversing the charge, E->K or inclusion of a bulky side chain, A->W). Constructs were then screened in 293T cells to evaluate the impact of the amino acid mutation(s) on NS1 secretion and 2B7 binding. Mutations at R299, G328, or W330, as well as constructs contained multiple amino acid substitutions displayed impaired secretion of NS1 into cell culture supernatant **(Figure 2A)**, despite successful transfection, as indicated by the presence of NS1 detected within transfected cells **(Figure 2B)**. Mutations at T301, A303, G305, E326 and D327 were secreted from cells and displayed diminished binding to 2B7 whereas D281P and V346E substitutions had no effect on either secretion or 2B7 binding ability compared to WT DENV2 NS1 **(Figure 2A)**. Based on these results, we moved 7 single substitution mutants forward for scaled production and further characterization: D281P, T301K, T301R, A303W, G305K, E326K, and D327K.

Binding to the 2B7 epitope core confers pan-flavivirus binding ability

We transfected NS1 constructs containing these mutations into 293F cells and purified NS1 from the supernatant using affinity chromatography. All mutants were expressed, secreted, oligomeric, stable, and of purity comparable to that of WT DENV2 NS1 made in-house or commercially available **(Figure 3)**. We then quantified the binding affinity of each mutant to 2B7 using a direct ELISA **(Figure 4A)**. All mutants, except D281P, had increased EC50 values compared to WT DENV NS1, indicating that T301, A303, G305, E326, and D327 all contribute 2B7's affinity to DENV NS1, with T301K, A303W, and G305K having the greatest binding defects to 2B7 **(Figure 4B)**. These mutations demonstrate that these amino acids are key determinants of 2B7 binding to DENV NS1.

T301 and G305 are conserved in NS1 across the flaviviruses, leading us to hypothesize that 2B7 has affinity for other flavivirus NS1. Indeed, 2B7 can bind to NS1 from the closely related ZIKV and the more distantly related WNV **(Figure 5A-B)**. We then generated ZIKV and WNV NS1 mutants with T301K and G305K substitutions to further evaluate the importance of the flavivirus-

conserved residues to 2B7 affinity to flavivirus NS1, **(Figure 5C-E)**. 2B7 was unable to bind any ZIKV or WNV NS1 containing these mutations **(Figure 5A-B)**, further demonstrating that these residues are key determinants of 2B7 binding and the basis for 2B7's cross-reactivity to other flavivirus NS1.

Mutations within the 2B7 epitope attenuate NS1-induced hyperpermeability independent of endothelial cell binding

Since 2B7 prevents NS1-induced endothelial dysfunction, we assessed whether these residues within the 2B7 epitope contribute to endothelial hyperpermeability *in vitro* using a trans-endothelial electrical resistance (TEER) assay. We treated human pulmonary microvascular endothelial cells (HPMEC) seeded in the apical chamber of a Transwell with either WT or mutated DENV2 NS1 and measured the TEER values between the apical and the basolateral chambers of the Transwell system over a 24-hour period. DENV2 NS1 mutants T301K and G305K mutant dropped TEER at similar levels to WT DENV2 NS1, whereas DENV2 NS1 mutants T301R, A303W, E326K and D327K were all defective in their capacity to mediate endothelial hyperpermeability, with NS1-A303W displaying the greatest functional defect **(Figure 6A-B)**. Interestingly, the inability of DENV2 NS1 mutants to induce endothelial hyperpermeability in HPMECs is not due to a defect in binding, as all DENV2 NS1 mutants tested bound HPMECs at similar levels to WT DENV2 NS1 **(Figure 7A-B)**. These results indicate that residues within the β-ladder are critical for NS1-mediated endothelial dysfunction at a step downstream of binding.

2B7 epitope NS1 mutants enable profiling of the α-NS1-Ab response from DENV-infected individuals.

Given the potency of 2B7 in preventing NS1-induced hyperpermeability and preventing mortality in a lethal model of DENV infection in mice, we next wondered whether α-NS1 Abs targeting residues within the 2B7 epitope are also elicited in human DENV infections. In order to profile this aspect of the α-NS1 Ab response in humans, we leveraged a multiplex antigen Luminex-based assay we had recently developed to profile Ab responses in plasma to compare the binding profiles of Ab binding to WT NS1 and to NS1 carrying the G305K mutation. The G305K mutation was selected as it contributed the most to 2B7 binding to NS1 by direct ELISA and was conserved across flaviviruses, thus enabling the profiling of a pan-flavivirus NS1 binding response. As a pilot study, we profiled 53 plasma samples from our longstanding Pediatric Dengue Hospital-based Study in Nicaragua. All samples were collected from patients experiencing either a secondary DENV2 or DENV3 infection 4 days post-symptom onset and stratified by disease severity **(Table 2)**. We profiled the samples for binding to DENV2 NS1 WT and DENV2 NS1 G305K and found that these responses varied across individuals; however, in most patients, at least a portion of the α-DENV2 NS1 response generated was lost with the G305K mutation **(Figure 8A-B).** This indicates that Abs generated against DENV NS1 in human infection can bind to epitopes similar to 2B7. The samples were also profiled using ZIKV NS1 WT and ZIKV NS1 G305K antigens to evaluate the cross-reactive potential of the α-NS1 Ab response towards the G305 epitope (**Figure 8C-D)**. All samples had antibodies that could cross react with ZIKV NS1 and many samples still showed a reduction in binding to the ZIKV NS1 G305K mutant, indicating that at least a portion of the α-NS1 Ab response has cross-reactive protection based on binding to the G305 residue. **(Figure 8E)**. Thus, we conclude that 2B7-like Abs with flavivirus cross-reactivity can be elicited in humans after DENV infection and can be detected using mutagenized NS1 as antigens.

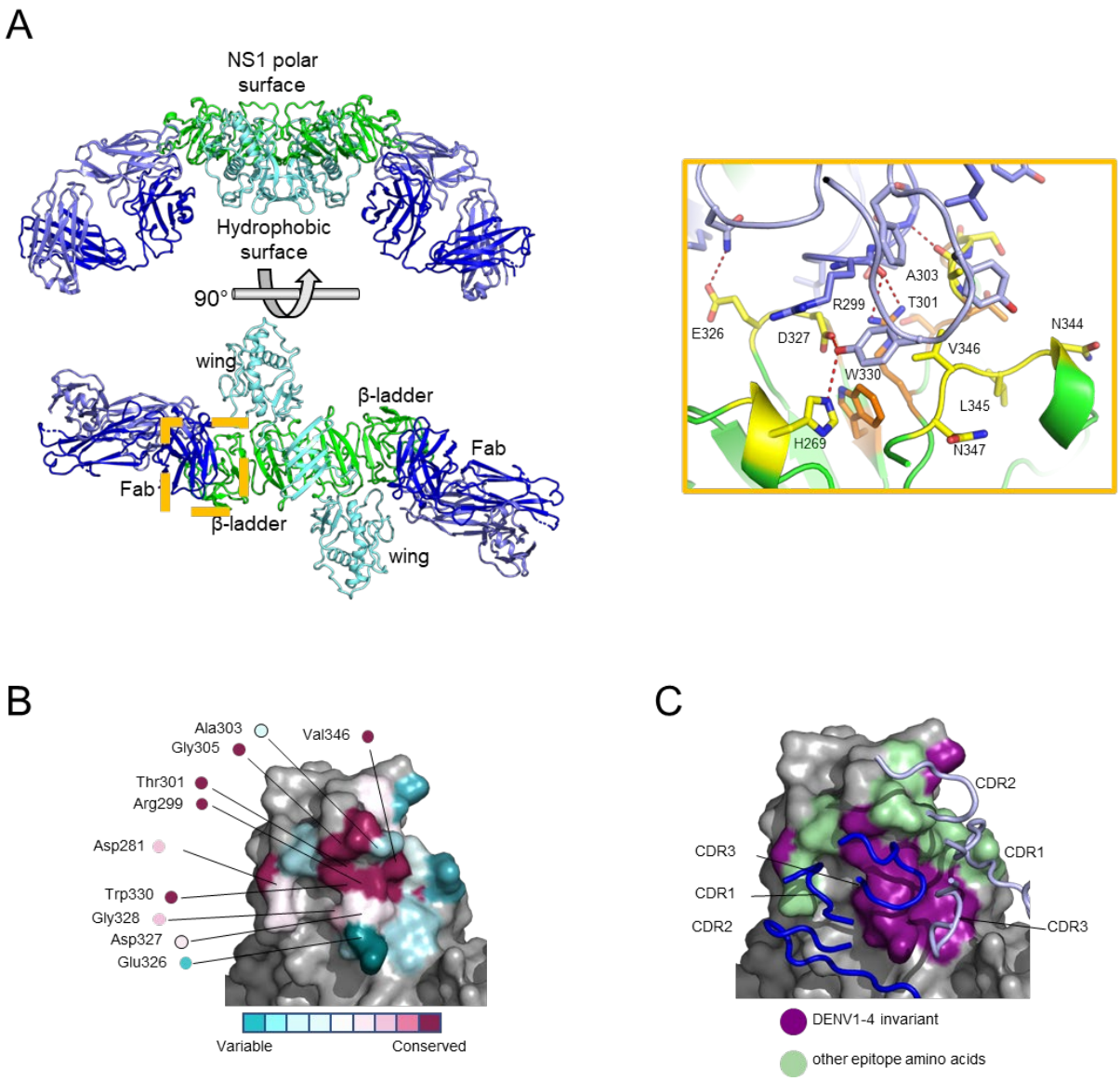

Figure 1: Crystal structure of the 2B7 Fab complexed with DENV NS1 maps the 2B7 epitope on the β-ladder. (A) Perpendicular views of a 3.2-Å crystal structure of 2B7 Fab (heavy chain, dark blue; light chain, light blue) and DENV1 NS1 dimer (β-ladder domains, green; β-roll and wing domains, cyan). The combining site is boxed (yellow) in the lower image, right monomer. Inset image: Detail of the 2B7 scFv and the DENV2 NS1–combining site highlighting the interacting amino acids. The 2B7 backbone is shown in blue, and NS1 is shown in green with key side chains shown as sticks. Pan-flavivirus conserved side chains (orange) are at the center of the discontinuous epitope; DENV-conserved side chains (yellow) are at the epitope periphery; and hydrogen bonds are shown as dashed lines**. (B)** DENV2 NS1 epitope for 2B7 scFv (colored by conservation across flaviviruses according to the key with surfaces outside the epitope in gray. Sites of mutagenesis are labeled. **(C)** 2B7 scFv complementarity-determining regions (CDRs, in tube rendering) for the heavy chain (dark blue) and light chain (light blue) overlaid on the DENV2 NS1 epitope surface. Surfaces of amino acids conserved across DENV 1-4 but variable in other flaviviruses are shown in purple; other epitope residues are shown in green; view as in (B). Figure is adapted from Biering et al (34).

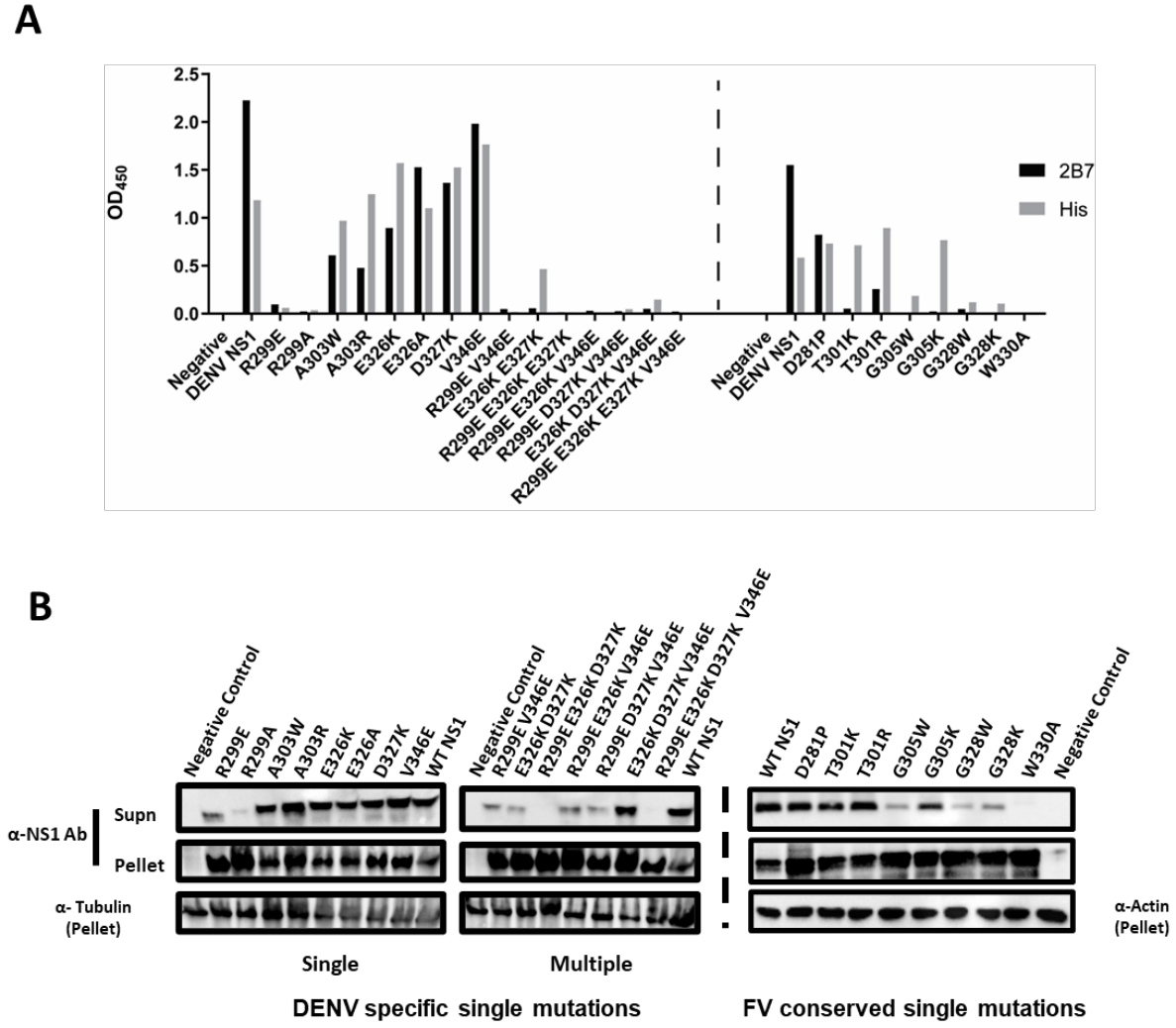

Figure 2: Screening and selection of DENV2 NS1 mutants (A) Capture ELISA with supernatants from DENV2 NS1 mutant-transfected 293T cells. Plates were coated with mAb (7E11) targeting the NS1 wing domain, and captured protein was detected using either 2B7 or an anti-6X histidine tag antibody. Detected proteins were measured via absorbance at 450 nm. Displayed is a single representative experiment from n=3 biological replicates. **(B)** Same samples as in A, with detection via Western blot analysis using the anti-NS1 wing mAb 7E11. Displayed is one representative experiment from n=3. FV=flavivirus. This data was adapted into Biering et al (34).

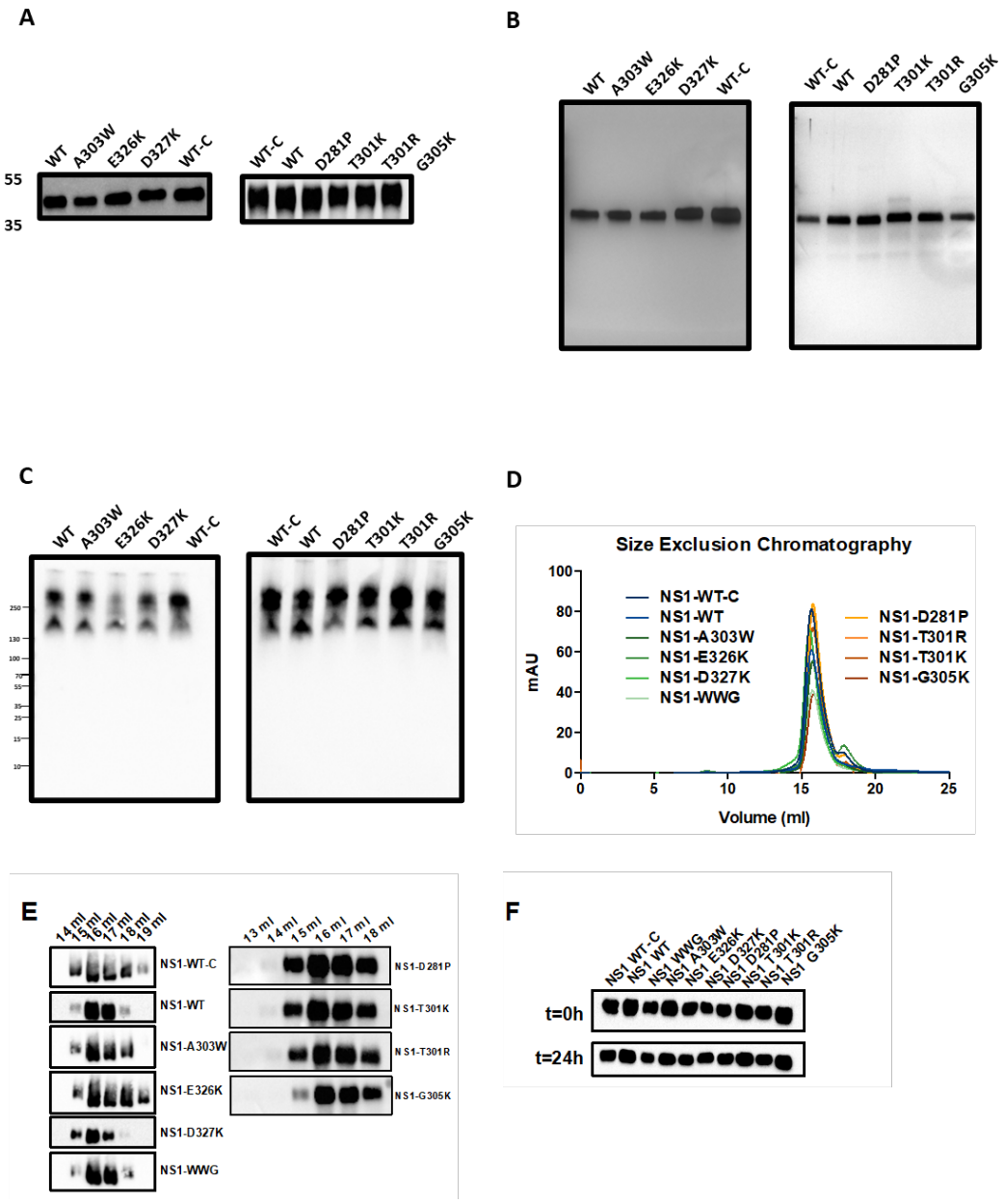

Figure 3. Production and quality control of DENV2 NS1 mutants (A) Western blot analysis (anti-HIS antibody) following SDS-PAGE of WT and mutant NS1 proteins after purification. **(B)** Silver stain following SDS-PAGE of purified WT and mutant NS1 proteins. **(C)** Western blot analysis (anti-His antibody) following native-PAGE of purified WT and mutant NS1 proteins. **(D)** Size-exclusion chromatography of purified WT and mutant NS1 proteins. **(E)** Western blot analysis (anti-His antibody) following SDS-PAGE of the indicated fractions from panel D. **(F)** Western blot analysis (anti-HIS antibody) following SDS-PAGE of WT and mutant NS1 proteins after incubation in endothelial cell medium at 37°C and 5% C02 for the indicated times. WT-C is the commercially purchased WT NS1, while NS1-WT is the in-house produced WT NS1. Unless otherwise indicated, the data presented are from n=3 biological replicates. (D) and (F) were done by Scott Biering. Figure is adapted from Biering et al (34).

A

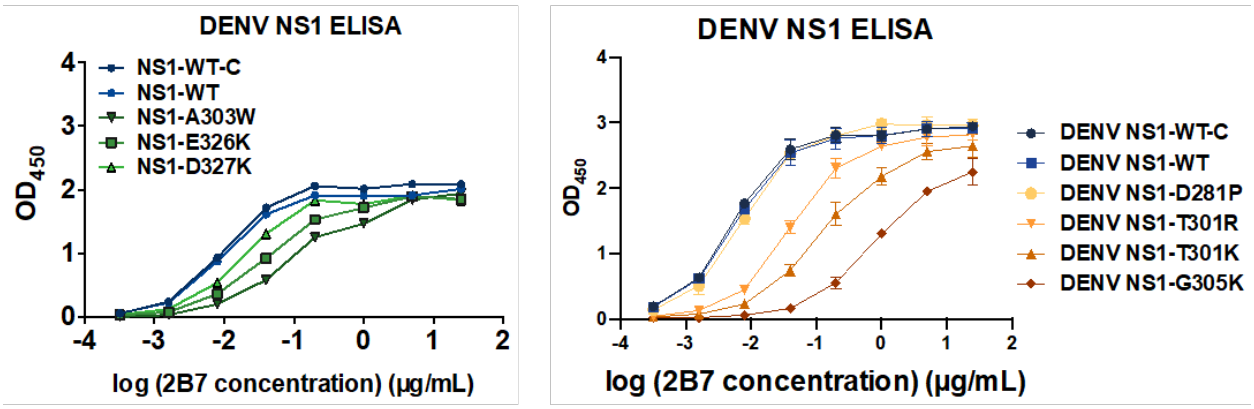

B

NS1	EC50 (ug/mL)	Fold increase (EC50)
DENV NS1 WT	0.006	
DENV NS1 D281P	0.008	1.28
DENV NS1 T301K	0.130	21.97
DENV NS1 T301R	0.041	6.99
DENV NS1 G305K	0.806	136.19
DENV NS1 A303W	0.120	20.29
DENV NS1 E326K	0.040	6.76
DENV NS1 D327K	0.018	2.99

Figure 4. Mutations within the 2B7 epitope core and periphery attenuate 2B7 binding to NS1. **(A)** ELISAs measuring 2B7 interaction with indicated DENV2 NS1–mutagenized proteins compared with the in-house–produced (NS1-WT) or commercially purchased (NS1-WT-C) control proteins. Plates were coated with 100ng of indicated NS1 protein and serial dilutions of 2B7 were added. Bound 2B7 was detected using a goat-α-mouse IgG HRP and plate was developed using a 3,3',5,5'-tetramethylbenzidine (TMB) substrate. **(B)** EC_{50} values calculated from curves in (A). Data displayed are n = 3 biological replicates. Figures were included in Biering et al (34).

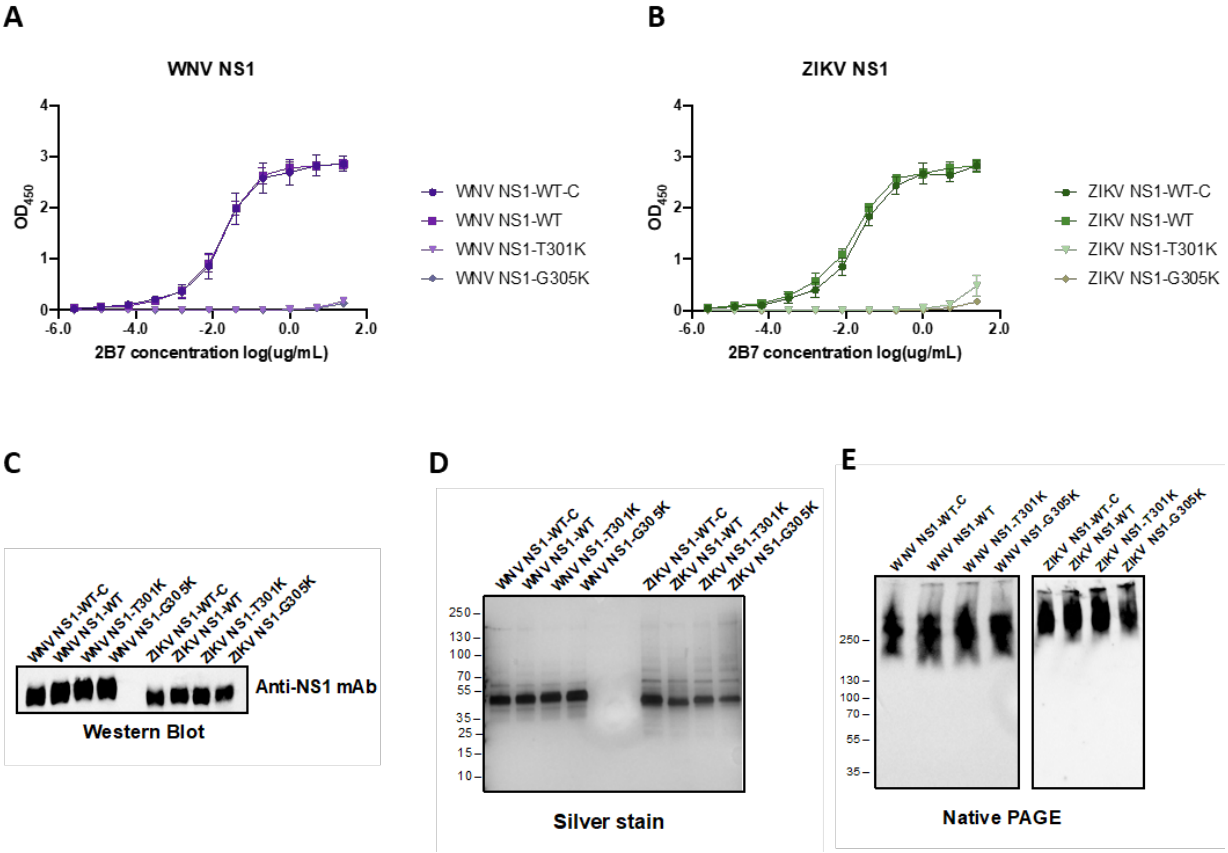

Figure 5. Conserved residues within the 2B7 epitope core impart flavivirus NS1 cross-reactivity to 2B7. (A-B) ELISAs measuring 2B7 interaction with indicated the indicated (A) WNV or (B) ZIKV NS1 WT or mutagenized proteins. Data displayed are n = 3 biological replicates. **(C)** Western blot analysis (anti-NS1 antibody, "7E11") following SDS-PAGE of WT and mutant WNV/ZIKV NS1 proteins after purification. **(D)** Silver stain following SDS-PAGE of purified WT and mutant WNV/ZIKV NS1 proteins. **(E)** Western blot analysis (anti-NS1 antibody, "7E11") following native-PAGE of purified WT and mutant WNV/ZIKV NS1 proteins. Figure is adapted from Biering et al (34).

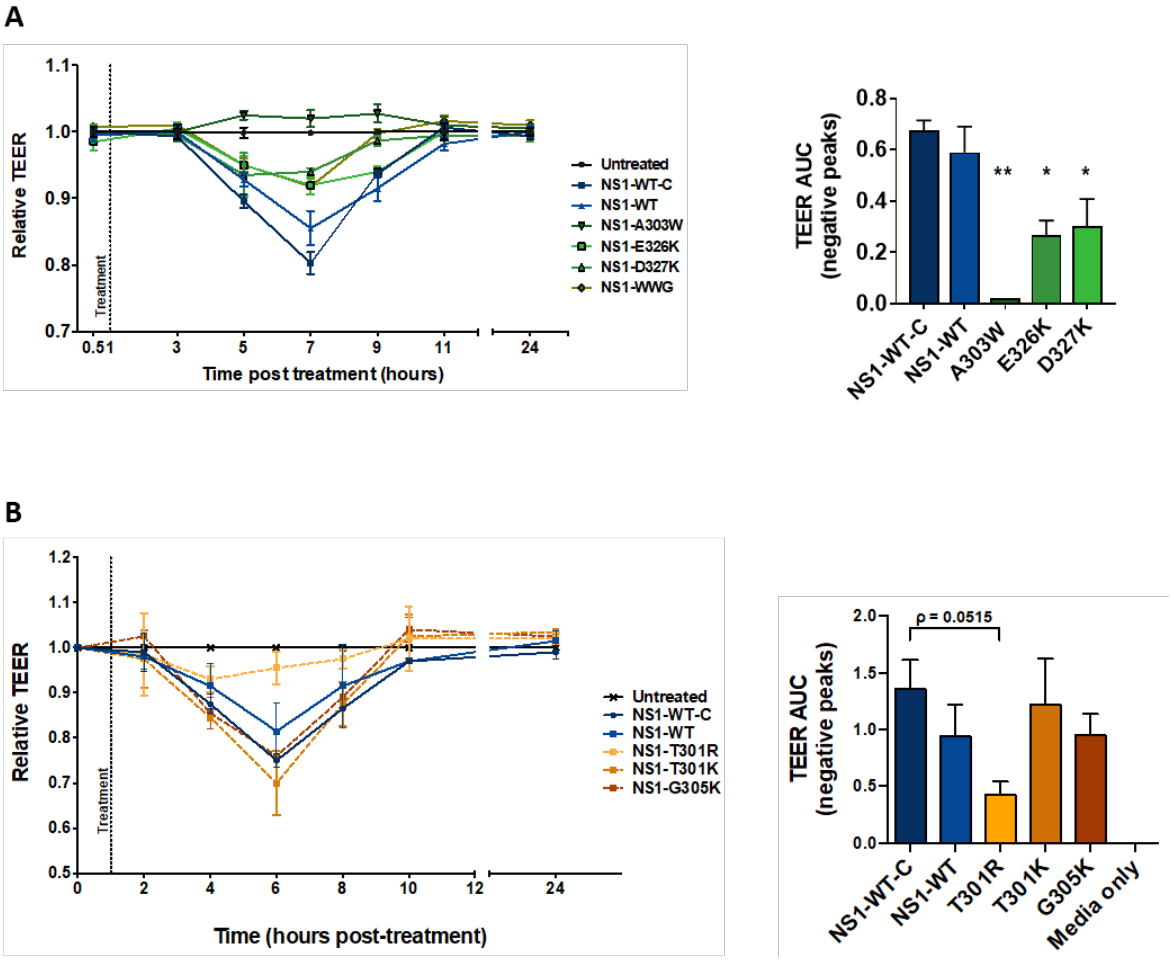

Figure 6. β-ladder mutations attenuate NS1-induced endothelial hyperpermeability. HPMEC monolayer was seeded in the apical chambers of 24-well Transwell inserts and treated with 10 μg/mL WT DENV NS1 or NS1 mutagenized at **(A, left panel)** DENV specific residues or **(B, left panel)** flavivirus-conserved residues within the 2B7 epitope. The trans-endothelial electrical resistance (TEER) between the apical and basolateral chamber were measured over time and normalized to the untreated controls at each respective timepoint. Quantification of the area between the curve and Y=1.0 ("area under curve"), correlating to a decrease in electrical resistance and an increase in permeability depicted **(A,B right panels)** *p<0.05, **p<0.01, by one-way ANOVA with multiple comparisons. Figures were included in Biering et al (34).

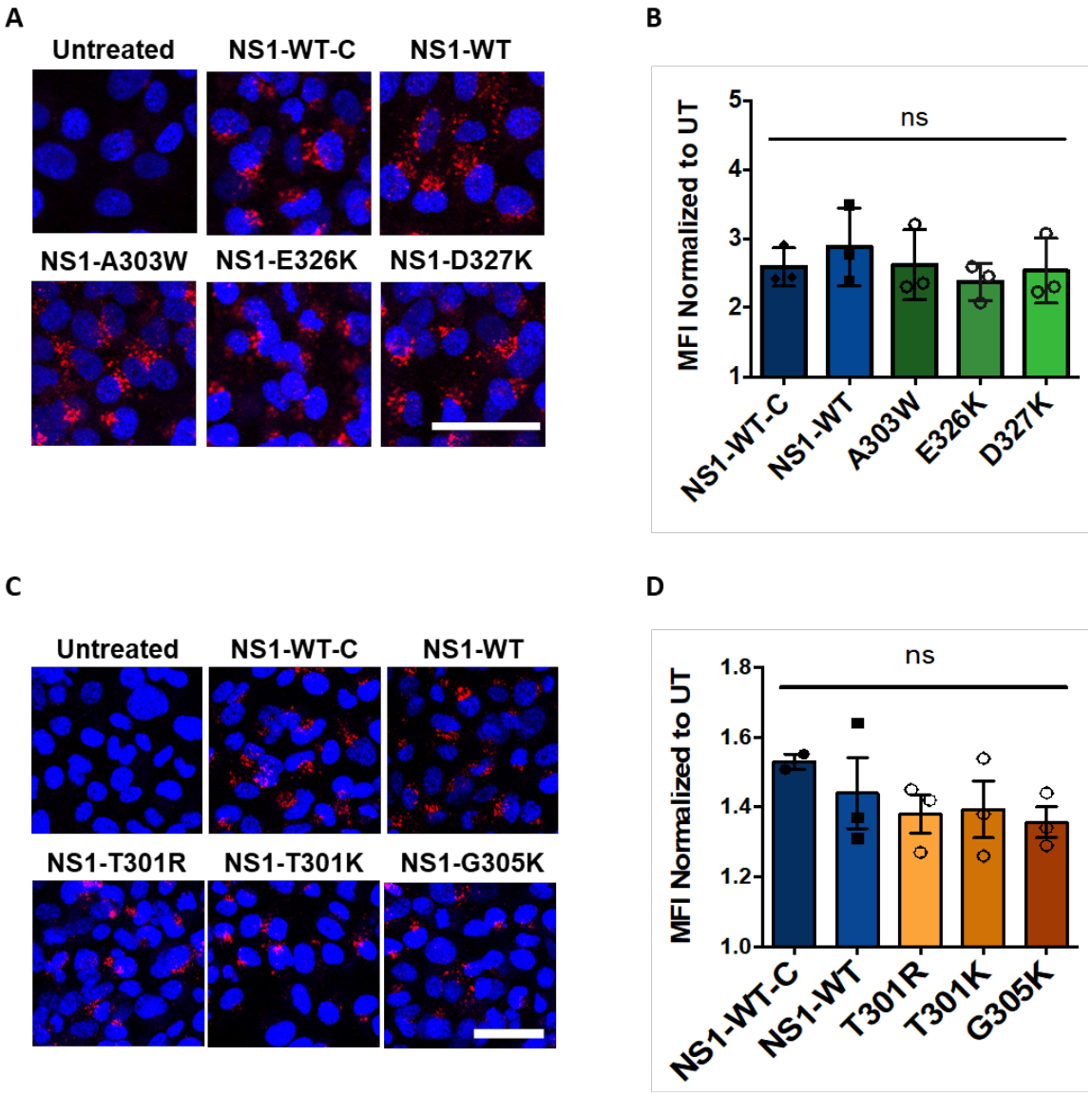

Figure 7. β-ladder mutations do not affect NS1 binding to endothelial cells. 10μg/mL of recombinant WT or NS1 mutagenized at **(A)** DENV specific residues or (**C)** flavivirus-conserved residues within the 2B7 epitope. was added to HPMEC and incubated at 37ºC for 1 hour. NS1 binding was assessed by immunofluorescence microscopy, and representative images from three experiments are shown. **(B)** Quantification of (A), normalized to untreated controls. **(D)** Quantification of (C), normalized to untreated controls. Images represent 3 independent experiments. Scale bars, 100 μm. Data plotted as mean ± SD. n.s., not significant. Figures were included in Biering et al (34).

Table 2. Characteristics of participants

	All		DF	DHF	DSS
Participants	53		20	20	13
Days since symptom onset	4		4	4	4
Age (mean (SD))	9 (3.5)		9.25 (3.5)	9.2 (3.6)	8.3 (3.7)
Female	33 *(62%)*		10	14	9
Male	20 *(38%)*		10	6	4
Secondary infection	53 *(100%)*		20	20	13
DENV2	28 *(53%)*		10	10	8
DENV3	25 *(47%)*		10	10	5
Dengue without Warning Signs	3		2	1	0
Dengue with Warning Signs	28		14	14	0
Severe Dengue	22		4	5	13

Percentage of participants per characteristic in italics. SD=standard deviation, DF = dengue fever, DHF = dengue hemorrhagic fever , DSS = dengue shock syndrome

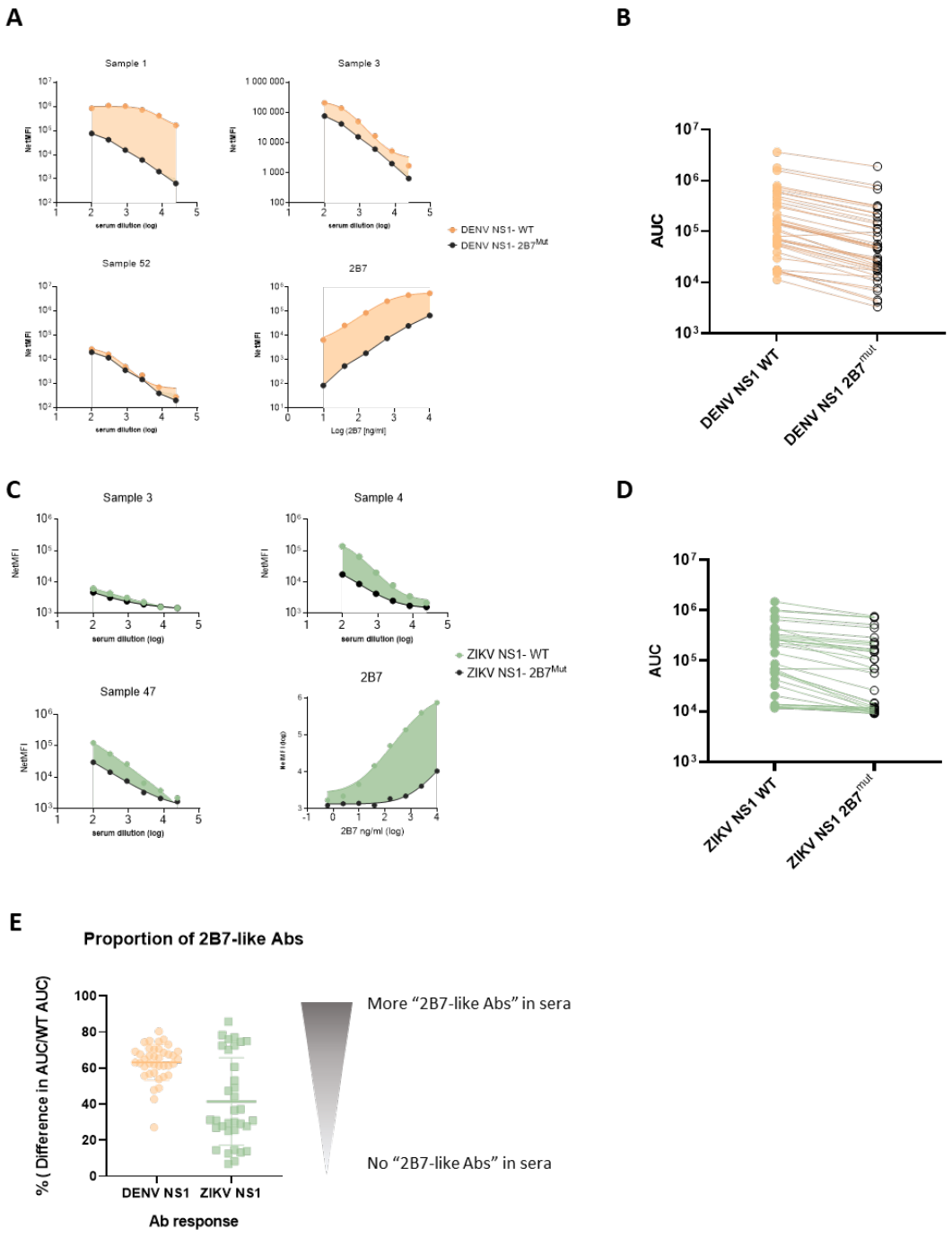

Figure 8. Antibody responses to the 2B7 epitope are prevalent in human DENV infections. (A-B) DENV NS1 WT or DENV NS1 G305K conjugated to Luminex beads were incubated with serially diluted sera from patients infected with DENV. α-NS1 Abs from sera bound to beads were detected using a phycoerythrin (PE)-conjugated goat α-human IgG on an Intellicyt iQue3 Screener. A 5-point dilution curve was created for each antigen, and the area under the curve (AUC) was quantified for each curve. Representative curves from 3 samples and mAb 2B7 are shown in (A). The AUC for all samples against WT DENV NS1 or DENV NS1 G305K (DENV NS1^{mut}) are shown in (B). **(C-D)** Same as in (A-B), except ZIKV NS1 WT or ZIKV NS1 G305K were conjugated to beads. Representative curves from 3 samples and mAb 2B7 are shown in (C). The AUC for all samples against WT ZIKV NS1 or ZIKV NS1 G305K (ZIKV

NS1^{mut}) are shown in (D). **(E)** The proportion of 2B7 epitope-binding Abs to the overall α-NS1 Ab response was calculated by dividing the difference in AUC between WT and NS^{mut} by the AUC of WT for the indicated antigens.

Table 3. List of primers used in this study

Backbone	Change	Primer	
DENV 2	D281P	Forward	GGACTTTGATTTCTGTCCAGGAACAACAGTGGTAGTG
		Reverse	CACTACCACTGTTGTTCCTGGACAGAAATCAAAGTCC
DENV 2	D281S	Forward	GGACTTTGATTTCTGTAGCGGAACAACAGTGGTAGTG
		Reverse	CACTACCACTGTTGTTCCGCTACAGAAATCAAAGTCC
DENV 2	R299E	Forward	GAGGACCCTCTTTGGAAACAACCACTGCCTC
		Reverse	GAGGCAGTGGTTGTTTCCAAAGAGGGTCCTC
DENV 2	R299A	Forward	GAGGACCCTCTTTGGCAACAACCACTGCC
		Reverse	GGCAGTGGTTGTTGCCAAAGAGGGTCCTC
DENV 2	T301K	Forward	GAGGACCCTCTTTGAGAACAAAGACTGCCTCTGG
		Reverse	CCAGAGGCAGTCTTTGTTCTCAAAGAGGGTCCTC
DENV 2	T301R	Forward	GAGGACCCTCTTTGAGAACAAGAACTGCCTCTGG
		Reverse	CCAGAGGCAGTTCTTGTTCTCAAAGAGGGTCCTC
DENV 2	A303W	Forward	TTGAGAACAACCACTTGGTCTGGAAAACTCATA
		Reverse	TATGAGTTTTCCAGACCAAGTGGTTGTTCTCAA
DENV 2	A303R	Forward	TTGAGAACAACCACTCGTTCTGGAAAACTCATA
		Reverse	TATGAGTTTTCCAGAACGAGTGGTTGTTCTCAA
DENV 2	G305W	Forward	CCACTGCCTCTTGGAAACTCATAACAGAATGGTGC
		Reverse	GCACCATTCTGTTATGAGTTTCCAAGAGGCAGTGG
DENV 2	G305K	Forward	CCACTGCCTCTAAGAAACTCATAACAGAATGGTGC
		Reverse	GCACCATTCTGTTATGAGTTTCTTAGAGGCAGTGG
DENV 2	E326K	Forward	GCTAAGATACAGAGGTAAGGATGGGTGCTGGTAC
		Reverse	GTACCAGCACCCATCCTTACCTCTGTATCTTAGC
DENV 2	E326A	Forward	CTAAGATACAGAGGTGCAGATGGGTGCTGGTAC
		Reverse	GTACCAGCACCCATCTGCACCTCTGTATCTTAG
DENV 2	D327K	Forward	CTAAGATACAGAGGTGAGAAGGGGTGCTGGTACGGGATG
		Reverse	CATCCCGTACCAGCACCCCTTCTCACCTCTGTATCTTAG
DENV 2	D327A	Forward	GATACAGAGGTGAGGCTGGGTGCTGGTACG
		Reverse	CGTACCAGCACCCAGCCTCACCTCTGTATC
DENV 2	G328W	Forward	CAGAGGTGAGGATTGGTGCTGGTACGG
		Reverse	CCGTACCAGCACCAATCCTCACCTCTG
DENV 2	G328K	Forward	CAGAGGTGAGGATAAGTGCTGGTACGG
		Reverse	CCGTACCAGCACTTATCCTCACCTCTG
DENV 2	W330A	Forward	GGTGAGGATGGGTGCGCATACGGGATGG
		Reverse	CCATCCCGTATGCGCACCCATCCTCACC
DENV 2	V346E	Forward	GAGAAAGAAGAGAATTTGGAGAACTCCTTGGTCACAGCTC
		Reverse	GAGCTGTGACCAAGGAGTTCTCCAAATTCTCTTCTTTCTC
DENV 2	V346F	Forward	GAGAAAGAAGAGAATTTGTTCAACTCCTTGGTCACAGC
		Reverse	GCTGTGACCAAGGAGTTGAACAAATTCTCTTCTTTCTC
DENV 2	E326K D327K	Forward	CTAAGATACAGAGGTAAGAAGGGGTGCTGGTACGGGATGG
		Reverse	CCATCCCGTACCAGCACCCCTTCTTACCTCTGTATCTTAG
DENV 2	E326A D327A	Forward	GATACAGAGGTGCAGCTGGGTGCTGGTACG
		Reverse	CGTACCAGCACCCAGCTGCACCTCTGTATC
WNV	T301K	Forward	GCCACTCGCACCAAGACAGAGAGCGGA
		Reverse	TCCGCTCTCTGTCTTGGTGCGAGTGGC
WNV	T301R	Forward	GCCACTCGCACCAGAACAGAGAGCGGA
		Reverse	TCCGCTCTCTGTTCTGGTGCGAGTGGC
WNV	G305K	Forward	CCACCACAGAGAGCAAAAAGTTGATAACAGATTGG
		Reverse	CCAATCTGTTATCAACTTTTTGCTCTCTGTGGTGG
ZIKV	T301K	Forward	CCATCTCTGAGATCAAAAACTGCAAGCGGAAGG
		Reverse	CCTTCCGCTTGCAGTTTTTGATCTCAGAGATGG
ZIKV	T301R	Forward	CCATCTCTGAGATCAAGAACTGCAAGCGGAAGG
		Reverse	CCTTCCGCTTGCAGTTCTTGATCTCAGAGATGG
ZIKV	G305K	Forward	CCACTGCAAGCAAAAGGGTGATCGAGGAATGG
		Reverse	CCATTCCTCGATCACCCTTTTGCTTGCAGTGG

Discussion

Our structure-guided interrogation of the 2B7:NS1 interaction has yielded several insights that have advanced our understanding of NS1 biology and the mechanism by which the α-NS1 antibodies like 2B7 protect against NS1-mediated pathogenesis. Mutagenesis of residues within the 2B7 epitope revealed previously unknown molecular determinants of NS1 secretion and NS1-mediated endothelial permeability. In addition, this work has determined key residues that form the structural basis of a highly protective and cross-reactive α-NS1 antibody response and identified that similar antibodies may be elicited in human DENV infection. Taken together, the work provided herein combined with the crystal structure of the DENV NS1:2B7 complex lead us to construct a model in which 2B7 inhibits DENV NS1-induced endothelial dysfunction through two distinct mechanisms: direct binding to amino acids in the β-ladder required for DENV NS1-induced endothelial hyperpermeability and prevention of NS1 binding to the endothelial cell surface through steric hinderance. This work, combined with data from *in vivo* experiments done in (34) and work done by Modhiran et al (35) defining another protective pan-flavivirus NS1 antibody binding a similar epitope to 2B7, thus illuminates the mechanistic basis of protective α-NS1 antibodies to flavivirus infection.

The function of distinct domains within NS1 were unknown at the start of the studies described herein. The mutagenesis of the 2B7 epitope presented in this work led us to hypothesize that the β-ladder to is essential for NS1-mediated endothelial pathogenesis is at a step downstream of binding and that the amino acids responsible to NS1 binding to cells is outside of the 2B7 epitope. Indeed, subsequent work by Lo et al using NS1 domain and amino acid swaps between DENV, ZIKV and WNV firmly establishes that the wing domain, specifically amino acids 91-93, are the molecular determinants of NS1 binding to endothelial cells (36). Previously, our group identified a glycosylation mutant within the β-ladder, N207Q, that was also deficient in inducing endothelial dysfunction but could still bind to endothelial cells due to a defect in internalization. (37). The reduced capacity of T301R, A303W, E326K, and D327K mutants to induce endothelial hyperpermeability despite displaying equal ability to bind to endothelial cells compared to WT DENV NS1 provides further evidence that the β-ladder domain of DENV NS1 is responsible for inducing endothelial hyperpermeability at a step distinct from and downstream of binding to the surface of endothelial cells.

The mechanism behind the attenuation of β-ladder mutants remains an open question. DENV NS1 activates multiple cellular pathways in endothelial cells to induce dysfunction, resulting in the activation of enzymes including MMP-9, cathepsin-L and heparanases, degradation of the endothelial glycocalyx, and mislocalization of tight and adherens junctions (14,16,38). Recent studies in the lab also indicate that the beta-2 adrenergic receptor (β2AR) and the endothelial growth factor receptor (EGFR) are also involved in mediating NS1-induced endothelial dysfunction. Preliminary experiments indicated that A303W, E326K, and D327K mutants may be less able to activate cathepsin-L, a cysteine protease activated by DENV NS1. However, recent work in the Harris lab has demonstrated that while NS1-induced pathways are interconnected, disruption of one pathway does not necessarily affect all downstream outcomes. Future studies characterizing the β-ladder mutants could evaluate whether attenuation extends to other phenotypes such as degradation of sialic acid and heparan sulfate, nuclear localization of β-catenin,

or localized vascular leak *in vivo*. These studies would begin to elucidate how specific residues within the β-ladder serve as molecular determinants to NS1-induced endothelial dysfunction.

One important observation of our work is that residues within the epitope core (AA 299-305) impart pan-flavivirus binding ability to 2B7 due to the conservation of these residues across multiple flavivirus NS1. This pan-flavivirus binding is not unique to 2B7; another α-NS1 mAb. 1G5.3 also binds to the 2B7 epitope core and has cross-reactivity to ZIKV and WNV NS1 (35). 2B7 and 1G5.3 can both block ZIKV/WNV NS1-induced endothelial hyperpermeability *in vitro* and 1G5.3 improves survival of mice challenged with DENV, ZIKV, and WNV (34,35). Thus, the 2B7 epitope core opens the door for NS1-directed therapeutics and vaccines with pan-flavivirus potential. Our study suggests that T301 and G305 are key residues that should be considered when designing small molecules, mAbs, or immunogens aimed at making a broadly efficacious therapeutic or vaccine against multiple flavivirus infections.

The effectiveness of polyclonal α-NS1 antibodies and monoclonals like 2B7 in preventing DENV disease severity in mice has been clearly demonstrated (8,34,35); however, the role of α-NS1 antibodies in preventing dengue disease severity in humans is less understood. The risk of symptomatic DENV infection and severe disease are elevated by prior ZIKV or DENV infections, where it is thought that low titers of pre-existing DENV antibodies mediate antibody-dependent enhancement (ADE) (5). However, under ADE conditions, α-NS1 antibody responses are also present; thus, the degree to which α-NS1 antibody responses are protective in human DENV infection is unclear, due in part to our incomplete understanding of what constitutes a protective α-NS1 antibody response. The β-ladder mutants generated in this work provide additional utility as antigens to profile the α-NS1 antibody response in humans. The work presented here represents a proof-of-concept study demonstrating that 2B7-like antibodies can be found in plasma after infection with DENV in a multiplex, Luminex-based format. Combined with NS1 domain chimeras generated in the lab, we now have the ability to profile α-NS1 antibody responses at the level of specific domains and epitopes. Analyzing these responses in pre-infection samples may reveal correlations between domain/epitope-specific responses and protection (or lack thereof) against symptomatic DENV infection or severe dengue disease, informing next-generation dengue vaccine design.

Elucidating the structural basis of binding of a single protective mAb against NS1-induced endothelial dysfunction has provided valuable insight into the roles specific amino acids have for NS1 secretion and NS1-induced pathogenesis and provides a roadmap for targets of protective NS1 antibodies. In addition, the mutants generated over the course of this work will continue to be valuable tools for interrogating intracellular pathways activated by NS1 as well as for profiling α-NS1 antibody responses in humans. Taken together, these results have deepened our knowledge of DENV NS1 biology and the antibody response to NS1, laying the groundwork for future therapeutics targeting NS1-induced pathogenesis and providing a roadmap for next-generation vaccines against DENV.

Materials and Methods

Cell lines

FreeStyle 293F suspension cells (Thermo Fisher Scientific) were used for production ofrecombinant NS1 proteins. 293F cells were cultured in FreeStyle 293 Expression medium (Thermo Fisher Scientific) containing 1% penicillin/streptomycin (P/S) and grown in a CO2 incubator at 37°C with 8% CO2 and maintained on a cell shaker at ~130 rpm. HEK-293T cells (ATCC) were cultured in Dulbecco's Modified Eagle Medium (DMEM) supplemented with 10% fetal bovine serum (FBS) and 1% P/S. HPMEC (HPMEC-ST1.6r) were kindly donated by Dr. J.C. Kirkpatrick at Johannes Gutenberg University, Germany, and were used for NS1 cell binding and TEER assays. HPMECs were propagated (passages 5–10) and maintained in endothelial growth medium 2 (EGM-2) using the EGM-2 bullet kit from Lonza following the manufacturer's specifications and grown at 37ºC with 5% CO2.

293T Screen

HEK-293T cells were seeded in 24-well plate and allowed to grow to confluency over 2 days. On the day of experiment, media was changed with fresh DMEM. NS1 plasmids were incubated with lipofectamine transfection reagents (Invitrogen) at room temperature for 20 minutes, then added to cells. 24 hours post-transfection, supernatant was collected. Cell pellets were washed 1x with PBS and permeabilized with RIPA buffer containing protein inhibitor (Roche) by incubating with shaking at 4ºC for 10 minutes, then stored at -80ºC. Cell pellets were analyzed by western blot. Supernatant was aliquoted and analyzed by western blot or NS1 capture ELISA.

NS1 mutagenesis, 293F transfection, and purification of NS1 proteins

NS1 mutants were produced using a site-directed mutagenesis kit (QuikChange XL Site-Directed Mutagenesis Kit, Agilent) following the manufacturer's instructions, with the primers from **Table 3** The pMAB protein expression vector encoding DENV2 NS1 (Thailand/16681) or WNV NS1 (NY99) with a N-terminal CD33 signal sequence and a C-terminal His tag were used (a kind gift from Dr. Michael Diamond, Washington University, St. Louis, MO). The ZIKV NS1 sequence (Nica1-16) was synthesized by Bio Basic Inc. and cloned into the pMAB vector (*35*). Transfections were conducted with FreeStyle 293F cells using polyethylenimine (PEI) (Sigma) according to the manufacturer's instructions. Forty-eight to seventy-two hours post-transfection, NS1-containing supernatants were collected and stored at -80°C prior to the protein purification step. The NS1-containing supernatants were thawed, then mixed 1:1 with binding buffer (20 mM sodium phosphate, 500 mM sodium chloride, 20 mM imidazole, pH 7.4) and bound to HisPur cobalt resin (Thermo Fisher Scientific) with shaking for 2 hours at room temperature. Afterwards, the NS1-resin was transferred to a column and washed 5X in 1 column volume of wash buffer (20 mM sodium phosphate, 500 mM sodium chloride, 30 mM imidazole, pH 7.4). NS1 was then eluted from the Ni-NTA resin with 1.5mL elution buffer (20 mM sodium phosphate, 500 mM sodium chloride, 200 mM imidazole, pH 7.4). The purified NS1 stocks were then subjected to dialysis against 1X PBS for 48 hours at 4°C, then concentrated in an Amicon filter with a 10-kDa size cutoff (Millipore). A mini-BCA protein quantitation kit (Thermo Fisher Scientific) was used to quantify the purified recombinant proteins. Unless stated otherwise, these NS1 proteins, as well as the Native Antigen NS1 proteins listed above, were used for all *in vitro* cell line, phage display and *in vivo* experiments. To compare mutagenized NS1 stability to NS1-WT at conditions relevant to cell culture experiments, 100 ng of the indicated proteins were mixed with EGM-2 media (Lonza)

and incubated in a tissue-culture incubator for the times indicated in the figures and protein levels were measured by Western blot analysis.

Size-exclusion chromatography

For size-exclusion chromatography, 0.125 mg (500 µL of a 0.25 mg/mL stock) of the indicated purified and dialyzed NS1 proteins was injected into a Superose 6 Increase 10/300 GL column (GE Life Sciences) previously equilibrated with 1X PBS; the eluate was monitored by absorbance at 280 nm. Peak fractions were analyzed by SDS-PAGE (2.5 µL of each 1-mL fraction) and probed with anti-His antibody.

NS1 cell-binding assay

To measure binding of DENV NS1 to HPMEC, $6x10^4$ (HPMEC) cells were seeded on 0.2% gelatin- (Sigma) coated glass coverslips in 24-well plates. Cells were allowed to form a fully confluent monolayer for three days, with medium changes every other day. On the day of the experiment, 10 µg/mL (3 µg total protein) of the NS1 proteins indicated in the figures was preincubated with antibodies for 30 min at 37°C and then added to wells. NS1 and cells were allowed to incubate for 1 hour, and then a mouse anti-His antibody conjugated to Alexa Fluor 647 (Novus Biologicals) was diluted 1:200 in the media of live cells and allowed to incubate for an additional 30 min. Cells were then washed twice in 1X PBS followed by fixation in 4% formaldehyde (Thermo Fisher Scientific). Nuclei were stained by adding Hoechst 33342 (Immunochemistry) at a dilution of 1:200 along with antibodies mentioned above. Coverslips were mounted onto microscope slides on a drop of ProLong Gold (Thermo Fisher Scientific) and imaged using a Zeiss LSM 710 inverted confocal microscope (CRL Molecular Imaging Center, UC Berkeley).

Enzyme-linked immunosorbent assay (ELISA)

Direct NS1 ELISAs were conducted to measure binding of 2B7 to different flavivirus NS1 proteins as well as to distinct recombinant NS1 domains. MaxiSorp ELISA plates (Thermo Fisher Scientific/Nunc) were coated with the indicated NS1 protein at a concentration of 0.5 µg/mL in 100 µL 1X PBS and allowed to incubate overnight at 4°C. The next day, plates were blocked in 1X PBS + 1% BSA for 2 hours then washed thrice with 1X PBS. 2B7 was then diluted, as indicated in the figures, in blocking buffer, and 100 µL was added to plates. After a 1-hour incubation at 37°C, plates were washed 5X in 1X PBS + 0.1% Tween20. Plates were then incubated for 1 hour at 37°C with an HRP-conjugated secondary antibody diluted at 1:5000 in blocking buffer. After five additional wash steps, plates were developed using the 3,3',5,5'-tetramethylbenzidine (TMB) substrate (Sigma). Plates were allowed to develop for ~10 min before the addition of a 2N H_2SO_4 stop buffer. Absorbance was read at a wavelength of 450 nm using a microplate reader. For the mutagenesis screening, the assay was conducted as above except plates were first coated with an anti-NS1 antibody specific for the wing domain of NS1 (7E11) diluted to 2 µg/mL in PBS and allowed to incubate overnight at 4°C. After blocking, NS1 containing supernatants were then incubated with plates for 1 hour at 37°C, and the bound NS1 was then detected using either biotinylated 2B7 diluted 1:1,000 in blocking buffer or a rabbit- anti-His antibody diluted 1:5,000 in blocking buffer. Strepavidin-HRP or donkey-α-rabbit IgG HRP-conjugated antibody diluted 1:5000 were used as secondaries.

Trans-endothelial Electrical Resistance assay (TEER)

A transendothelial electrical resistance assay was used to measure the capacity of NS1 proteins to trigger endothelial hyperpermeability of HPMECs. In brief, $6x10^4$ (HPMEC) or $1x10^5$ (HBMEC) cells were seeded in 300 µL of medium into the apical chamber of 24-well transwell polycarbonate membrane inserts (Transwell permeable support, 0.4 µm, 6.5 mm insert; Corning). Next, 1.5 mL of medium was added to the basolateral chamber, and a full cell monolayer was allowed to grow for three days with media changes from both apical and basolateral chambers every day. On the day of the experiment, 5 µg/mL of the indicated NS1 proteins (1.5 µg total protein) was premixed, or not, with antibodies at the concentrations indicated in the figure legends for 30 min at 37°C. After incubation, NS1 and antibody mixtures were added to the apical chambers of transwells. Electrical resistance values were measured in ohms (Ω) at the time-points indicated in the figures using an Epithelial Volt Ohm Meter (EVOM) with "chopstick" electrodes (World Precision Instruments). Untreated endothelial cells grown on transwells, as well as transwell inserts containing only medium but no cells, were used as negative controls to calculate the baseline electrical resistance. Relative TEER is calculated as a ratio of resistance values as (Ω experimental condition-Ω medium alone)/(Ω non-treated endothelial cells-Ω medium alone). For the area under the curve (AUC) analyses, the net AUC was taken from all curves using a baseline of Y=1 while also taking into consideration peaks that went below the baseline.

SDS-PAGE and western blot

Total cell lysates or recombinant proteins were collected in protein sample buffer (0.1 M Tris pH 6.8, 4% SDS, 4 mM EDTA, 286 mM 2-mercaptoethanol, 3.2 M glycerol, 0.05% bromophenol blue) and then resolved by SDS-PAGE. For native gels, the same protocol was followed except the sample buffer contained no SDS or 2-mercaptoethanol. Proteins were then transferred onto nitrocellulose membranes and probed with primary antibodies diluted in Tris-buffered saline with 0.1% Tween20 (TBS-T) containing 5% skim milk. Membranes and antibodies were incubated overnight rocking at 4°C. The next day, membranes were washed three times with TBS-T before being probed with anti-mouse HRP secondary antibodies diluted in 5% milk in TBS-T at a dilution of 1:5,000 at room temperature for 1 hour. Afterwards, membranes were washed with TBST three more times before being developed with ECL reagents and imaged on a ChemiDoc system with Image Lab software (Bio-Rad). The following antibodies were used: mouse anti-His (MA1-21315, Thermo Scientific), mouse anti-NS1 mAb (7E11), mouse anti-NS1 mAb (2B7), mouse anti-α-tubulin (ab4074, Abcam), mouse anti-β-actin (sc-47778, Santa Cruz Biotechnology), goat anti-mouse HRP (405306, Biolegend).

Luminex profiling of human sera

Antibody responses to the 2B7 epitope of DENV or ZIKV NS1 were measured using a multiplex-bead based assay. To generate antigen-conjugated beads, mouse biotinylated-α-His-Ab was conjugated to Magplex-Avidin microspheres ThermoFisher) by end-over-end mixing for 30 minutes at room temperature. Beads were washed twice in 1X PBS-1% BSA and then WT DENV NS1, G305K DENV NS1, WT ZIKV NS1, or G305K ZIKV NS1 produced in-house were captured on the conjugated beads by end-over-end mixing for 60 minutes at room temperature. Beads were washed twice in 1X PBS-1% BSA and resuspended at a concentration of $1x10^6$ beads/mL. Patient sera was initially diluted 1:100 in 1X PBS-1% BSA and serially diluted with 3-fold dilutions in 1X PBS-1% BSA. Diluted sera was incubated with antigen-conjugated beads (WT and G305K DENV NS1 or WT and G305K ZIKV NS1) in a 384-well plate for 90 minutes at room temperature.

Plate was washed and then a PE-conjugated goat-α-human IgG was added to the plate and allowed to incubate for 45 minutes are room temperature on a plate shaker shaking at 1200rpm. Plate was then washed and then analyzed on a Intellcyt iQue3 Screener. A 5-point dilution curve was created for each antigen and the area under the curve (AUC) was quantified for each curve. The proportion of 2B7 epitope-binding Abs to the overall α-NS1 Ab response was calculated by dividing the difference in AUC between WT and NSmut over the AUC of WT for the indicated antigens

Statistics

All quantitative analyses were conducted, and all data were plotted, using GraphPad Prism 8 software. Experiments were repeated at least 2 times, to ensure reproducibility. All experiments were designed and performed with both positive and negative controls (indicated in the figures), which were used for inclusion/exclusion determination. For immunofluorescence microscopy experiments, images of random fields were captured. For all experiments with quantitative analysis, data are displayed as mean ± standard error of the mean (SEM). All cell binding and TEER quantitative data were analyzed using a One-way ANOVA analysis with Tukey's multiple comparisons test. The resulting p-values from the above statistical tests were displayed as n.s., not significant; $p > 0.05$; *$p < 0.05$; **$p < 0.01$; ***$p < 0.001$; ****$p < 0.0001$.

References

1. Cattarino L, Rodriguez-Barraquer I, Imai N, Cummings DAT, Ferguson NM. Mapping global variation in dengue transmission intensity. Science Translational Medicine [Internet]. 2020 Jan 29 [cited 2020 May 29];12(528). Available from: https://stm.sciencemag.org/content/12/528/eaax4144

2. Muller DA, Depelsenaire ACI, Young PR. Clinical and Laboratory Diagnosis of Dengue Virus Infection. J Infect Dis. 2017 Mar 1;215(suppl_2):S89–95.

3. Halstead SB. Dengvaxia sensitizes seronegatives to vaccine enhanced disease regardless of age. Vaccine. 2017 Nov 7;35(47):6355–8.

4. Sridhar S, Luedtke A, Langevin E, Zhu M, Bonaparte M, Machabert T, et al. Effect of Dengue Serostatus on Dengue Vaccine Safety and Efficacy. New England Journal of Medicine. 2018 Jul 26;379(4):327–40.

5. Katzelnick LC, Gresh L, Halloran ME, Mercado JC, Kuan G, Gordon A, et al. Antibody-dependent enhancement of severe dengue disease in humans. Science. 2017 Nov 17;358(6365):929–32.

6. Katzelnick LC, Bos S, Harris E. Protective and enhancing interactions among dengue viruses 1-4 and Zika virus. Curr Opin Virol. 2020 Aug;43:59–70.

7. Amorim JH, Diniz MO, Cariri FAMO, Rodrigues JF, Bizerra RSP, Gonçalves AJS, et al. Protective immunity to DENV2 after immunization with a recombinant NS1 protein using a genetically detoxified heat-labile toxin as an adjuvant. Vaccine. 2012 Jan 20;30(5):837–45.

8. Beatty PR, Puerta-Guardo H, Killingbeck SS, Glasner DR, Hopkins K, Harris E. Dengue virus NS1 triggers endothelial permeability and vascular leak that is prevented by NS1 vaccination. Science Translational Medicine. 2015 Sep 9;7(304):304ra141-304ra141.

9. Glasner DR, Puerta-Guardo H, Beatty PR, Harris E. The Good, the Bad, and the Shocking: The Multiple Roles of Dengue Virus Nonstructural Protein 1 in Protection and Pathogenesis. Annu Rev Virol. 2018 Sep 29;5(1):227–53.

10. Paranavitane SA, Gomes L, Kamaladasa A, Adikari TN, Wickramasinghe N, Jeewandara C, et al. Dengue NS1 antigen as a marker of severe clinical disease. BMC Infect Dis. 2014 Oct 31;14:570.

11. Avirutnan P, Hauhart RE, Somnuke P, Blom AM, Diamond MS, Atkinson JP. Binding of flavivirus nonstructural protein NS1 to C4b binding protein modulates complement activation. J Immunol. 2011 Jul 1;187(1):424–33.

12. Chao CH, Wu WC, Lai YC, Tsai PJ, Perng GC, Lin YS, et al. Dengue virus nonstructural protein 1 activates platelets via Toll-like receptor 4, leading to thrombocytopenia and hemorrhage. PLoS Pathog. 2019 Apr;15(4):e1007625.

13. Chan KWK, Watanabe S, Jin JY, Pompon J, Teng D, Alonso S, et al. A T164S mutation in the dengue virus NS1 protein is associated with greater disease severity in mice. Science Translational Medicine. 2019 Jun 26;11(498):eaat7726.

14. Puerta-Guardo H, Glasner DR, Harris E. Dengue Virus NS1 Disrupts the Endothelial Glycocalyx, Leading to Hyperpermeability. PLoS Pathog. 2016;12(7):e1005738.

15. Glasner DR, Ratnasiri K, Puerta-Guardo H, Espinosa DA, Beatty PR, Harris E. Dengue virus NS1 cytokine-independent vascular leak is dependent on endothelial glycocalyx components. PLOS Pathogens. 2017 Nov 9;13(11):e1006673.

16. Puerta-Guardo H, Biering SB, Sousa FTG de, Shu J, Glasner DR, Li J, et al. Flavivirus NS1 Triggers Tissue-Specific Disassembly of Intercellular Junctions Leading to Barrier Dysfunction and Vascular Leak in a GSK-3β-Dependent Manner. Pathogens [Internet]. 2022 Jun [cited 2023 Nov 9];11(6). Available from: https://www.ncbi.nlm.nih.gov/pmc/articles/PMC9228372/

17. Akey DL, Brown WC, Dutta S, Konwerski J, Jose J, Jurkiw TJ, et al. Flavivirus NS1 crystal structures reveal a surface for membrane association and regions of interaction with the immune system. Science. 2014 Feb 21;343(6173):881–5.

18. Winkler G, Randolph VB, Cleaves GR, Ryan TE, Stollar V. Evidence that the mature form of the flavivirus nonstructural protein NS1 is a dimer. Virology. 1988 Jan;162(1):187–96.

19. Scaturro P, Cortese M, Chatel-Chaix L, Fischl W, Bartenschlager R. Dengue Virus Non-structural Protein 1 Modulates Infectious Particle Production via Interaction with the Structural Proteins. PLOS Pathogens. 2015 Nov 12;11(11):e1005277.

20. Płaszczyca A, Scaturro P, Neufeldt CJ, Cortese M, Cerikan B, Ferla S, et al. A novel interaction between dengue virus nonstructural protein 1 and the NS4A-2K-4B precursor is required for viral RNA replication but not for formation of the membranous replication organelle. PLoS Pathog. 2019 May 9;15(5):e1007736.

21. Flamand M, Megret F, Mathieu M, Lepault J, Rey FA, Deubel V. Dengue virus type 1 nonstructural glycoprotein NS1 is secreted from mammalian cells as a soluble hexamer in a glycosylation-dependent fashion. J Virol. 1999 Jul;73(7):6104–10.

22. Gutsche I, Coulibaly F, Voss JE, Salmon J, d'Alayer J, Ermonval M, et al. Secreted dengue virus nonstructural protein NS1 is an atypical barrel-shaped high-density lipoprotein. Proc Natl Acad Sci U S A. 2011 May 10;108(19):8003–8.

23. Shu B, Ooi JSG, Tan AWK, Ng TS, Dejnirattisai W, Mongkolsapaya J, et al. CryoEM structures of the multimeric secreted NS1, a major factor for dengue hemorrhagic fever. Nat Commun. 2022 Nov 9;13(1):6756.

24. Henchal EA, Henchal LS, Schlesinger JJ. Synergistic Interactions of Anti-NS1 Monoclonal Antibodies Protect Passively Immunized Mice from Lethal Challenge with Dengue 2 Virus. Journal of General Virology. 1988;69(8):2101–7.

25. Espinosa DA, Beatty PR, Reiner GL, Sivick KE, Hix Glickman L, Dubensky TW, et al. Cyclic Dinucleotide-Adjuvanted Dengue Virus Nonstructural Protein 1 Induces Protective Antibody and T Cell Responses. J Immunol. 2019 Feb 15;202(4):1153–62.

26. Wan SW, Chen PW, Chen CY, Lai YC, Chu YT, Hung CY, et al. Therapeutic Effects of Monoclonal Antibody against Dengue Virus NS1 in a STAT1 Knockout Mouse Model of Dengue Infection. J Immunol. 2017 Oct 15;199(8):2834–44.

27. Lai YC, Chuang YC, Liu CC, Ho TS, Lin YS, Anderson R, et al. Antibodies Against Modified NS1 Wing Domain Peptide Protect Against Dengue Virus Infection. Sci Rep. 2017 Aug 1;7:6975.

28. Tien SM, Chang PC, Lai YC, Chuang YC, Tseng CK, Kao YS, et al. Therapeutic efficacy of humanized monoclonal antibodies targeting dengue virus nonstructural protein 1 in the mouse model. PLoS Pathog. 2022 Apr;18(4):e1010469.

29. Churdboonchart V, Bhamarapravati N, Peampramprecha S, Sirinavin S. Antibodies against dengue viral proteins in primary and secondary dengue hemorrhagic fever. Am J Trop Med Hyg. 1991 May;44(5):481–93.

30. Shu PY, Chen LK, Chang SF, Yueh YY, Chow L, Chien LJ, et al. Dengue NS1-specific antibody responses: isotype distribution and serotyping in patients with Dengue fever and Dengue hemorrhagic fever. J Med Virol. 2000 Oct;62(2):224–32.

31. Sharma M, Glasner DR, Watkins H, Puerta-Guardo H, Kassa Y, Egan MA, et al. Magnitude and Functionality of the NS1-Specific Antibody Response Elicited by a Live-Attenuated Tetravalent Dengue Vaccine Candidate. J Infect Dis. 2020 Mar 2;221(6):867–77.

32. Hertz T, Beatty PR, MacMillen Z, Killingbeck SS, Wang C, Harris E. Antibody epitopes identified in critical regions of dengue virus nonstructural 1 protein in mouse vaccination and natural human infections. J Immunol. 2017 May 15;198(10):4025–35.

33. Jayathilaka D, Gomes L, Jeewandara C, Jayarathna GeethalSB, Herath D, Perera PA, et al. Role of NS1 antibodies in the pathogenesis of acute secondary dengue infection. Nat Commun. 2018 Dec 7;9:5242.

34. Biering SB, Akey DL, Wong MP, Brown WC, Lo NTN, Puerta-Guardo H, et al. Structural basis for antibody inhibition of flavivirus NS1–triggered endothelial dysfunction. Science. 2021 Jan 8;371(6525):194–200.

35. Modhiran N, Song H, Liu L, Bletchly C, Brillault L, Amarilla AA, et al. A broadly protective antibody that targets the flavivirus NS1 protein. Science. 2021 Jan 8;371(6525):190–4.

36. Lo NTN, Roodsari SZ, Tin NL, Wong MP, Biering SB, Harris E. Molecular Determinants of Tissue Specificity of Flavivirus Nonstructural Protein 1 Interaction with Endothelial Cells. Journal of Virology. 2022 Sep 15;96(19):e00661-22.

37. Wang C, Puerta-Guardo H, Biering SB, Glasner DR, Tran EB, Patana M, et al. Endocytosis of flavivirus NS1 is required for NS1-mediated endothelial hyperpermeability and is

abolished by a single N-glycosylation site mutation. PLOS Pathogens. 2019 Jul 29;15(7):e1007938.

38. Pan P, Li G, Shen M, Yu Z, Ge W, Lao Z, et al. DENV NS1 and MMP-9 cooperate to induce vascular leakage by altering endothelial cell adhesion and tight junction. PLOS Pathogens. 2021 Jul 26;17(7):e1008603.

Chapter 4

Development and Implementation of Dried Blood Spot-based COVID-19 Serological Assays for Epidemiologic Studies

This chapter was published in:

Wong MP, Meas MA, Adams C, Hernandez S, Green V, Montoya M, Hirsch BM, Horton M, Quach HL, Quach DL, Shao X, Fedrigo I, Zermeno A, Huffaker J, Montes R, Madden A, Cyrus S, McDowell D, Williamson P, Contestable P, Stone M, Coloma J, Busch MP, Barcellos LF, Harris E. Development and Implementation of Dried Blood Spot-Based COVID-19 Serological Assays for Epidemiologic Studies. *Microbiol Spectr*. 2022 Jun 29;10(3):e0247121. doi: 10.1128/spectrum.02471-21.

Abstract

Serological surveillance studies of infectious diseases provide population-level estimates of infection and antibody prevalence, generating crucial insight into population-level immunity, risk factors leading to infection, and effectiveness of public health measures. These studies traditionally rely on detection of pathogen-specific antibodies in samples derived from venipuncture, an expensive and logistically challenging aspect of serological surveillance. During the COVID-19 pandemic, guidelines implemented to prevent the spread of SARS-CoV-2 infection made collection of venous blood logistically difficult at a time when SARS-CoV-2 serosurveillance was urgently needed. Dried blood spots (DBS) have generated interest as an alternative to venous blood for SARS-CoV-2 serological applications due to their stability, low cost, and ease of collection; DBS samples can be self-generated via fingerprick by community members and mailed at ambient temperatures. Here, we detail the development of four DBS-based SARS-CoV-2 serological methods and demonstrate their implementation in a large serological survey of community members from 12 cities in the East Bay region of the San Francisco metropolitan area using at-home DBS collection. We find that DBS perform similarly to plasma/serum in enzyme-linked immunosorbent assays and commercial SARS-CoV-2 serological assays. In addition, we show that DBS samples can reliably detect antibody responses months post-infection and track antibody kinetics after vaccination. Implementation of DBS enabled collection of valuable serological data from our study population to investigate changes in seroprevalence over an eight-month period. Our work makes a strong argument for the implementation of DBS in serological studies, not just for SARS-CoV-2, but any situation where phlebotomy is inaccessible.

Introduction

Serological surveillance of infectious diseases provides estimates of the incidence and prevalence of infections, generating actionable public health knowledge – such as which populations are disproportionately affected by an infectious disease outbreak or the effectiveness of public health measures in curbing infections. SARS-CoV-2, the causative agent of the COVID-19 pandemic, is responsible for at least 770 million infections and 6 million deaths since its emergence in late 2019 to date (1). Given that approximately 35% of all SARS-CoV-2 infections are asymptomatic (2, 3), with proportions varying substantially by age, serological surveillance studies are a critical tool to enable estimation of the incidence of recent infection and prevalence of past infections at the population level. Most serological studies rely on venous blood from study participants to derive plasma or serum and therefore require an invasive phlebotomy procedure and an intact cold chain for collection, shipment, and storage to ensure sample stability prior to testing. However, during the COVID-19 pandemic, implementation of public health guidelines to curb the spread of SARS-CoV-2, such as lockdowns and social distancing, made the collection of blood to obtain serum or plasma for serosurveillance studies logistically challenging, especially for sizeable community-based studies focused on a large geographic region.

Dried blood spots (DBS) are an alternative blood collection method for serological testing and have been used extensively in screening for other viruses, including Hepatitis B, HIV, and Ebola in both clinical and non-clinical settings (4–6). DBS have advantages over traditional venous blood sampling (7): DBS are stable at room temperature for extended periods of time and can be easily shipped by mail and stored (8), DBS require considerably less blood than traditional phlebotomy, and DBS can be collected by study participants themselves via fingerprick. These qualities make DBS an attractive alternative to venous blood collection, especially when traditional phlebotomy is inaccessible, such as in resource-poor settings or because of pandemic-related public health restrictions.

There has been interest in developing DBS-based serological methods for SARS-CoV-2 serosurveillance. Several studies have investigated the feasibility and performance of DBS-based serological assays, including enzyme-linked immunosorbent assays for anti-spike (S) and receptor binding domain (RBD) antibodies (9–13), as well as multiplexed assay formats for simultaneous detection of spike, RBD, and nucleocapsid (N) antibodies (14). Commercial assays on automated platforms like the Roche Elecsys, which can detect anti-N or anti-S antibodies, have also been evaluated for use with DBS samples. These assays have the advantage of high-throughput processing and lower personnel requirements (15, 16). Based on testing paired plasma/serum and DBS samples, these studies demonstrated robust agreement between the sample types. In addition, several studies have shown that serological assays performed on DBS samples prepared by study participants in the home and mailed to labs for processing can reliably detect SARS-Cov-2 antibodies, providing evidence that DBS are a promising alternative to plasma or serum for SARS-CoV-2 serosurveillance (13–15, 17). However, implementation of DBS-adapted serological methods for large community-based serological surveillance has not been widely demonstrated for tracking immune responses due to natural infections and COVID-19 vaccines.

In this study, we present the validation of four DBS-based serological assays against SARS-CoV-2 S and N antibodies and detail their implementation in a large, serological survey with at-home sample collection, as well as in ancillary longitudinal vaccine studies. We assessed the performance of DBS-based lab-developed anti-S and anti-N IgG ELISAs and two commercial assays (the Ortho anti-S and Roche anti-N Total Ig assays) and evaluated their ability to detect long-term antibody responses and vaccine-induced antibody kinetics. Using these assays in a serial testing algorithm, we analyzed a total of 14,782 DBS samples from a longitudinal cohort of individuals living in 12 cities in the East Bay region of the San Francisco metropolitan area at 3 timepoints between July 2020 and April 2021 for antibodies against SARS-CoV-2 S and N. Results from this study demonstrate that DBS are a practical sampling method for serology-based epidemiology studies, enabling in-home self-sampling for serosurveillance in situations where traditional phlebotomy is inaccessible, impractical, or too costly.

Results

DBS are a viable replacement for plasma in multiple serological assay formats

To evaluate whether DBS samples could be a viable replacement for plasma in serosurveillance studies, we first validated the performance of DBS eluates on both an in-house ELISA detecting anti-S IgG and the Ortho CoV2T. To generate DBS for the validation study, we mixed COVID convalescent plasma (CCP) samples from 39 RT-PCR-confirmed SARS-CoV-2-positive patients and 100 pre-2020 negative controls with anticoagulated plasma depleted whole blood to reconstitute whole blood and applied the mixture to the DBS cards (~15 ul per DBS). Eluates from these reconstituted DBS and their paired plasma samples were then tested by both serological assays.

We first tested DBS eluates in our previously validated anti-S IgG ELISA (18). We determined a new cut-off for the anti-S IgG ELISA using DBS eluate as the input (DBS ELISA) as an optical density (OD_{450}) value of 0.34 via receiver-operator curve (ROC) analysis using the convalescent samples following PCR diagnoses and the pre-2020 samples as the reference standards. This cut-off resulted in an overall sensitivity of 97.62% and specificity of 100% for the ELISA, which demonstrated 100% concordance in the SARS-CoV-2-positive samples between the reconstituted DBS eluate and plasma (Figure 2A-B, S1). When the recommended threshold (S/Co $\geq$1) on the Ortho CoV2T for detection of anti-S antibodies in plasma/serum was used for DBS eluates, ROC analysis yielded a sensitivity of 79.50% (95% CI: 63.29% to 88.00%) and specificity of 100% (95% CI: 90.59% to 100.0%), with an 80% concordance in the SARS-CoV-2-positive samples between the reconstituted DBS eluates and plasma (Figure 2C-D). Both assays showed a linear relationship between plasma and DBS values (ELISA, r^2=0.93; Vitros r^2=0.78; Figure 2 A,C).

We found that the reduced sensitivity of the Ortho CoV2T assay could be explained by the diluted nature of the DBS eluate, as compared to the Ortho CoV2T assay using undiluted plasma. We found that diluting plasma 1:40 gave similar values as the DBS eluates (Figure S2). In contrast, the in-house ELISA was developed using a 1:100 dilution of plasma; thus, DBS eluates performed similarly to plasma in this assay format.

Validation of anti-N serological assays

The introduction of S-based vaccines during the study period necessitated the implementation of N-based serology testing to distinguish between vaccinated and naturally infected individuals in the EBCOVID study. Therefore, we validated an anti-N IgG ELISA for both DBS and plasma as well as the Roche N assay for use with DBS eluates. We validated our anti-N IgG ELISA first on plasma using convalescent plasma samples collected >8 days post-symptom onset from 60 hospitalized, RT-PCR-confirmed severe COVID-19 cases, 57 mild or subclinical cases, and 131 samples collected before 2020 from unexposed persons as described previously (18) and determined the positivity cut-off for the anti-N IgG ELISA as an OD_{490} value of 0.32 via ROC analysis. This cutoff resulted in a sensitivity of 97.10% (95% CI: 90.03% to 99.48%) and specificity of 91.51% (95% CI: 84.65% to 95.47%) when testing serum samples (Figure S3A).

We performed validation of DBS eluates for the N DBS ELISA using the reconstituted DBS sample set used for the validation of our anti-S antibody assays and determined a positivity cut-

off for DBS eluates as an OD_{490} value of 0.32 via ROC analysis (Figure S3B). This cut-off gave the ELISA an overall sensitivity of 89.74% (95% CI: 76.42% to 95.94%), specificity of 90.48% (95% CI: 83.35% to 94.74%) and 87.17% concordance in the SARS-CoV-2 positive samples between the reconstituted DBS eluate and plasma (Figure 3A-B). Overall, the DBS eluates and plasma performed similarly in the anti-N IgG ELISA, comparable to our results for the anti-S IgG ELISA.

Due to limited sample availability from our validation sample set, we validated the use of DBS eluates on the Roche N assay using reserved eluates from our Round 2 sampling that preceded vaccine approvals and rollout (Figure 1C). Using our anti-S IgG DBS ELISA as the reference standard, we determined a new positivity cut-off for the Roche N assay (S/Co ≥0.045). With this cut-off, the Roche N assay displayed a sensitivity of 86.7% and specificity of 97.9% using the DBS format (Figure 3C-D).

Anti-S antibodies remain stable over time whereas anti-N antibodies appear to wane

Since a key characteristic needed for our study as well as other serosurveillance studies is the ability to accurately track cumulative incidence of infection, we empirically assessed whether the DBS format affected the ability of our serological assays to detect long-term, persistent antibody responses to S and N. We generated a panel of plasma and reconstituted whole blood DBS from 10 COVID-19 convalescent plasma donors sampled longitudinally between 0 and 246 days from their first donation and tested this panel using our in-house indirect IgG ELISAs for S and N, the Ortho CoV2T (S) assay, and the Roche N Total Ig assay. The Ortho CoV2T assay showed stable antibody reactivity over time in plasma and DBS eluates; however, the DBS eluate signal was substantially lower than the signal from neat plasma samples. Our in-house indirect S IgG ELISA also showed antibody stability in both DBS and plasma formats over time, but with similar reactivity observed for plasma and DBS eluates (Figure 4A-B). In contrast, both the Roche N Total Ig and our in-house indirect N IgG ELISA showed a decrease in antibody reactivity over time in 6 of 10 donors tested (Figure 5A-B), although every donor would have still been considered antibody reactive. The signal magnitude of the in-house N ELISA, in both DBS and plasma formats, were comparable to each other as well as to the Roche N plasma results, whereas the Roche N DBS results displayed an overall reduction in signal (Figure 5B). Overall, we found that our serological assays in both plasma and DBS formats were suitable for detection of long-term antibodies against S and N.

DBS eluates reflect antibody responses after vaccination

We next evaluated the ability of our assays to measure the antibody response after vaccination against SARS-CoV-2. We generated a longitudinal panel of DBS following 12 vaccinated individuals sampled before their first dose, after their first dose, and after their second dose and tested this panel using the Ortho CoV2T assay and anti-S ELISA. We found that the while both assays were able to capture the increase of antibodies after the first dose of vaccine, the anti-S DBS ELISA did not show subsequent boosting of the antibody response after the second dose when plotted by optical density (OD) (Figure 6A-C). We reasoned that this was due to saturation of the OD of the anti-S-ELISA; therefore, we performed dilutions of the DBS eluate and generated an endpoint titer for each sample. Determining the endpoint titer effectively increased the dynamic range of the anti-S DBS ELISA and allowed us to capture boosting of the antibody response due to the second dose of vaccine (Figure 6D). We further validated this concept by following the

vaccine antibody response via weekly DBS sampling of a small cohort of 4 individuals over a period of 6 months. Comparisons between the single-dilution OD reading and the endpoint titers revealed that while the single-dilution OD stayed stable across the sampling period, the endpoint titers showed an increase in titers up to four weeks after the second dose and subsequent decline over the next six months (Figure 6E-F). 2 of the individuals also showed an increase in titers after receiving booster doses. These results suggest that our anti-S DBS ELISA is not only able to qualitatively detect persistent antibodies after infection and vaccination but also able to track antibody kinetics by using an endpoint titer method.

DBS enables serosurveillance in a large longitudinal study during a pandemic

Our validation studies demonstrated that DBS are a reliable replacement for plasma, and thus we implemented the use of DBS cards as part of the EBCOVID study. The DBS collected from participants were assessed for quality before processing. Only samples with adequate numbers of saturated DBS were processed in our serological assays; samples that did not meet this criterion were labelled as "Insufficient Sample" (IS)", as described above. Overall, we tested 14,782 qualified DBS samples from study participants over three rounds of testing.

In our first round of testing (July to September 2020), we analyzed 4,670 DBS samples using the Ortho CoV2T Assay and detected anti-S antibodies in 29 individuals as positive (S/Co$\geq$1.0), giving an unweighted seroprevalence of 0.62%. Analysis of Round 1 results revealed that 1.08% of samples had S/Co ratios between 0.7 and 1.5, close to the positivity cutoff of 1.0 set by the manufacturer (Figure S4). Given the linear relationship of DBS eluate to plasma and the dilutional effect attributable to DBS elution seen in our validation of the Ortho CoV2T assay, we reasoned that these samples were likely antibody-positive samples with lower seroreactivity. To better resolve samples with grey-zone reactivity in the Ortho CoV2T in subsequent rounds, we devised an algorithm utilizing the in-house S DBS ELISA to retest samples with Ortho CoV2T S/Co results that fell between 0.7 and 2.0. The algorithm performance was determined on all reconstituted DBS samples used for validation (Figures 2-4); we were able to correctly classify 182/184 samples as positive for past SARS-CoV-2 infections and 100/100 pre-2020 samples as negative for past SARS-CoV-2 infections. This yielded a positive predictive value of 100% and a negative predictive value of 98% for our Round 2 algorithm.

We implemented this algorithm in Round 2 (October to December 2020), testing 5,308 samples by the Ortho Total Ig assay. Of these, 317 samples with S/Co values >0.7 and <2.0 were reflexed to the anti-S IgG ELISA, resulting in 33 S antibody-positive samples, giving an unweighted seroprevalence of 0.62% in the cohort in Round 2 (Figure 7).

During Round 3 (February to April 2021), vaccines became available to the public, including our study participants. To distinguish between natural infection and vaccine-induced antibody responses, we modified our testing algorithm to include reflex testing for anti-N antibody using the Roche N assay. Round 3 samples were tested first on the Ortho CoV2T assay, and all anti-S-antibody reactive samples with an S/Co ratio >0.7 and <2.0 were reflexed to the anti-S IgG ELISA, while all anti-S-antibody samples with an S/Co >0.7 were reflexed to the Roche N DBS assay. We considered a confirmed natural infection as any sample that was positive by anti-S IgG ELISA or

had an Ortho CoV2T Assay S/C ratio greater than 2.0 and was positive in the Roche N DBS assay. Using this algorithm, we determined that, of 4,641 samples tested, 1,452 (31.3%) had anti-S antibodies and 84 (1.81%) had anti-NC antibodies due to natural infection (Figure 8). While we could not validate the performance of our Round 3 algorithm before its implementation due to the lack of vaccines and vaccinated individuals preceding Round 3 (before February 2021), a retrospective analysis showed that our Round 3 algorithm correctly identified 435/453 (96%) individuals who self-reported themselves to be fully vaccinated (14 days after the second dose of vaccine).

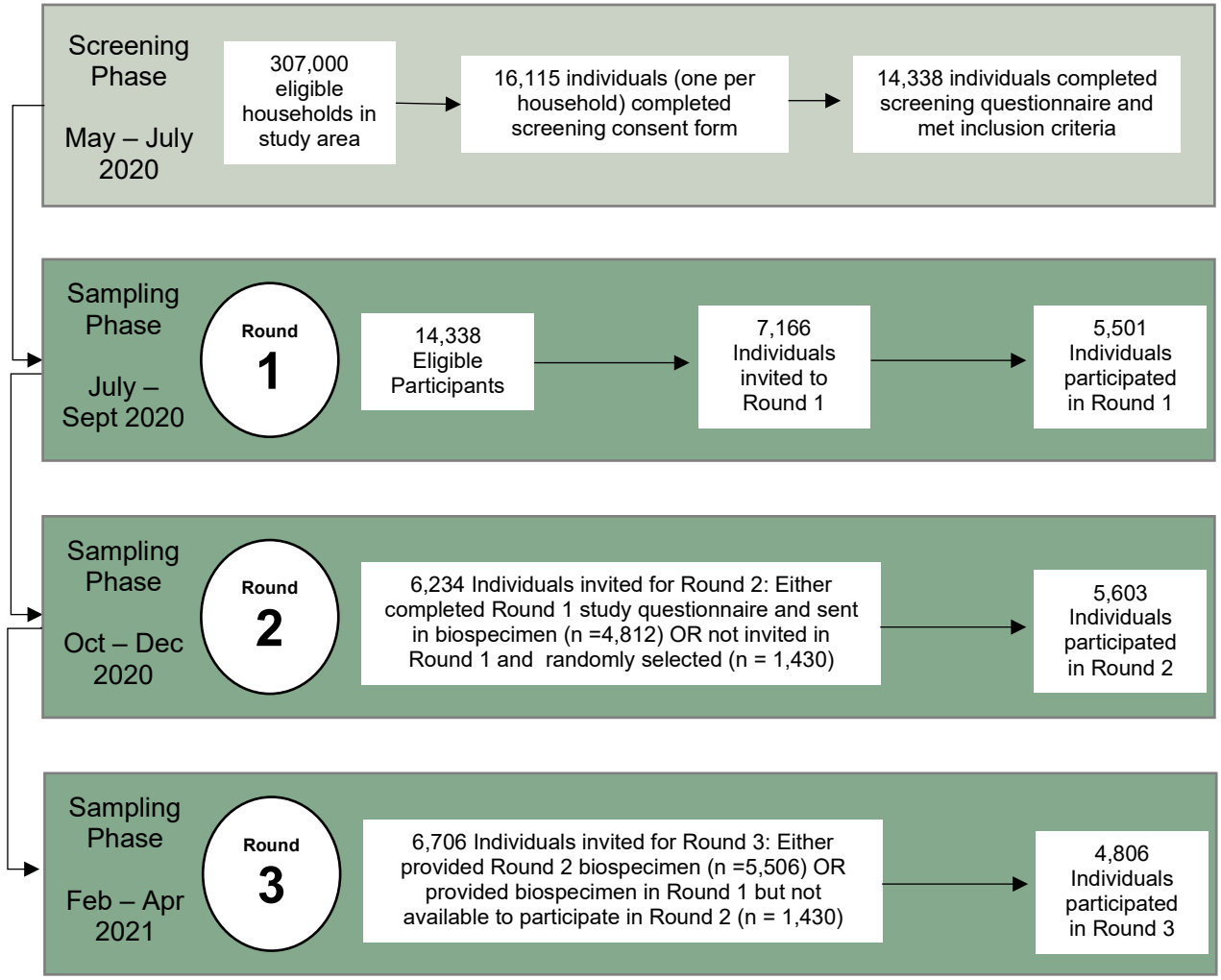

Figure 1. Schematic of the East Bay COVID (EBCOVID) study. There were 2 phases to the study: (A) the screening phase, where participants were recruited and screened for eligibility for inclusion into our study, and (B-D) the sampling phase, where study participants were invited to provide biospecimens, including DBS, in 3 separate rounds.

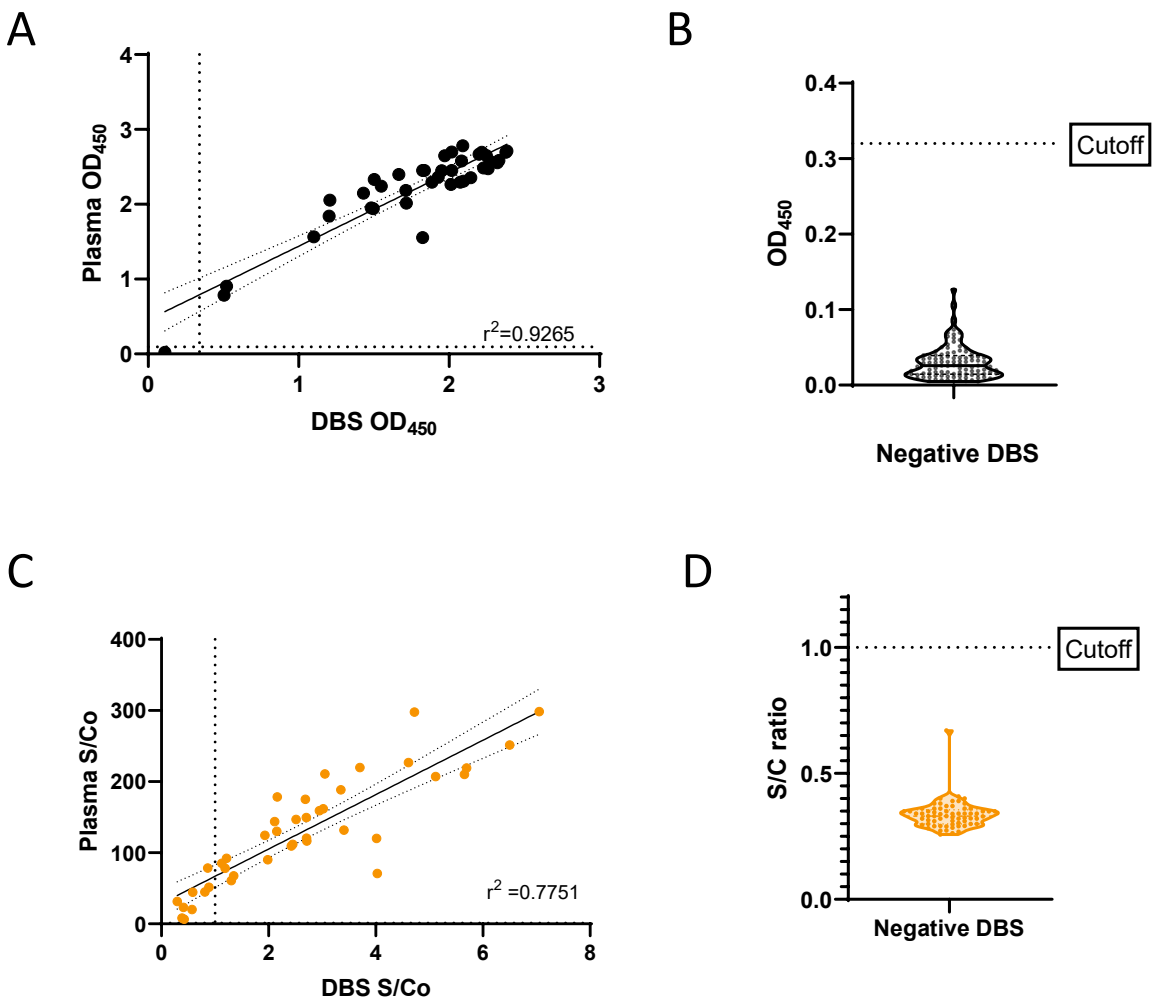

Figure 2. Validation of DBS in anti-S serological assays. Paired DBS and plasma samples (n=39) from previously SARS-CoV-2-infected individuals were compared in (A) the anti-S IgG ELISA and (C) the Ortho COV2T assay. DBS samples (n=100) from individuals without previous SARS-CoV-2 infection were analyzed by (B) the anti-S IgG ELISA and (D) the Ortho COV2T assay. Cut-offs for the assays are denoted by dashed lines. Linear regression comparing IgG levels between sample types (A and C) is depicted by a solid line with 95% confidence intervals (CI).

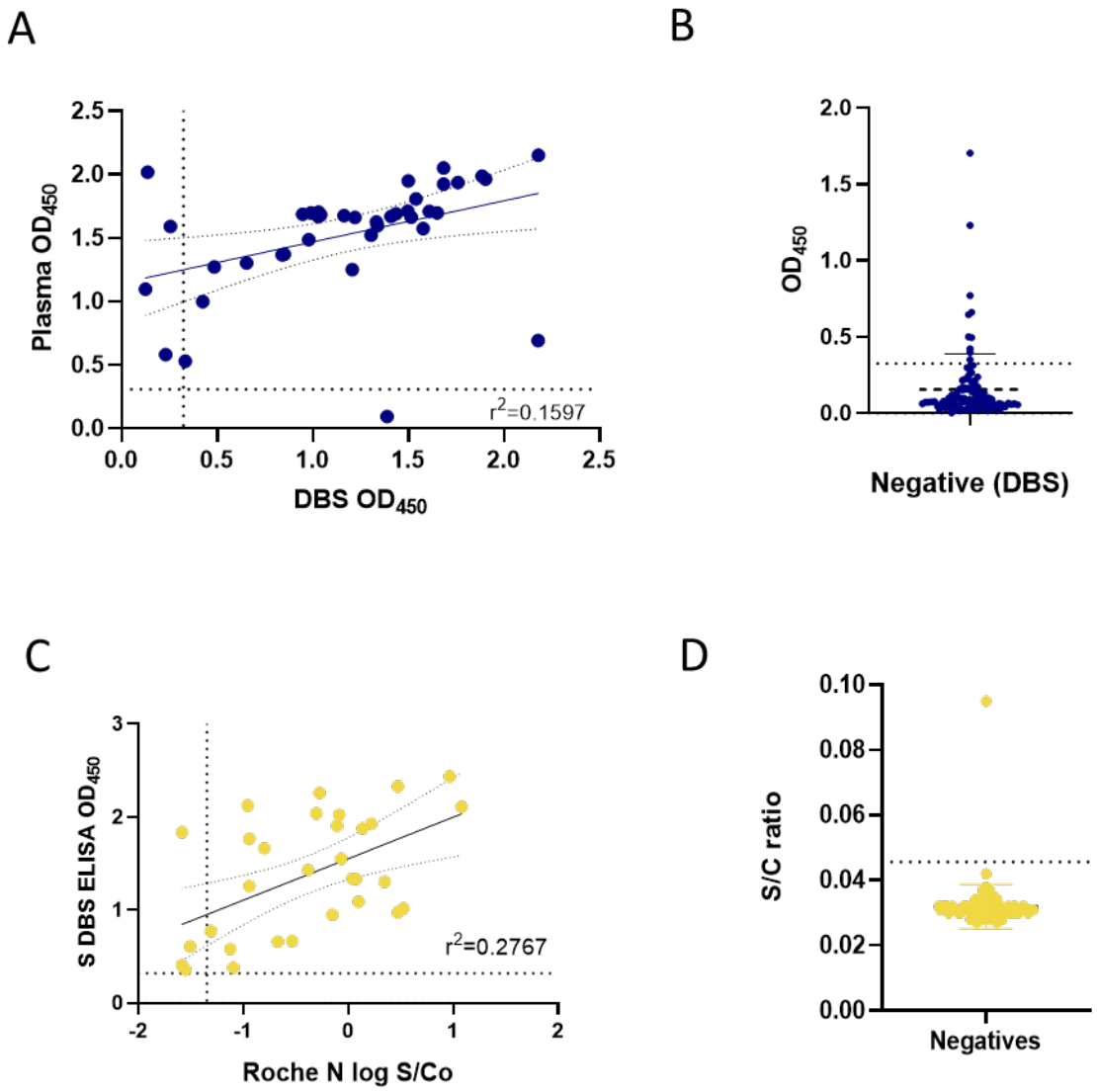

Figure 3. Validation of DBS in anti-N serological methods. Paired DBS and plasma samples (n=39) from previously SARS-CoV-2-infected individuals were compared in (A) the anti-N IgG ELISA. DBS samples (n=100) from individuals without previous SARS-CoV-2 infection were analyzed by (B) the anti-N IgG ELISA. Validation of DBS on the Roche N assay was performed on DBS samples derived from study participants in Round 2 of the EBCOVID study. (C) Samples considered SARS-CoV-2-seropositive (n = 33) from the anti-S IgG DBS ELISA were analyzed by the Roche N assay. (D) Samples considered SARS-CoV-2-seronegative (n=99) by the Ortho COV2T assay were analyzed by the Roche N assay. Cut-offs for the assays are denoted by dashed lines. Linear regression comparing IgG levels between sample types is depicted by a solid line with 95% CI.

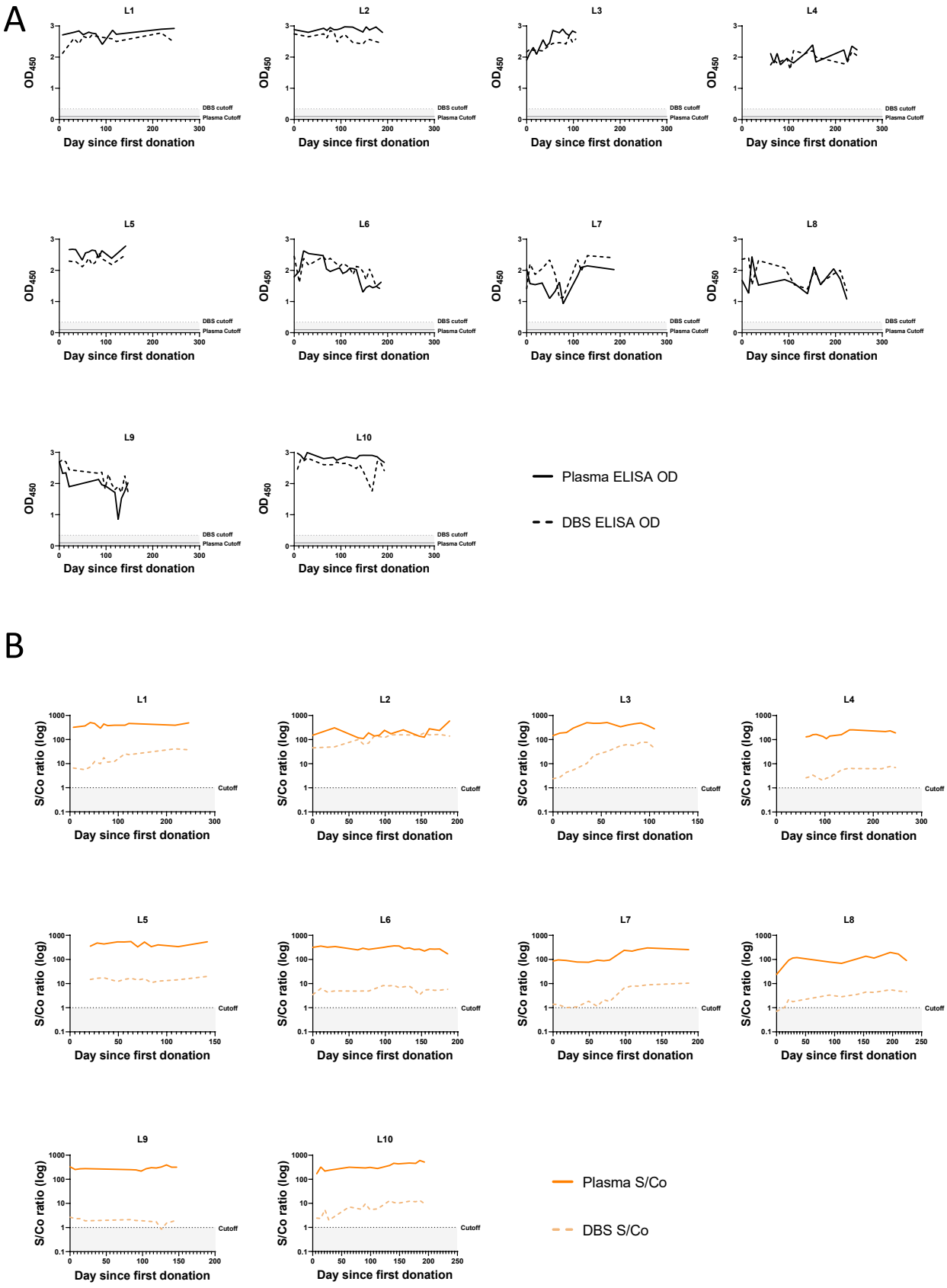
A
L1
L2
L3
L4
L5
L6
L7
L8
L9
L10
OD450
DBS cutoff
Plasma Cutoff
Day since first donation
Plasma ELISA OD
DBS ELISA OD
B
S/Co ratio (log)
Cutoff
Plasma S/Co
DBS S/Co

Figure 4. Durable SARS-CoV-2 antibody responses to S can be detected by DBS. Paired plasma (solid lines) and DBS samples (dashed lines) from 10 COVID-19 convalescent plasma donors (L1-L10) sampled longitudinally between 0 and 246 days from their first donation were analyzed by (A) the anti-S IgG ELISA and (B) the Ortho CoV2T assay . In 4A, the positivity cutoff for plasma is OD450 ≥ 0.095 (solid gray line) and DBS is OD450 ≥ 0.32 (dotted, shaded line). In 4B, the positivity for both plasma and DBS is S/Co ≥1 (dotted, shaded line)

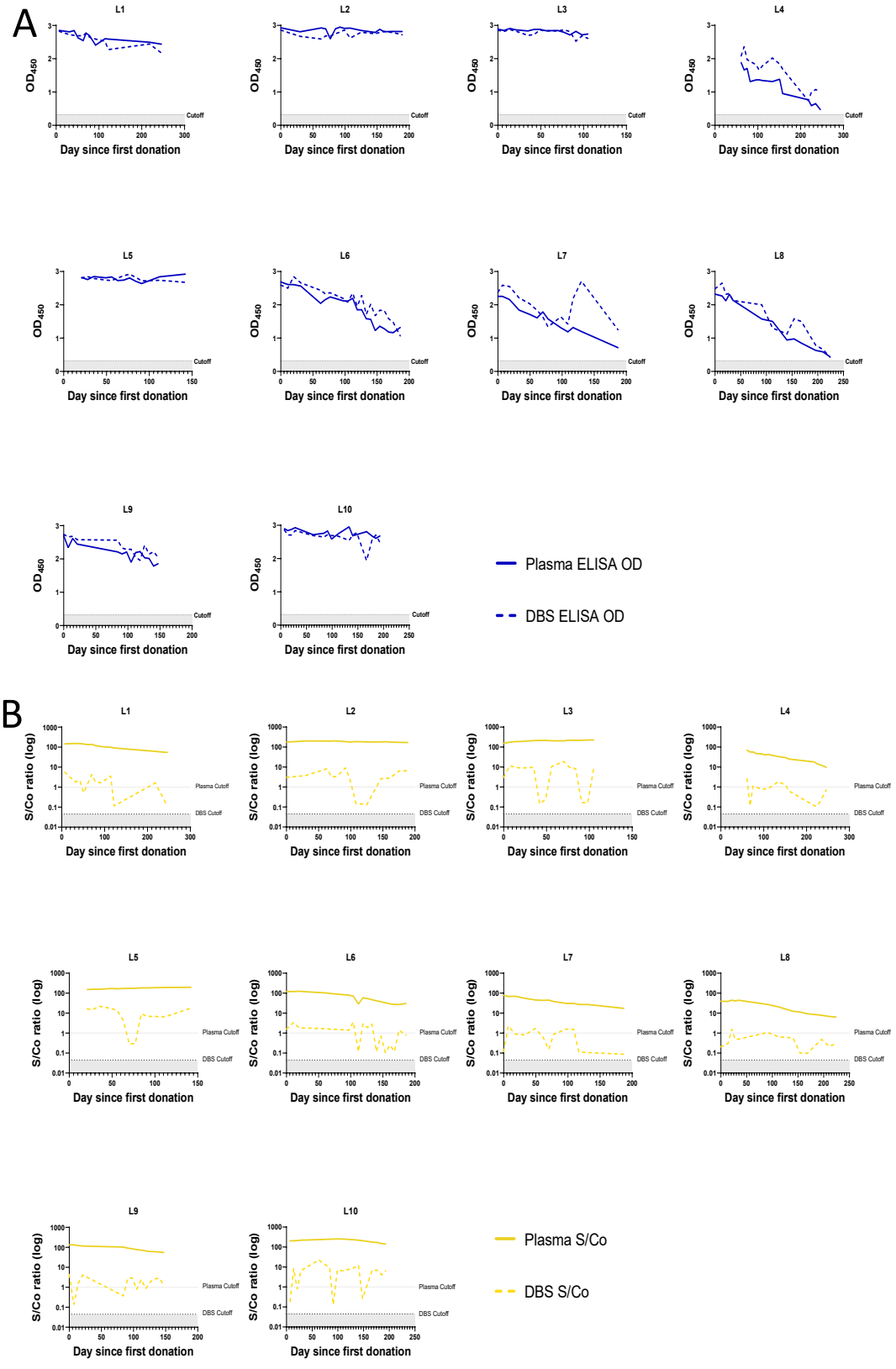
A
L1
L2
L3
L4
L5
L6
L7
L8
L9
L10
OD450
Cutoff
Day since first donation
Plasma ELISA OD
DBS ELISA OD
B
S/Co ratio (log)
Plasma Cutoff
DBS Cutoff
Plasma S/Co
DBS S/Co

Figure 5. **SARS-CoV-2 antibody responses to N wane over time can be detected by DBS.** Paired plasma (solid lines) and DBS samples (dashed lines) from 10 COVID-19 convalescent plasma donors (L1-L10) sampled longitudinally between 0 and 246 days from their first donation were analyzed by (A) the anti-N-IgG ELISA and (B) the Roche N assay. In 5A, the positivity cutoff for both plasma and DBS is OD450 ≥ 0.32 (dotted, shaded line). In 5B, the positivity cutoff for plasma is S/Co ≥ 1 (solid gray line) and DBS is S/Co ≥ 0.045 (dotted, shaded line).

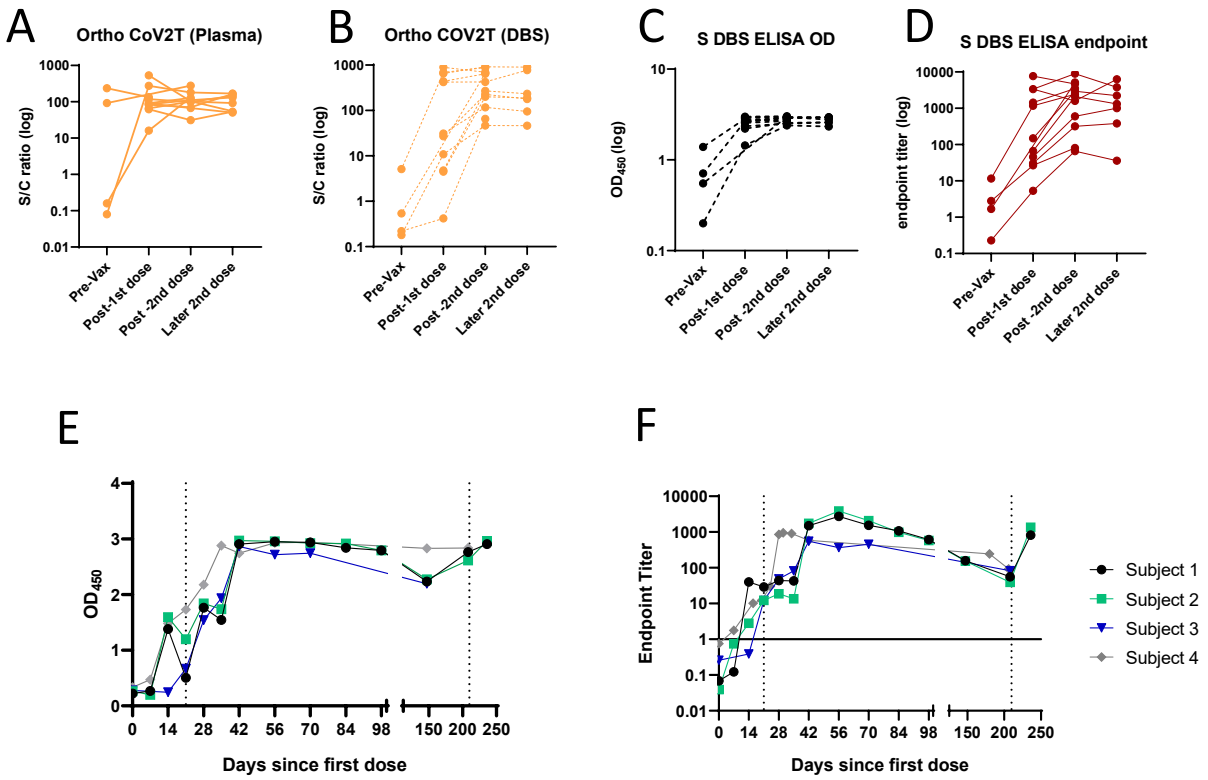

Figure 6. Vaccine-elicited SARS-CoV-2 antibody kinetics can be detected by DBS. (A-B) Plasma and DBS generated from 12 SARS-CoV-2 S-vaccinated individuals sampled before their first dose, after their first dose, and after their second dose were analyzed using the Ortho COV2T assay. DBS from these same individuals were analyzed by the anti-S IgG DBS ELISA as (C) OD_{450} values or (D) endpoint titers. DBS from 4 other vaccinated individuals sampled weekly after their first, second and third doses were analyzed by the anti-S IgG DBS ELISA as (E) OD_{450} value or (F) endpoint titer. Solid line in (F) represents positivity cut-off. Dashed lines in (E-F) denote days where additional doses of vaccine were administered.

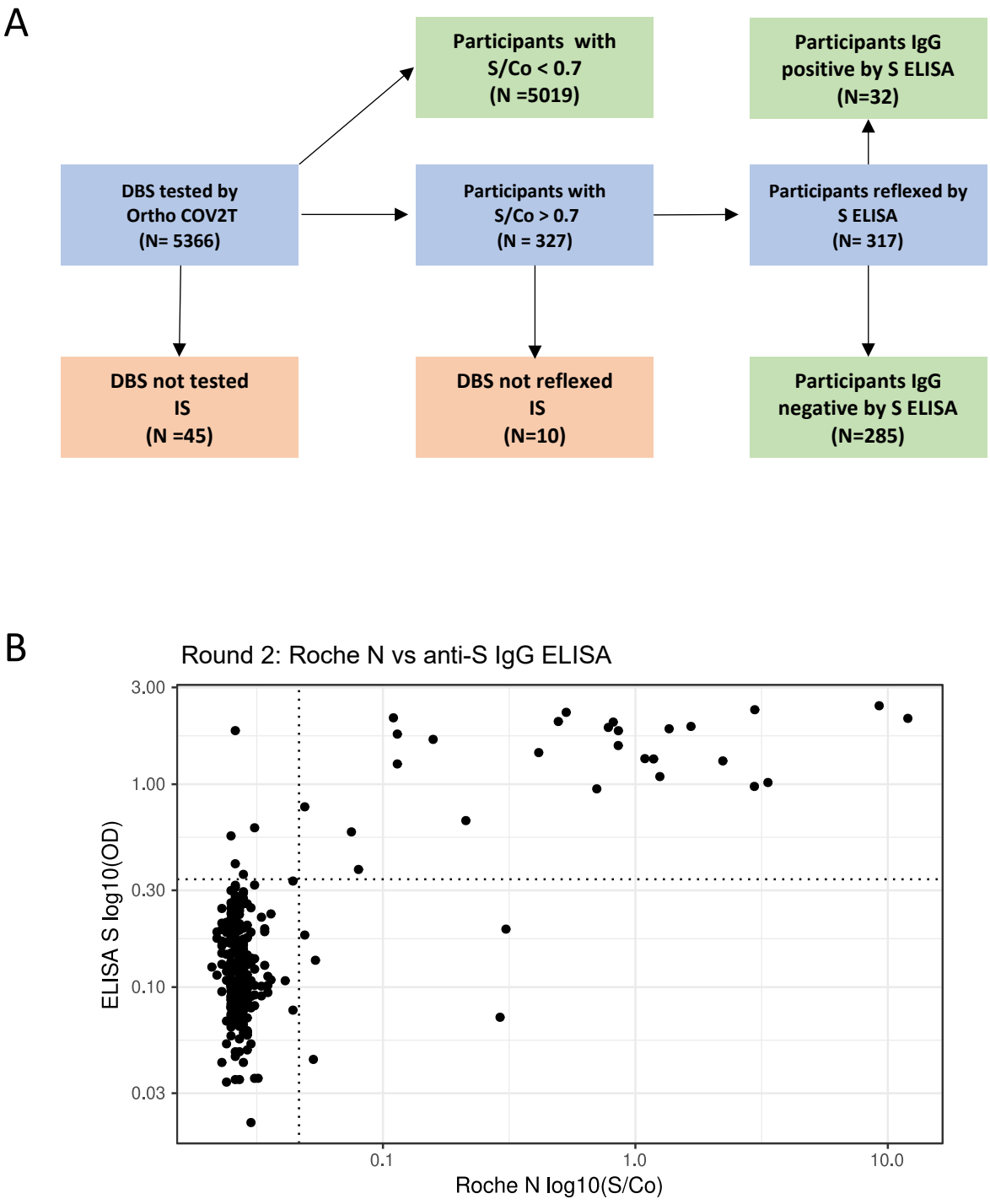

Figure 7. Testing algorithm and results from EBCOVID Round 2. (A) Schematic of the testing algorithm used for Round 2 of the EBCOVID study. (B) Round 2 EBCOVID results comparing DBS reflexed according to the testing algorithm on the anti-S IgG ELISA and the Roche N assays. IS=Insufficient sample.

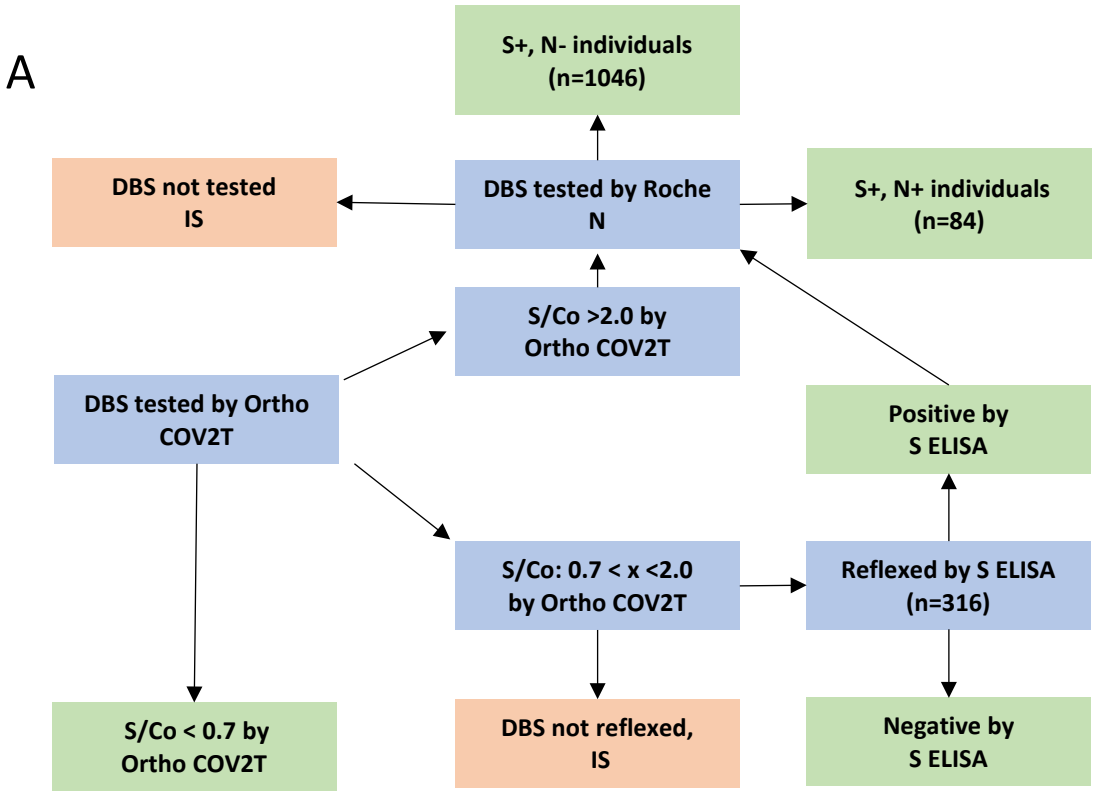

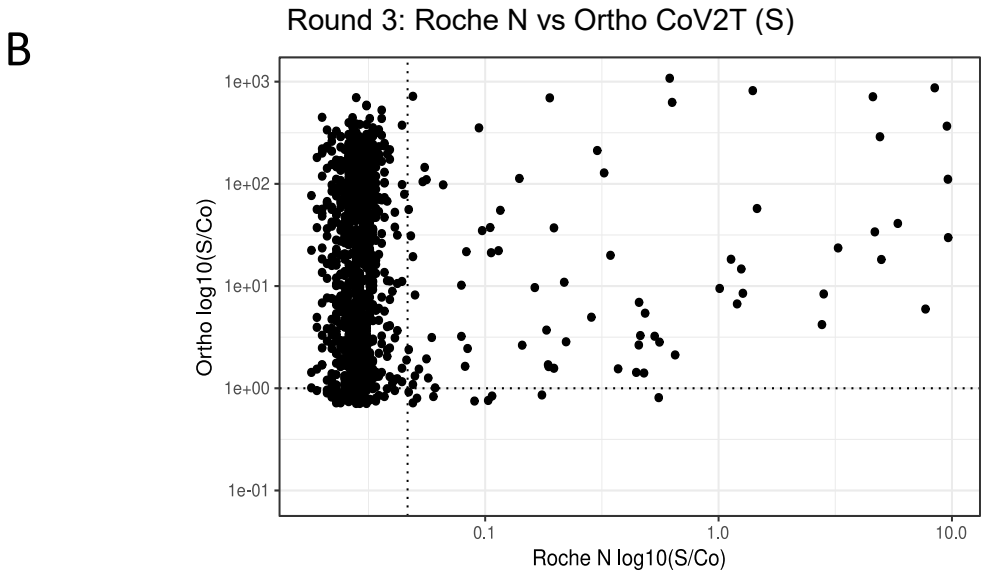

Figure 8. Testing algorithm and results from EBCOVID Round 3. (A) Schematic of the testing algorithm used for Round 3 of the EBCOVID study. (B) Round 3 EBCOVID results comparing DBS reflexed according to the testing algorithm on the Ortho CoV2T (Ortho S), the anti-S-IgG ELISA and the Roche N assays. IS=Insufficient sample

Discussion

This study demonstrates that DBS are a suitable replacement for plasma or serum in serological assays and that fingerstick-derived DBS can be effectively implemented for community-based epidemiologic studies. We validated four distinct DBS serological assays with different assay formats and demonstrated that DBS performed similarly to plasma, can be used to detect antibody responses up to 246 days (or more) after infection, and can be used to track antibody kinetics after vaccination. These assays were implemented in a large longitudinal serological survey of 12 cities in the East Bay region of the San Francisco metropolitan area with at-home biospecimen collection, demonstrating the utility of the DBS format for large-scale serosurveillance.

Recent work on the topic of SARS-CoV-2 DBS serology has shown that DBS samples and serum/plasma samples perform comparably in most serological assay formats (9, 12, 16, 17, 19). One recent study reported that DBS samples could also be adapted for epitope profiling by phage display and for SARS-CoV-2 pseudovirus neutralization (19). These investigators, along with others, validated their serological assays on DBS self-collected by study participants at home and mailed to investigators, providing proof-of-concept that a serological study could be performed using DBS (17, 19, 20). However, these studies analyzed relatively small number of participants, which limited insights into the scalability of this approach for large epidemiologic studies. Several studies adapted the Roche N assay, a high-throughput semi-automated commercial assay, for use on DBS eluates to process a larger number of samples. However, since the Roche N assay only detects antibodies to N, anti-S antibody responses at the population level have yet to be measured in the DBS format. Here, we present extensive validation of both commercial and in-house-derived serological assays against S and N and demonstrate the implementation of these methods in a large longitudinal cohort study involving at-home DBS collection by the study participants.

Our S ELISA showed 100% agreement with plasma and DBS in our validation studies. The Ortho CoV2T assay showed an 80% concordance between DBS and plasma format at the recommended S/Co cutoff of 1.0, displaying somewhat reduced sensitivity. This loss of sensitivity was attributed to the dilutional effect that occurs during the DBS elution process. We determined that our DBS elution method results in an approximately 1:40 dilution compared to plasma, which is in line with other studies that compared total IgG levels between DBS and plasma (19). This dilutional effect explains why ELISAs perform well when adapted to the DBS format; since most indirect ELISAs are performed with a serum/plasma dilution step, they are less affected by any dilution introduced during the DBS elution step. In contrast, the Ortho and Roche Total Ig sandwich assays are performed using undiluted serum/plasma. When optimizing the Roche N assay, we were able to adjust the S/Co threshold from 1 to 0.04 based on our performance data and thus improve the sensitivity of the assay in the DBS format. We compensated for the loss of sensitivity in the Ortho S CoV2T assay by reflexing DBS samples with Ortho CoV2T S/Co values that fell within the range of 0.7 to 2 to the in-house anti-S ELISA.

In this study, we were interested in understanding the prevalence of SARS-CoV-2 infection in our study population. Since we used seropositivity as a marker for past infection, it was important to evaluate whether serological assays in the DBS format would be able to detect durable antibody responses months after initial infection. Studies have shown that the durability of SARS-CoV-2 antibody responses are variable and depend on assay format, target antigens and severity of disease (20–22). While most individuals had persistent detectable antibodies over 42 weeks post-infection,

other individuals demonstrated waning of the antibody response, which correlated with being male, older, and/or having milder disease (21). One study comparing SARS-CoV-2 serological assays using a set of COVID-19 convalescent plasma from a longitudinal cohort 63-129 days following resolution of symptoms showed that some assays, like the Ortho COV2T and the Roche N assays, show stable antibody reactivity over time, while others showed a decline in reactivity (23). We assessed the longitudinal performance of all four serological assays employed in our study using a longitudinal sample set derived from 10 SARS-CoV-2 infected convalescent plasma donors with intervals between resolution of disease symptoms and last donation up to 246 days, using both reconstituted whole blood derived DBS and matched plasma samples. We found that all our assays were consistently able to detect a stable antibody response in previously SARS-CoV-2-infected individuals, although N antibody responses did show some waning.

Recent interest has developed in the waning of SARS-CoV-2 antibody responses after vaccination (24–26). Studies have shown that the antibody response induced by the commonly used mRNA vaccine BNT162b2 (Pfizer-BioNTech) shows a peak in antibody titers several weeks after the administration of the second dose with subsequent decline in total antibody levels and neutralizing antibody titers over a 6-month period (24, 25). We showed that an anti-S DBS ELISA could accurately detect these kinetics by performing an endpoint titer on the DBS eluate, adding greater utility to the DBS format. Thus, DBS samples for SARS-CoV-2 can provide valuable information about both seroprevalence at the population level and antibody titers over time at the individual level.

Finally, we have demonstrated the feasibility of using DBS samples in a large longitudinal study. At-home sample collection and the implementation of DBS enabled the collection of valuable serological data from our study population to investigate changes in seroprevalence over three time-points. Additional examples of how DBS serology data derived from large samples can be successfully used to conduct epidemiologic investigations include our own recent studies. We combined DBS results with comprehensive questionnaire and other publicly available data to estimate population-adjusted SARS-CoV-2 seroprevalence and differences by age, sex, race/ethnicity, zip code, and other demographic strata, and to characterize mitigation behaviors and their effects on SARS-CoV-2 seroprevalence (28). In addition, DBS serology results as described here were also used to assess the relationship between vaccination antibody response and several study participant characteristics including age, sex, vaccine type, vaccine side effects and other health-related factors (O. Solomon and L. Barcellos, unpublished data).

In summary, the use of DBS has gained recent interest as an alternative to venous blood sampling due to the COVID-19 pandemic. Many of the strengths of the DBS format (stability at room temperature, less sample volume required, cost-effectiveness) that make them well-suited for serological studies in resource-limited settings also make them an attractive option for SARS-CoV-2 serological surveillance since they enable at-home sampling from study participants. Samples can be returned by mail, safeguarding the health of study participants by avoiding clinic-based phlebotomy. While DBS has been an attractive option for biological sampling in many fields, lack of validation of DBS on commercial assays/platforms and limited examples of successful implementation have led to reluctance in implementation of DBS sampling for serosurveillance (7, 27). Our study presents the validation of two commercial assays, highlighting potential pitfalls due to the dilute nature of the DBS eluate. We also present solutions to mitigate the subsequent

reduction in sensitivity when switching from plasma/serum to DBS. We, and others, found that ELISAs were easily modified to accommodate DBS eluates with minimal optimization and with equivalent sensitivity and specificity to plasma/serum. Because ELISAs are also relatively low-cost compared to commercial diagnostic assays, a DBS-based ELISA assay for serosurveillance would be advantageous in resource-limited settings. In addition to providing diagnostic utility, our work and that of others show that DBS eluates can also be used to track antibody kinetics, and can be employed in epitope mapping studies, and even in neutralization assays (19). Our work, combined with evidence from others, makes a strong case for the implementation of DBS, not just for SARS-CoV-2 serological studies but in any other setting where phlebotomy would be impractical.

Materials and Methods

Materials

We obtained DBS cards (Tropbio Filter Paper Blood Collection Disks) from Cellabs. Reagents for the DBS Elution Buffer (63mM K_2HP0_4, 28mM KH_2PO_4, 139mM NaCl, 5g/L Sodium Azide, 5g/L Caesin, 50g/L Probumin BSA in H_20) were obtained from Sigma-Aldrich. SARS-CoV-2 soluble trimeric S and N proteins used in ELISAs developed at UC Berkeley were provided by Dr. John Pak (Chan-Zuckerberg Biohub) and Dr. Aubree Gordon (University of Michigan), respectively.

Human Subjects Ethics Statement

Samples for DBS validation studies were collected from participants consented under IRB #11-06262 approved by the University of California, San Francisco Committee on Protection of Human Subjects. Use of samples from convalescent plasma donors but did not involve human subjects based on anonymization of data and routine consent for blood donation testing that includes use of residual samples for research purposes. Samples for validation of the S and N IgG ELISAs were obtained from Dr. Benjamin Pinsky (Stanford University) and Dr. Bryan Greenhouse (UC San Francisco) and were pre-collected and de-identified.

All participants in the East Bay COVID study provided informed consent for the initial screening phase of the study. All those participating in the sampling phase of the study provided their informed consent for each sample/data collection round. The study was approved by the University of California, Berkeley Committee on Protection of Human Subjects (Protocol #2020-03-13121).

Validation Studies

Plasma and DBS samples were collected from COVID-19 convalescent patients and SARS-CoV-2-infected individuals. Reconstituted DBS were generated by mixing plasma with anticoagulated, plasma-depleted whole blood at a 1:1 ratio and spotted on DBS cards. Four sets of samples were generated for validation studies. The first sample set consisted of 39 paired plasma and reconstituted DBS samples from previously SARS-CoV-2-infected individuals and 100 paired samples from individuals without previous SARS-CoV-2 infection. The second sample set consisted of paired plasma and reconstituted DBS from 10 COVID-19 convalescent plasma donors sampled longitudinally between 0 and 246 days from their first donation. The third set of samples consisted of paired plasma and fingerstick DBS samples generated from 12 vaccinated individuals sampled before their first dose, after their first dose, and after their second dose. Four other vaccinated individuals were sampled by fingerstick DBS over a period of 210 days, after their first, second, and third doses. The plasma-based S and N IgG ELISAs IgG ELISA were validated using convalescent plasma samples collected >8 days post-symptom onset from 60 hospitalized, PCR-confirmed severe COVID-19 cases, 57 mild or subclinical cases, and samples collected before 2020 from 131 unexposed persons as described previously (18).

East Bay COVID (EBCOVID) Study Design

Recruitment and selection of study participants was completed in a screening phase followed by a longitudinal sampling phase with three timepoints or "rounds" (Figure 1). In the screening phase, all residential addresses within the East Bay cities and communities of Albany, Berkeley, El Cerrito, El Sobrante, Emeryville, Hercules, Kensington, Oakland, Piedmont, Pinole, Richmond, and San Pablo (~307,000 residential households) were mailed an invitation to participate. The

household member aged 18 or older with the next birthday was invited to complete a consent form and screening questionnaire. Spanish versions of study invitations and all study materials were also utilized.

Of the 16,115 residents who consented and completed the screening procedures between May-July 2020, 1,777 individuals did not meet the inclusion criteria and were excluded (Figure 1). Eligible participants were required to be the household member with the next birthday, live within the study region, be willing to provide biospecimens (including DBS) and questionnaire responses, read and speak English or Spanish, and have internet access and a valid email address.

The target sample size for the sampling phase was 5,500 participants. To obtain a sample that resembled the racial and ethnic proportions reported in the 2018 American Community Survey (ACS) for the study region, we ranked screening participants for study inclusion. Black and/or Hispanic individuals were ranked the highest (n=1,556) followed by other non-White individuals (n=1,939). White individuals were randomly ranked to complete the remaining participant slots. Individuals ranked between 1 and 5,500 were offered study enrollment, and non-respondents were replaced with the next highest ranked individuals who had not yet been offered study entry.

Biospecimens and questionnaire data were collected during three sampling rounds. Approximate dates for each round were July-September 2020, October-December 2020, and February-April 2021. For each round of data and biospecimen collection, individuals who had participated in the previous round were contacted to confirm their willingness to participate in the next round. If participation was declined, individuals from the pool of screening participants who had not yet participated in a sampling round were invited as needed. This resulted in 5,501 participants in Round 1, 5,603 participants in Round 2, and 4,806 participants in Round 3 (Figure 1). This corresponds to participation rates of 76.8%, 89.8%, and 87.3% across the study rounds, respectively. A biospecimen collection kit was developed and assembled by investigators and sent to each participant via Federal Express (FedEx). Both written instructions and an instructional video for at-home sample collection, including fingerstick blood sampling and preparation of DBS, were provided to all study participants. Both English and Spanish versions were made available.

Quality Control of DBS

DBS received from participants were assessed for quality. We evaluated each DBS on a scale from 0 to 3, with 0 representing a blank DBS, 1 representing an incompletely filled DBS on one side, 2 representing a DBS card saturated fully on only one side, and 3 representing a DBS fully saturated on both sides. Participants who provided at least two DBS samples with a cumulative score of 2 or higher were processed in our serological assays; samples that did not meet this criterion were labelled as “Insufficient Sample” (IS).

Reconstitution of Blood Spots

Two DBS were removed from the Tropbio disk and placed in a 2-mL screwcap tube. Five hundred uL of elution buffer was added into the tube and vortexed for 20 seconds. If DBS numbers were limited, one spot was eluted in 250uL of elution buffer instead. DBS were incubated in elution buffer overnight at 4°C, then spun down at 10,600xg for 10 minutes (min) at 4°C. The DBS eluate was then transferred to a fresh tube and stored at 4°C until analysis.

ELISA (N and S)
DBS eluates and plasma were evaluated for the presence of IgG against SARS-CoV-2 S and NC using an in-house direct ELISA as previously described (18). Briefly, SARS-CoV-2 antigens were coated in 96-well Nunc Maxisorp ELISA plates (ThermoFisher) overnight at 4°C. Plates were then blocked in 2.5% non-fat dry milk in PBS for 2 hours (h) at 37°C. Plates were washed 3X with PBS (Gibco), and 100uL of DBS eluate or 100 uL of a 1:100 dilution of plasma (1 uL of plasma diluted in 99uL of 1% non-fat dry milk) were added and incubated at 37°C for 1h. Plates were then washed 5 times with 0.05% PBS-Tween-20, and 100uL of goat-α-human IgG horseradish peroxidase (HRP) secondary antibody (Fisher) diluted in 1% non-fat dry milk was added. After incubating for 1h at 37°C, plates were washed 5 times in 0.05% PBS-Tween-20 and once in PBS. Wells were developed with TMB (3,3',5,5'-Tetramethylbenzidine, ThermoFisher) for exactly 5 minutes, and the reaction was stopped with 2M H_2SO_4. Plates were read on a plate reader at 490nm. Endpoint-titer ELISAs were performed as above, except that the DBS eluate was serially diluted 1:4 or 1:5 eight times in DBS eluate before addition to the plate. Endpoint titers were calculated using the five-parameter logistic equation function in GraphPad Prism 8, using 0.34 as the negative cut-off.

Commercial Assays (Ortho S & Roche N Total IgG Assays)
DBS eluates prepared as above (or paired plasma samples for assay validation) were tested with the Ortho VITROS® Anti-SARS-CoV-2 S1 Total Ig assay (https://www.fda.gov/media/136967/download) or the Roche Elecsys ® Anti-SARS-CoV-2 N Total Ig assay (https://www.fda.gov/media/137605/download) according to the manufacturers' instructions. Briefly, the Ortho VITROS Anti-SARS-CoV-2 total (CoV2T, Ortho-Clinical Diagnostics, Inc.) was used to detect total (IgG, IgM, and IgA) antibodies to SARS-CoV-2 Spike S1 protein. DBS eluates or plasma samples were loaded on Ortho VITROS XT-7600 or 3600 instruments (Ortho-Clinical Diagnostics, Inc.) and programmed for the CoV2T test following the manufacturer's instructions. The S1 antigens coated on the assay wells bind anti-S1 antibodies from human serum which, in turn, bind to a secondary HRP-labeled S1 antigen in the conjugate reagent, forming a sandwich. The addition of signal reagent containing luminol generates a chemiluminescence reaction that is measured by the system and quantified as the ratio of the signal relative to the cut-off value (S/Co) generated during calibration. A S/Co ≥1 was considered positive in plasma, while a S/Co ≥0.7 in DBS eluate was considered indeterminate or grey zone (see Results).

The Roche Elecsys Anti-SARS-CoV-2 immunoassay (Roche N) was processed on the Cobas e441 analyzer (Roche Diagnostics) to detect total antibodies against the SARS-CoV-2 N protein. DBS eluates or plasma samples are initially incubated with biotinylated and ruthenium-labeled SARS-CoV-2 recombinant N antigens, and any anti-N antibody present in the solution is sandwiched between the two. Subsequently, streptavidin-coated microparticles are added to the mixture to bind the biotin. The magnetic particles drive the complexes to the electrode, where a chemiluminescent signal is emitted and measured as the ratio between the signal and the cut-off obtained during calibration. A S/Co≥1 in plasma was considered positive, while a S/Co ≥0.045 in DBS eluate was considered positive (see Results).

Statistics
Statistical analysis was performed using GraphPad Prism Version 8 (GraphPad Software) and the R statistical programming package.

Acknowledgments

We would like to thank John Pak and Aubree Gordon for the provision of S and N proteins used in the study. We also thank Patrick Hsu and Spotlight Therapeutics for donation of S protein used for assay development. This study was supported by Open Philanthropy Projects, Fast Track grants from Emergent Ventures, the UC Berkeley Innovative Genomics Institute, and the UC Berkeley School of Public Health Center for Population Health.

References

1. WHO Coronavirus (COVID-19) Dashboard.

2. Oran DP, Topol EJ. 2021. The Proportion of SARS-CoV-2 Infections That Are Asymptomatic. Ann Intern Med 174:655–662.

3. Sah P, Fitzpatrick MC, Zimmer CF, Abdollahi E, Juden-Kelly L, Moghadas SM, Singer BH, Galvani AP. 2021. Asymptomatic SARS-CoV-2 infection: A systematic review and meta-analysis. Proc Natl Acad Sci U S A 118:e2109229118.

4. Mössner BK, Staugaard B, Jensen J, Lillevang ST, Christensen PB, Holm DK. 2016. Dried blood spots, valid screening for viral hepatitis and human immunodeficiency virus in real-life. World J Gastroenterol 22:7604–7612.

5. Stefic K, Guinard J, Peytavin G, Saboni L, Sommen C, Sauvage C, Lot F, Laperche S, Velter A, Barin F. 2019. Screening for Human Immunodeficiency Virus Infection by Use of Fourth-Generation Antigen/Antibody Assay and Dried Blood Spots: In-Depth Analysis of Sensitivity and Performance Assessment in a Cross-Sectional Study. J Clin Microbiol58:e01645-19.

6. Sarkar S, Singh MP, Ratho RK. 2015. Dried blood spot for Ebola testing in developing countries. Lancet Infect Dis 15:1005.

7. Lim MD. 2018. Dried Blood Spots for Global Health Diagnostics and Surveillance: Opportunities and Challenges. Am J Trop Med Hyg 99:256–265.

8. Behets F, Kashamuka M, Pappaioanou M, Green TA, Ryder RW, Batter V, George JR, Hannon WH, Quinn TC. 1992. Stability of human immunodeficiency virus type 1 antibodies in whole blood dried on filter paper and stored under various tropical conditions in Kinshasa, Zaire. J Clin Microbiol 30:1179–1182.

9. Morley GL, Taylor S, Jossi S, Perez-Toledo M, Faustini SE, Marcial-Juarez E, Shields AM, Goodall M, Allen JD, Watanabe Y, Newby ML, Crispin M, Drayson MT, Cunningham AF, Richter AG, O'Shea MK. 2020. Sensitive Detection of SARS-CoV-2-Specific Antibodies in Dried Blood Spot Samples. Emerg Infect Dis 26:2970–2973.

10. McDade TW, McNally EM, Zelikovich AS, D'Aquila R, Mustanski B, Miller A, Vaught LA, Reiser NL, Bogdanovic E, Fallon KS, Demonbreun AR. 2020. High seroprevalence for SARS-CoV-2 among household members of essential workers detected using a dried blood spot assay. PloS One 15:e0237833.

11. Zava TT, Zava DT. Validation of dried blood spot sample modifications to two commercially available COVID-19 IgG antibody immunoassays. Bioanalysis 10.4155/bio-2020–0289.

12. Toh ZQ, Higgins RA, Anderson J, Mazarakis N, Do LAH, Rautenbacher K, Ramos P, Dohle K, Tosif S, Crawford N, Mulholland K, Licciardi PV. 2021. The use of dried blood spots for the serological evaluation of SARS-CoV-2 antibodies. J Public Health 22:fdab011.

13. Moat SJ, Zelek WM, Carne E, Ponsford MJ, Bramhall K, Jones S, El-Shanawany T, Wise MP, Thomas A, George C, Fegan C, Steven R, Webb R, Weeks I, Morgan BP, Jolles S.

2021. Development of a high-throughput SARS-CoV-2 antibody testing pathway using dried blood spot specimens. Ann Clin Biochem 58:123–131.

14. Roxhed N, Bendes A, Dale M, Mattsson C, Hanke L, Dodig-Crnković T, Christian M, Meineke B, Elsässer S, Andréll J, Havervall S, Thålin C, Eklund C, Dillner J, Beck O, Thomas CE, McInerney G, Hong M-G, Murrell B, Fredolini C, Schwenk JM. 2021. Multianalyte serology in home-sampled blood enables an unbiased assessment of the immune response against SARS-CoV-2. Nat Commun 12:3695.

15. Beyerl J, Rubio-Acero R, Castelletti N, Paunovic I, Kroidl I, Khan ZN, Bakuli A, Tautz A, Oft J, Hoelscher M, Wieser A. 2021. A dried blood spot protocol for high throughput analysis of SARS-CoV-2 serology based on the Roche Elecsys anti-N assay. EBioMedicine 70:103502.

16. Mulchandani R, Brown B, Brooks T, Semper A, Machin N, Linley E, Borrow R, Wyllie D, Taylor-Philips S, Jones H, Oliver I, Charlett A, Hickman M, Brooks T, Mulchandani R, Wyllie D. 2021. Use of dried blood spot samples for SARS-CoV-2 antibody detection using the Roche Elecsys ® high throughput immunoassay. J Clin Virol 136:104739.

17. Karp DG, Danh K, Espinoza NF, Seftel D, Robinson PV, Tsai C. 2020. A serological assay to detect SARS-CoV-2 antibodies in at-home collected finger-prick dried blood spots. Sci Rep 10:20188.

18. Lewnard J, Mora A, Nkwocha O, Kogut K, Rauch S, Morga N, Hernandez S, Wong M, Huen K, Andrejko K, Jewell N, Parra K, Holland N, Harris E, Cuevas M, Eskenazi B. 2021. Prevalence and Clinical Profile of Severe Acute Respiratory Syndrome Coronavirus 2 Infection among Farmworkers, California, June–November 2020. Emerg Infect Dis J 2021;27(5):1330-1342

19. Itell HL, Weight H, Fish CS, Logue JK, Franko N, Wolf CR, McCulloch DJ, Galloway J, Matsen FA, Chu HY, Overbaugh J. SARS-CoV-2 Antibody Binding and Neutralization in Dried Blood Spot Eluates and Paired Plasma. Microbiol Spectr 0:e01298-21.

20. Dorigatti I, Lavezzo E, Manuto L, Ciavarella C, Pacenti M, Boldrin C, Cattai M, Saluzzo F, Franchin E, Del Vecchio C, Caldart F, Castelli G, Nicoletti M, Nieddu E, Salvadoretti E, Labella B, Fava L, Guglielmo S, Fascina M, Grazioli M, Alvisi G, Vanuzzo MC, Zupo T, Calandrin R, Lisi V, Rossi L, Castagliuolo I, Merigliano S, Unwin HJT, Plebani M, Padoan A, Brazzale AR, Toppo S, Ferguson NM, Donnelly CA, Crisanti A. 2021. SARS-CoV-2 antibody dynamics and transmission from community-wide serological testing in the Italian municipality of Vo'. Nat Commun 12:4383.

21. Vanshylla K, Di Cristanziano V, Kleipass F, Dewald F, Schommers P, Gieselmann L, Gruell H, Schlotz M, Ercanoglu MS, Stumpf R, Mayer P, Zehner M, Heger E, Johannis W, Horn C, Suárez I, Jung N, Salomon S, Eberhardt KA, Gathof B, Fätkenheuer G, Pfeifer N, Eggeling R, Augustin M, Lehmann C, Klein F. 2021. Kinetics and correlates of the neutralizing antibody response to SARS-CoV-2 infection in humans. Cell Host Microbe 29:917-929.e4.

22. den Hartog G, Vos ERA, van den Hoogen LL, van Boven M, Schepp RM, Smits G, van Vliet J, Woudstra L, Wijmenga-Monsuur AJ, van Hagen CCE, Sanders EAM, de Melker HE, van der Klis FRM, van Binnendijk RS. 2021. Persistence of antibodies to SARS-CoV-2 in

relation to symptoms in a nationwide prospective study. Clin Infect Dis Off Publ Infect Dis Soc Am ciab172.

23. Di Germanio C, Simmons G, Kelly K, Martinelli R, Darst O, Azimpouran M, Stone M, Hazegh K, Grebe E, Zhang S, Ma P, Orzechowski M, Gomez JE, Livny J, Hung DT, Vassallo R, Busch MP, Dumont LJ. 2021. SARS-CoV-2 antibody persistence in COVID-19 convalescent plasma donors: Dependency on assay format and applicability to serosurveillance. Transfusion 61:2677–2687.

24. Campo F, Venuti A, Pimpinelli F, Abril E, Blandino G, Conti L, De Virgilio A, De Marco F, Di Noia V, Di Domenico EG, Di Martino S, Ensoli F, Giannarelli D, Mandoj C, Mazzola F, Moretto S, Petruzzi G, Petrone F, Pichi B, Pontone M, Vidiri A, Vujovic B, Piaggio G, Sperandio E, Rosati V, Cognetti F, Morrone A, Ciliberto G, Pellini R. 2021. Antibody Persistence 6 Months Post-Vaccination with BNT162b2 among Health Care Workers. Vaccines 9:1125.

25. Levin EG, Lustig Y, Cohen C, Fluss R, Indenbaum V, Amit S, Doolman R, Asraf K, Mendelson E, Ziv A, Rubin C, Freedman L, Kreiss Y, Regev-Yochay G. 2021. Waning Immune Humoral Response to BNT162b2 Covid-19 Vaccine over 6 Months. N Engl J Med oa2114583

26. Bayart J-L, Douxfils J, Gillot C, David C, Mullier F, Elsen M, Eucher C, Van Eeckhoudt S, Roy T, Gerin V, Wieers G, Laurent C, Closset M, Dogné J-M, Favresse J. 2021. Waning of IgG, Total and Neutralizing Antibodies 6 Months Post-Vaccination with BNT162b2 in Healthcare Workers. Vaccines 9:1092.

27. Lange B, Cohn J, Roberts T, Camp J, Chauffour J, Gummadi N, Ishizaki A, Nagarathnam A, Tuaillon E, van de Perre P, Pichler C, Easterbrook P, Denkinger CM. 2017. Diagnostic accuracy of serological diagnosis of hepatitis C and B using dried blood spot samples (DBS): two systematic reviews and meta-analyses. BMC Infect Dis 17:700.

28. Adams C, Horton M, Solomon O, Wong MP, Wu SL, Fuller S, Shao X, Fedrigo I, Quach HL, Quach DL, Meas M, Lopez L, Broughton A, Barcellos AL, Shim J, Seymens Y, Hernandez S, Montoya M, Johnson DM, Lewnard J, Beckman KB, Busch MP, Coloma J, Harris E, Barcellos LF. 2021. Impact of individual-level characteristics and virus mitigation behaviors on SARS-CoV-2 infection and seroprevalence in a large Northern California cohort. Medrxiv. https://doi.org/10.1101/2021.12.02.21266871

Chapter 5

Conclusions and Future Directions

Summary

In this dissertation, I aimed to understand how innate and adaptive immune responses to NS1 prevent severity during DENV infections. First, I demonstrate that DENV NS1 is sensed by a class of innate immune sensors known as the inflammasome pathway. I show that NS1-induced inflammasome activation is independent of the NLRP3 inflammasome but is dependent on CD14 and caspase-1/11. I generated two new mouse lines (*Casp1/11* $^{+/-}$*Ifnar* $^{-/-}$ and *Nlrp3* $^{+/-}$*Ifnar* $^{-/-}$) to assess the effect of inflammasome activation during DENV infection and found that caspase-1/11-deficient mice are more susceptible to DENV infection compared to their caspsase-1/11-functional littermates, whereas NLRP3 deficiency in mice does not affect the outcome of DENV infection. Overall, this work suggests that activation of pro-inflammatory immune responses during DENV infection does not always lead to detrimental outcomes, as previously hypothesized, and suggests that innate immune sensing of NS1 can contribute to protective responses to dengue disease.

Next, I helped elucidate the mechanistic basis of antibody-mediated inhibition of DENV NS1-induced permeability and identified key amino acids targeted by the protective monoclonal antibody 2B7 that contribute to NS1 secretion and NS1-induced endothelial hyperpermeability. Structure-guided mutagenesis and mutant screening identified R299, G328, and W330 as residues required for NS1 secretion. These residues have not been previously identified as affecting NS1 secretion but are in close proximity to regions reported to be essential for NS1 secretion by other groups. I also identified four β-ladder mutants (T301K, A303W, E326K, D327K) that are deficient in inducing endothelial hyperpermeability, with A303W displaying the greatest defect, at a step downstream of binding (1). Finally, I found that binding to residues T301 and G305, which are conserved across the flaviviruses, imparts pan-flavivirus affinity to 2B7, and I used a G305K mutant to profile anti-NS1-antibody responses in DENV-infected humans. Taken together, these results have revealed new insights into DENV NS1 biology and generated new tools to profile the antibody response to NS1.

Lastly, I document our efforts to develop serological assays for a newly emergent pathogen, SARS-CoV-2, and their adaptation into a DBS format, enabling seroepidemiological studies when pandemic-imposed social distancing restrictions limited the ability to collect sera by venipuncture (2). These assays were implemented successfully in several studies. We used these serological methods to determine SARS-CoV-2 infection and antibody prevalence as well as to identify risk factors associated with SARS-CoV-2 infection in communities of migrant farmworkers living in Salinas Valley, California (3,4).The DBS format enabled assessment of SARS-CoV-2 seroprevalence in a longitudinal, population-based study in the East Bay Area of Northern California. Data from this study allowed us to investigate the association between geographic and demographic characteristics as well as transmission mitigation behavior and SARS-CoV-2 prevalence (5). SARS-CoV-2 vaccines were also rolled out over the study period, and we were able use antibody data collected from vaccinees to characterize the differences in side-effects and antibody responses by vaccine type, sex, and age, as well as to describe responses in subjects with pre-existing health conditions that are known risk factors for more severe COVID-19 infection (6).

Future Directions and Concluding Thoughts

NS1 is a fascinating viral protein with many diverse functions in the viral lifecycle. How one protein plays such disparate roles in viral replication, immune evasion, and pathogenesis has been a major research question for many years. Ever since DENV NS1 was shown to mediate both endothelial dysfunction and immune activation, much work has been done to understand the mechanisms underlying these functions as well as their contribution to DENV pathogenesis. This dissertation begins to shed light on the complex ways in which NS1 can act both as a target of protective immune responses and as a mediator of disease. Importantly, the work described herein opens new intriguing avenues of inquiry into inflammasome biology, the biology of DENV NS1, and DENV pathogenesis, laying the groundwork for novel therapeutic targets against severe dengue disease.

The work presented in Chapter 2 demonstrates, for the first time, a protective role for the inflammasome during DENV infection. While several groups have postulated that DENV-mediated inflammasome activation may contribute to a pathogenic cytokine storm, very few have assessed this role experimentally.

One study by Pan and colleagues =ascribed a pathogenic role to inflammasome activation during DENV infection, since DENV-infected *Ifnar* $^{-/-}$ mice that are therapeutically administered recombinant IL-1 receptor antagonist (IL-1RA) lose less weight and have diminished vascular leakage compared to untreated controls, implicating IL-1β in DENV pathology (7). In contrast, we find that blocking the inflammasome activation through capase-1/11 deficiency leads to increased morbidity and mortality, implicating inflammasome activation as protective. The use of genetic models in our study implicates a protective role for inflammasome activation early in DENV infection, though our data does not preclude the possibility of inflammasome activation being pathogenic in later stages of infection. Of note, the study by Pan et al. administered IL-1RA at day 0 and day 4 after infection. Thus, inflammasome activation can be both protective and pathogenic depending on the context of the infection. It is reasonable to hypothesize that early activation of the inflammasome can jumpstart protective immune responses that help to control viremia and reduce mortality, whereas excess inflammation late in infection, when viremia is high, may be detrimental to the host. Future studies characterizing the effect of inflammasome antagonism at various points during DENV infection will be crucial to understanding more fully the roles that inflammasomes play in host defense and immunopathology as well as guiding the timing of potential inflammasome-based host-directed therapies against DENV.

While we were able to determine that caspase-1/11 is necessary for protection against DENV, we did not identify the exact mediator of this protection, and further studies are needed to understand the mechanistic basis of caspase-1/11-mediated protection during DENV infection. It would be interesting to interrogate how IL-1β or another caspase-1 substrate, such as IL-18 or IL-33, is important for mediating protection during viral infection (8). IL-18, for example, is known to induce the activation of Th1 and NK cells through the induction of interferon-γ (IFN-γ), and IFN-γ is a key mediator of anti-viral defense against DENV (9,10). IL-33 is another IL-1 family cytokine that is expressed primarily in endothelial and epithelial cells associated with allergic inflammation and anti-viral responses (11–13). *In vivo* work interrogating which cytokines and

cell types are necessary for caspase-1/11-mediated protection would also be useful in understanding how inflammasome activation can lead to protection against DENV.

While we establish that DENV NS1 induces inflammasome activation independently of the NLRP3 inflammasome using multiple orthogonal genetic and chemical approaches, the identity of the inflammasome activated by DENV NS1 remains elusive. Future genetic screens targeting other inflammasomes may help to identify which inflammasome senses DENV NS1. This will prove useful for illuminating new areas of inflammasome biology, which is an active area of research. This may also help us better understand the biology of DENV NS1. While we have begun to uncover which host pathways are affected by DENV NS1, we have yet to discover the mechanisms by which DENV NS1 perturbs these pathways. By understanding how DENV NS1 is sensed by the innate immune system, we may also glean insight into how DENV NS1 functions.

Interestingly, we found that DENV NS1-induced inflammasome activation does not result in measurable cell death and is dependent on CD14. This pattern of inflammasome activation is reminiscent of other recent reports, which find that certain oxidized phospholipids commonly associated with dying cells can also activate the inflammasome without cell death in a CD14-dependent manner. Since secreted DENV NS1 contains a lipid cargo and other studies have found that the lipid content of NS1-associated lipids can modulate DENV NS1's inflammatory capacity, DENV NS1 may be able to act as a carrier of oxidized phospholipids generated from infected cells and subsequently be detected by macrophages at sites distal from infection, activating an inflammasome and cytokine response. We were unable to determine whether oxidized phospholipids were present within the lipid cargo of our NS1 in this study; however, it would be interesting to explore whether the inflammatory capacity of NS1 can be modulated by the lipids within the lipid cargo and how this might affect DENV NS1's protective or pathogenic qualities.

Ultimately, the data presented in chapter 2 suggest that further investigation into understanding the balance in which innate immune activation can be protective and/or pathogenesis during DENV infection is sorely needed. While the DENV mouse model remains an imperfect system for modelling severe dengue, significant insights can be gained from careful perturbation of specific host responses *in vivo*. Understanding more clearly how inflammasomes, and other innate immune mediators, sense and contribute to DENV protection or pathogenesis will be crucial for developing new host-directed therapies and identifying the best biomarkers to assess risk of progression to severe disease.

Although major advances have been made with respect to understanding NS1-induced endothelial dysfunction, important questions still remain regarding the mechanisms of induction of endothelial hyperpermeability. As a result of our interrogations of the mAb 2B7 binding epitope, we have generated several new NS1 mutants deficient in secretion and pathogenesis. Future studies characterizing the β-ladder mutants such as A303W could evaluate whether the inability of mutant A303W to decrease TEER extends to other phenotypes such as EGL degradation, mislocalization of TJ/AJ proteins, or localized vascular leak *in vivo*. This characterization is important given that work in our lab has recently found discrepancies between the NS1-induced hyperpermeability as measured by the TEER phenotype *in vitro* compared to binding and vascular leak in the dorsal dermis mouse model. Specifically, mutants defective in binding to endothelial cells are unable to induce TEER and localized dermal leak, whereas DENV NS1 N207Q, which can bind to cells but not induce TEER, can still induce localized dermal leak. Careful characterization of the phenotypes

affected by mutations like A303W could begin to map specific phenotypes induced by NS1 in cells to specific residues within the β-ladder and clarify the mechanisms underlying NS1-induced endothelial dysfunction. Structural studies aimed at analyzing NS1 interaction partners in complex with NS1 could also leverage the mutants generated in this dissertation to evaluate, for example, how the A303W substitution might disrupt a key interaction between NS1 and its cognate receptor. Lastly, well-characterized mutations could be incorporated into DENV infectious clones to evaluate the impact of *in vitro* defects on DENV infection *in vivo.*

The mutants generated in Chapter 3 also serve as ideal antigens for profiling the NS1 antibody response in DENV-infected humans. While we have demonstrated that a single NS1 monoclonal antibody can be protective in mice, our knowledge of what a protective NS1 antibody response is in humans is limited. Data presented in Chapter 3 represents a proof-of-concept study demonstrating that 2B7-like antibodies can be found in plasma after infection with DENV using a multiplex, Luminex-based format. Combined with NS1 domain chimeras generated in our lab, we now have the ability to profile α-NS1 antibody responses at the level of specific domains and epitopes. Ongoing studies will analyze these responses in pre-infection samples and attempt to find correlations between NS1 domain/epitope-specific responses and protection (or lack thereof) against dengue severity, thus growing our understanding of the utility of anti-NS1 antibody responses. Combining this with efforts to characterize the profile of anti-E-antibodies at the domain level will shed key insights into the makeup of protective and pathogenic antibody responses to DENV, informing next-generation dengue vaccines that can provide protection without the risk of ADE.

The central role of secreted NS1 in the flavivirus lifecycle has been hypothesized to be in opening barriers to enable spread of the virus to tissues distal from the initial infection site. In other flaviviruses, such as ZIKV and WNV, NS1 enables viral dissemination into tissues normally guarded by specialized barriers, like the placenta and brain (14,15).Work from our group has shown that secreted DENV NS1 also promotes viral dissemination in mice, triggering leak into key organs throughout the body due to the broad tropism of DENV NS1 to many endothelial cells types (Biering and Harris, unpublished data). However, the data from this dissertation suggest that this strategy can be countered through immune responses to NS1. Inflammasomes may act as an early alarm system by sensing secreted NS1 and triggering pro-inflammatory responses in distal tissues, priming them for defense against DENV in a primary infection. Antibodies against DENV NS1 can act during a secondary infection to inhibit NS1-induced endothelial dysfunction, confining viral spread. On the other hand, excessive inflammation induced by DENV NS1 itself or by DENV infection may result in poor outcomes and contribute to immunopathology. In many ways, dengue disease can be defined by this balance between protective and pathogenic responses. Cross-reactive antibodies to E, for example, can mediate both strong neutralization and ADE, depending on their titers and epitopes targeted (16,17). Understanding the complex interplay between immunity to E, immunity to NS1, and NS1-induced pathogenesis will yield new insights into how to target and treat severe dengue disease. Despite much progress, as described in this dissertation and elsewhere, in uncovering new aspects of DENV NS1 biology and its relationship to dengue disease, many questions remain about how it carries out these many functions. Further exploration of pathways triggered by DENV NS1 and their contributions to protection or pathogenesis will surely reveal many fascinating answers about this enigmatic, multifaceted viral protein.

References

1. Biering SB, Akey DL, Wong MP, Brown WC, Lo NTN, Puerta-Guardo H, et al. Structural basis for antibody inhibition of flavivirus NS1–triggered endothelial dysfunction. Science. 2021 Jan 8;371(6525):194–200.

2. Wong MP, Meas MA, Adams C, Hernandez S, Green V, Montoya M, et al. Development and Implementation of Dried Blood Spot-Based COVID-19 Serological Assays for Epidemiologic Studies. Microbiol Spectr. 2022 Jun 29;10(3):e0247121.

3. Lewnard J, Mora A, Nkwocha O, Kogut K, Rauch S, Morga N, et al. Prevalence and Clinical Profile of Severe Acute Respiratory Syndrome Coronavirus 2 Infection among Farmworkers, California, June–November 2020. Emerging Infectious Disease journal [Internet]. 2021;27(5). Available from: https://wwwnc.cdc.gov/eid/article/27/5/20-4949_article

4. Mora AM, Lewnard JA, Kogut K, Rauch SA, Hernandez S, Wong MP, et al. Risk Factors Associated With SARS-CoV-2 Infection Among Farmworkers in Monterey County, California. JAMA Netw Open. 2021 Sep 1;4(9):e2124116.

5. Adams C, Horton M, Solomon O, Wong M, Wu SL, Fuller S, et al. Health inequities in SARS-CoV-2 infection, seroprevalence, and COVID-19 vaccination: Results from the East Bay COVID-19 study. PLOS Glob Public Health. 2022;2(8):e0000647.

6. Solomon O, Adams C, Horton M, Wong MP, Meas M, Shao X, et al. COVID-19 vaccine antibody response is associated with side-effects, chronic health conditions, and vaccine type in a large Northern California cohort [Internet]. medRxiv; 2022 [cited 2023 Dec 1]. p. 2022.09.30.22280166. Available from: https://www.medrxiv.org/content/10.1101/2022.09.30.22280166v1

7. Pan P, Zhang Q, Liu W, Wang W, Yu Z, Lao Z, et al. Dengue Virus Infection Activates Interleukin-1β to Induce Tissue Injury and Vascular Leakage. Front Microbiol [Internet]. 2019 [cited 2020 Jun 28];10. Available from: https://www.frontiersin.org/articles/10.3389/fmicb.2019.02637/full

8. Dinarello CA. Overview of the IL-1 family in innate inflammation and acquired immunity. Immunol Rev. 2018;281(1):8–27.

9. Uno N, Ross TM. Dengue virus and the host innate immune response. Emerg Microbes Infect. 2018 Oct 10;7:167.

10. Kaplanski G. Interleukin-18: Biological properties and role in disease pathogenesis. Immunol Rev. 2018 Jan;281(1):138–53.

11. Molofsky AB, Savage A, Locksley RM. Interleukin-33 in tissue homeostasis, injury and inflammation. Immunity. 2015 Jun 16;42(6):1005–19.

12. Bonilla WV, Fröhlich A, Senn K, Kallert S, Fernandez M, Johnson S, et al. The alarmin interleukin-33 drives protective antiviral $CD8^+$ T cell responses. Science. 2012 Feb 24;335(6071):984–9.

13. Norris GT, Ames JM, Ziegler SF, Oberst A. Oligodendrocyte-derived IL-33 functions as a microglial survival factor during neuroinvasive flavivirus infection. PLoS Pathog. 2023 Nov 20;19(11):e1011350.

14. Puerta-Guardo H, Tabata T, Petitt M, Dimitrova M, Glasner DR, Pereira L, et al. Zika Virus Nonstructural Protein 1 Disrupts Glycosaminoglycans and Causes Permeability in Developing Human Placentas. J Infect Dis. 2020 Jan 15;221(2):313–24.

15. Wessel AW, Dowd KA, Biering SB, Zhang P, Edeling MA, Nelson CA, et al. Levels of Circulating NS1 Impact West Nile Virus Spread to the Brain. J Virol. 95(20):e00844-21.

16. Katzelnick LC, Zambrana JV, Elizondo D, Collado D, Garcia N, Arguello S, et al. Dengue and Zika virus infections in children elicit cross-reactive protective and enhancing antibodies that persist long term. Sci Transl Med. 2021 Oct 6;13(614):eabg9478.

17. Katzelnick LC, Bos S, Harris E. Protective and enhancing interactions among dengue viruses 1-4 and Zika virus. Curr Opin Virol. 2020 Aug;43:59–70.